An assessment of factors influencing the spatial variability of iron concentrations in groundwater in selected areas of the Western Cape Province.

Presanta Bissonram

A thesis submitted in partial fulfilment of the requirements for the degree of MSc. Environmental and Water Science in the Department of Earth Science, University of the Western Cape.

August 2022

Supervisor: Dr. Sumaya Clarke

Co-Supervisor: Dr. Thokozani Kanyerere

KEYWORDS

Hydrochemistry

Iron Clogging

Iron Precipitation

Geochemistry

Water Quality

Sampling Techniques

Spatial Variation

Incremental Modelling

Site-specific Conditions

Borehole Management

Abstract

Groundwater in South Africa, and more specifically the Western Cape Province (WCP), has become of major interest in recent years due to the unpredictable climatic conditions and the uncertainty of surface water to continuously meet the current and future water demands. With the exploration of groundwater (through the drilling of boreholes) to meet the current water demand and to ensure water security there comes the related problem of iron (Fe) and Manganese (Mn) oxidation and precipitation. The precipitation of Fe and Mn in boreholes reduce the yield and quality of the water, resulting in borehole clogging. This study took place in the WCP and the sites sampled at were hospitals as part of the business continuity project that was initiated during the drought in that took place in Cape Town in 2017. There are 4 objectives for this study which are to assess spatial variations in Fe and Mn concentrations, to establish site-specific processes controlling the concentration of Fe and Mn in groundwater, to model the likelihood of precipitation of Fe and Mn based on detected solution composition and to assess the best practice method/techniques for sampling Fe and Mn.

This research project made use of quantitative and qualitative research methods. The first two objectives was addressed by using historical data which included groundwater chemistry data, pumping test data and geological data of the WCP. In addition to the historical data being used sampling was done at selected sites to understand the current groundwater chemistry, while interviews were conducted with site maintenance personnel to further understand the management of the boreholes. The third objective made use of the PHREEQC software to determine the saturation indices of samples collected and modelling of the effect of change in Fe, Mn, redox potential, pH and temperature has on the precipitation of Fe and Mn minerals. The last objective was achieved through the sampling conducted which provided the opportunity to test the best practice sampling methods of Fe and Mn in groundwater.

Research findings indicate that the occurrence of Fe and Mn found spatially within the WCP are at low concentrations but are of concern. The Fe^{2+} concentrations were split into 5 ranges from the data used, the ranges are 0.00mg/L to 3.79mg/L, 3.79mg/L to 16.92mg/L, 16.92mg/L to 41.66mg/L, 41.66mg/L to 74.30mg/L and lastly 74.30mg/L to 285.70mg/L. The Mn^{2+} map was also split into 5 ranges from the data used, the ranges are 0.00mg/L to 0.39mg/L, 0.39mg/L to 1.55mg/L, 1.55mg/L to 4.21mg/L, 4.21mg/L to 9.23mg/L and 9.23mg/L to 17.43mg/L. These concentrations are mainly made up of a range between 0.00mg/L and 3.79mg/L. The points between 3.79mg/L and 16.92mg/L are spread from the south-western to south-eastern

parts of the province. Ranges between 16.92mg/L and 41.68mg/L are mainly found at the lower south-easterly area of the province. Higher concentrations between 41.68mg/L and 74.30mg/L are found closer to the areas where there are concentrations between 16.92mg/L and 41.68mg/L. There was only one point of a range between 74.30mg/L and 285.70mg/L found on the western side of the province. The highest concentrations of Fe^{2+} are 285.70mg/L whereas the highest concentrations of Mn^{2+} are 17.43mg/L. Most of Mn^{2+} are concentrated towards the north-western, south-western and south-easterly part of the province. Concentrations between 0.39mg/L and 1.55mg/L are also found in the north-western and south-eastern parts of the province. Points between 1.55mg/L and 4.21mg/L mirror the previous range of concentrations. The concentrations of 4.21mg/L and 9.23mg/L are mainly found at the north-western part of the province. The points between 9.23mg/L and 17.43mg/L are both found on the western part of the province.

The geological map and lithological logs indicate that there is a strong influence of geology on the concentration of Fe and Mn found in groundwater. The geologic formations found are the Malmesbury Group, TMG and Cape Granite Suite. The influence of recharge was assessed briefly by looking at the land use, the results show that there was no significant impact on the Fe and Mn concentrations from landuse activities. The influence of geology is further enhanced and understood through the interviews conducted at the sites with the site personnel which showed the importance of borehole management and maintenance. The interviews shows that the maintenance have an influence on the quality of groundwater that was pumped. For DP Marais Hospital BH1 and DP Marais Hospital BH2 the minerals Gibbsite, Goethite and Hematite were oversaturated. At Sonstraal hospital, the mineral Gibbsite was oversaturated. UWC BH4 the minerals Calcite, Gibbsite, Goethite and Hematite were oversaturated. UWC BH5 the minerals Gibbsite, Goethite, Hausmannite and Hematite were oversaturated. All mineral phases were undersaturated for the Paarl hospital site. The modelling of the effect that Mn, Fe, pH, temperature and redox potential on the concentration of Fe and Mn showed that the pH, temperature and redox potential have a strong influence on the concentration of Fe and Mn in groundwater and its spatial occurrence.

The following sampling techniques were used to compare to establish the best practice techniques; sampling directly from the pipe outlet, filtered using a 0,45-micron filter, preservation with nitric acid, using a flow through cell to minimize contact with oxygen prior to sampling and in field analysis by DR900. The results were inconclusive as errors occurred from handling and storage of samples. It was concluded that the sampling technique for Fe and

Mn should include the immediate analysis of these minerals as the exposure to oxygen and time before analyses at an accredited lab will allow for chemical changes to occur allowing for inaccurate data.

This research that reflects the ways in which Fe and Mn concentrations are influenced from site to site will aid in future considerations of borehole drilling, management and monitoring as well as groundwater monitoring and management across the WCP. It is suggested that future research should take into consideration the following recommendations. Not only site-specific processes that take place influence the Fe and Mn concentrations in groundwater but there is also a strong microbial influence that needs to be considered in the future. The sampling technique should be repeated with decreased time between sample collection and lab analysis. The sampling technique used should also be mentioned when reporting on Fe and Mn as this provides insight to the quality of the data and results which will be useful when it comes to decision making. This study does provide errors that highly influence and alter the results therefore thee sampling techniques practiced should be repeated in future studies for further understanding and recommendations.

Declaration

I declare that *An assessment of factors influencing the spatial variability of iron concentrations in groundwater in selected areas of the Western Cape Province* is my own work, that it has not been submitted for any degree or examination in any other university, and that all the sources I have used or quoted have been indicated and acknowledged by complete references.

Presanta Bissonram August 2022

Signed……………..

Acknowledgements

I would like to first thank Dr. Kevin Pietersen an Dr. Rodger Parsons who initiated this research project and providing me with the background knowledge of the larger business continuity project and data retrieval which played a crucial role in this study.

I would like to express immense gratitude to my supervisor, Dr. Sumaya Clarke for helping me refine the research project, gain practical experience, provide funding, motivating and encouraging me through this study. I am also grateful to my family, friend and staff at UWC Earth Science department for assisting me and supporting me through this research project. Lastly, I would like to thank God for blessing me with another opportunity to learn and grow and without whom none of this would have been possible.

TABLE OF CONTENTS

CHAPTER 1: INTRODUCTION 1

1.1 Background 1

1.2 Problem Statement 4

1.3 Research Question 4

1.4 Thesis Statement 4

1.5 Research Aims and Objectives 4

1.6 Motivation for Research 4

1.7 Contextualization of the Study 5

1.8 Study Area 6

1.9 Thesis Structure and Outline 8

CHAPTER 2: LITERATURE REVIEW 10

2.1 Introduction 10

2.1.1 Iron and Manganese 10

2.1.2 Iron 11

2.1.3 Manganese 14

2.1.4 Iron Oxides 17

2.1.5 Manganese Oxides 20

2.2.1 Iron in aquifers 27

2.2.2 Manganese in aquifers 29

2.3 Iron encrustation and iron-related clogging 29

2.3.1 Borehole iron encrustation 30

2.3.2 Iron and manganese biofouling 31

2.3.3 Management strategies 34

2.3.4 Rehabilitation methods 35

2.4 Methods used for sampling iron 39

2.4.1 Measuring iron and manganese 39

2.4.2 Importance of Field Determinants 39

2.4.3 Sample Collection Protocols 44

2.4.4 Data Analysis Interpretation of Fe and Mn 46

2.5 Factors impacting iron precipitation 47

2.5.1 Fe 47

2.5.2 Micronutrients 48

2.5.3 Plants impacts on soil Eh and pH 48

2.5.4 Dissolved Oxygen 48

CHAPTER 3: STUDY AREA 49

3.1 Introduction 49

3.2 Climate 49

3.3 Land Use 53

3.4 Geology 54

3.4.1 Malmesbury Group 54

3.4.2 Table Mountain Group 55

3.5 Hydrogeology 57

CHAPTER 4: METHODS 59

4.2 Methods 59

4.2.1 Fieldwork 59

4.2.2 Desktop Study 59

4.3 Field work measurements and analysis 61

4.3.1 Parameters to be measured 61

4.3.2 Periodate Oxidation Method 61

4.3.3 FerroVer Method 62

4.3.4 Sample collection method 64

1. Flow through cell sample 64

2. Preserved sample 64

3. Filtered sample 64

4. Pipe outlet sample..64

4.4 Sampling Sites..65

4.4.1 Sampling Equipment..65

4.5 Modelling & Statistics..65

4.6 Limitations of the Study..66

4.6.1 Sampling Errors 66

CHAPTER 5: RESULTS AND DISCUSSION..68

5.1 Spatial variation of Fe and Mn in the Western Cape Province 68

5.2 Site specific processes that control the concentrations of Fe and Mn in groundwater ..70

5.2.1 Geology and lithology of boreholes of the selected sites..70

5.2.2 Borehole maintenance and management..76

5.2.3 Water Quality 77

5.3 Likelihood of precipitation of Fe and Mn based on detected solution composition through PHREEQC modelling. 79

5.3.1 Saturation Indices of points sampled..79

5.3.2 Modelling..82

5.3.3 Correlation Analysis for Fe and Mn..91

5.4 Comparing various sampling techniques of iron and manganese 92

CHAPTER 6: CONCLUSION 98

Recommendations..99

APPENDICES 101

References……………………………………………………………………………..114

List of Figures

Figure 1: Fe oxidation reactions (Ahmad, 2012): 12

Figure 2: Borehole exposure to atmospheric conditions 22

Figure 3: Diagram indicating the clogging of a borehole screen and head (van Beek, Hofman-Caris and Zweere, 2020). 23

Figure 4: Map of the study area highlighting major towns and cities, damns, rivers and national roads in selected areas of the WCP 49

Figure 5: Map showing the annual mean maximum temperatures of the major cities and towns in the WCP. 51

Figure 6: Map showing the mean annual rainfall in the major cities and towns in selected areas of the WCP. 52

Figure 7: Map showing the mean minimum annual temperature of the major cities and towns in selected areas of the WCP. 52

Figure 8: Image of handheld HACH DR900 measuring device. 61

Figure 9: Spatial distribution map of Fe^{2+} in the WCP. 68

Figure 10: Histogram indicating the frequency of points per Fe2+ range. 69

Figure 11: Spatial distribution map of Mn2+ in the WCP. 69

Figure 12: Geological map and lithological log of Brooklyn Chest Hospital boreholes drilled during the drought. 71

Figure 13: Geological map and lithological log of DP Marais Hospital boreholes drilled during the drought. 72

Figure 14: Geological map and lithological log of Kraaifontein Community Health Clinic boreholes drilled during the drought. 73

Figure 15: Geological map and lithological log of Paarl Hospital boreholes drilled during the drought. 74

Figure 16: Geological map and lithological log of Sonstraal Hospital boreholes drilled during the drought. 75

Figure 17: Piper diagram indicating water types of 3 different sampling sites. 78

Figure 18a: Incremental modelling of Fe concentration against Fe (a.) and Mn (b.) minerals. 82

Figure 18b: Incremental modelling of Fe concentration against Fe (a.) and Mn (b.) minerals. 83

Figure 22: (a.) Image of filtered sampled collected at DP Marais Hospital and filter used to collect the sample. (b.) Image of the water being purged from DP Marais Hospital. 95

List of Tables

Table 1: Stratigraphic column of the geology of the WCP (Bargmann, 2003). 8
Table 2: List of all Fe oxides and description (Cornell and Schwertmann, 2007) 18
Table 3: List of all sampling sites and number of boreholes. 65
Table 4: Summary of sampling site interviews...77
Table 5: Saturation Indices of collected groundwater samples for all sampled sites. 80
Table 6: Correlation coefficients between the modelled parameters and Fe minerals. 91
Table 7: Correlation coefficients between the parameters modelled and Mn minerals...........92
Table 8: Comparison of sampling techniques to measure Fe and Mn concentrations............93

CHAPTER 1: INTRODUCTION

1.1 Background

Groundwater in South Africa, and more specifically the Western Cape Province (WCP), has become of major interest in recent years due to the unpredictable climate conditions and the uncertainty of surface water to continuously meet the current and future water demands. This study takes place in the WCP and the sites used were based in Cape Town and surrounding areas, situated in health care facilities. This was based on the drought that took place in Cape Town in 2015 that initiated the business continuity project to provide a secure water source for these health care facilities. With the exploration of groundwater (through the drilling of boreholes) to meet the current water demand and to ensure water security there comes the related problem of iron (Fe) and Manganese (Mn) oxidation and precipitation. The precipitation of Fe and Mn in boreholes reduce the yield and quality of the water, resulting in borehole clogging. Fe and Mn form a major part of soils and rock minerals and are dissolved and released when contact is made with groundwater (Khozyem *et al.*, 2019). Fe and Mn appear clear and colourless when dissolved in water, however, when oxygenation and/or aeration takes place, the water becomes cloudy and turbid (Khozyem *et al.*, 2019; Song *et al.*, 2020). This is due to Fe oxidizing from dissolved/soluble Fe (Fe^{2+}) to precipitated/insoluble Fe (Fe^{3+}) and Mn from dissolved/soluble Mn (Mn^{2+}) to precipitated/insoluble Mn (Mn^{4+}) which are their colloidal precipitated forms (Khozyem *et al.*, 2019; Song *et al.*, 2020). Fe oxidation and precipitation in boreholes is a global problem since Mn^{2+} and Fe^{2+} are natural ions found in anaerobic groundwater throughout the world (Olsthoorn, 2000). Globally, areas which experience elevated Fe concentrations or Fe clogging in their groundwater or boreholes respectively, are South Africa, USA, Germany, United Kingdom (Scotland), France, Egypt, Switzerland, India, Norway, Australia, South and South-East Asia (Bourg and Berlin, 1994; Mettler, Abdelmoula, *et al.*, 2001; Karakish, 2005; Smith, 2006; Homoncik *et al.*, 2010; Houben and Weihe, 2010; Prasad and Danso-Amoako, 2014; Nitzsche *et al.*, 2015; Oppong-Anane *et al.*, 2018; Khozyem *et al.*, 2019; van Beek, Hofman-Caris and Zweere, 2020; Moser *et al.*, 2021). One of the oldest plants built to remediate Fe and Mn clogging in Sweden in 1971 reported varying concentrations of Fe and Mn between levels of 0.3 – 15 mg/L and 0.2 – 4 mg/L respectively (Braester and Martinell, 1988). A municipality in Canada reported that for a number of years the groundwater contained between 7 – 15 mg/L and 1.8 – 2 mg/L of Fe and Mn respectively (Ellis, Bouchard and Lantagne, 2000). In the state of Maharashtra in India the reported groundwater Fe concentrations were between 0.08 – 1.51 mg/L and for Mn between 0.23 – 1.7 mg/L (Khadse, Patni and Labhasetwar, 2015). In Western Switzerland the groundwater contained dissolved Fe and Mn in concentrations between 0.3 – 1 mg/L and 0.1 – 0.2 mg/L, respectively (Mettler et al., 2001). In Vietnam the reported concentration of Fe in groundwater was 16.3 mg/L and 1.1 mg/L for Mn (Nitzsche *et al.*, 2015). In Norway the abstracted groundwater contains 25mg/L of Fe (van Beek, Hofman-Caris and Zweere, 2020). In the Upper Yamuna Basin, in India, the concentration of Fe in groundwater was found to be between 0.04 – 4 mg/L (Sarkar and Shekhar, 2018).

The World Health Organization (WHO) has stated that the acceptable concentrations for Fe in drinking water is 0.3 mg/L and Mn as 0.1 mg/L (Ellis et al., 2000; Karakish, 2005; Mettler et al., 2001; Nguyen and Ahn, 2018). Similar standards are also used in other countries for example in the USA, Canada 0.3 mg/L and 0.05 mg/L and in the European Union (1998) 0.2 mg/L and 0.05 mg/L for Fe and Mn respectively (Ellis et al., 2000; Mettler et al., 2001). In Egypt the concentrations are limited to 1.0 mg/L of Fe and 0.5 mg/L for Mn in drinking water, concentrations which exceed this may not have any direct effect on health but can cause aesthetic problems with the water as well as precipitation issues (Karakish, 2005). In India the Bureau of India Standards states that the maximum permissible limit for Fe concentration in drinking water is between 1.0 mg/L to – 0.3 mg/L (Sarkar and Shekhar, 2018). As stated above, due to many countries becoming heavily reliant on groundwater as a water resource there have been many cases of increased Fe and Mn concentrations. In South Africa, where this research project will be taking place, the national water quality guidelines for domestic use states that the water quality target range for Fe should be between 0.1 mg/L – 0.3 mg/L . This target range is described to have slight effects on taste and marginal other aesthetic effects and deposits in plumbing with associated problems may start to occur however, there are no health effects. With reference to allowable Mn concentrations for domestic water use, the South African water quality guidelines states that the water quality target range for Mn is 0.05 mg/L – 0.10 mg/L (Forestry, South African Water Quality Guidelines, 1996). This target range is described as a tolerable range with no health effects however, slight staining may occur (Forestry, South African Water Quality Guidelines (second edition). Volume 1: Domestic Use, 1996).

The cycling of Fe between their sources and sinks within an aquifer is dependent on the change in pH and redox conditions (Smith, 2006; Song *et al.*, 2020). Fe and Mn related issues associated with groundwater quality are mainly aesthetic and potable water problems (Robey, 2014). When Fe and Mn are present in concentrations exceeding 0.3 mg/L and 0.1 mg/L, respectively, it results in a harsh, metallic taste and the aesthetic problems include a reddish-brown or greyish-black water discolouration that results in staining of laundry, pumping fixtures, households appliances, walls and cooked food (Homoncik *et al.*, 2010; Robey, 2014; Khozyem *et al.*, 2019). The precipitation of Fe oxide minerals within a borehole leads to encrustation of borehole equipment or form a coating which later will slough off and subsequently clog equipment such as pumps, screens and pipes causing the decrease in water quality and yield (Smith, 2006; Emerson, Fleming and McBeth, 2010; Robey, 2014; Sarkar and Shekhar, 2018; van Beek, Hofman-Caris and Zweere, 2020). High concentrations of Fe and Mn in drinking water also pose a health risk to humans, such as chromic intoxication, lung embolism, bronchitis, impotence, nerve damage and parkinsonism as well as other diseases such as kidney failure and damage to neurological systems (Zhang *et al.*, 2020; Friends of Groundwater in the World Water Quality Alliance, 2021; Usman *et al.*, 2021).

Fe – related clogging of boreholes is an expensive problem to treat once it has occurred. Some of the methods in use currently such as the Blended Chemical Heat Treatment (BCHT) method is both a potential hazard to the aquifer in which it is being used as well as the people who are treating the borehole (Smith & Roychoudhury, 2013). A treatment process called In-Situ Iron Removal (ISIR) is commonly used for drinking water production. This involves the aeration of anoxic groundwater that contains high concentrations of Fe^{2+} thus allowing Fe oxyhydroxide's to precipitate (Appelo, 2009). Once the Fe oxy-hydroxide has precipitated the insoluble Fe^{3+} can be filtered out (Appelo, 2009). Some common oxidizing agents used for Fe^{2+} oxidation include ClO_2, O_3 and $KMnO_4$ (Nguyen, 2018). This method is both cost-effective and environmentally-friendly, however, this technology is limited by the uncontrollable transportation of injected oxygen that can be consumed by other side reactions and mediate for unwanted underground processes to take place (Nguyen, 2018).

Although it may be an international setback, the cause for the oxidation and precipitation in groundwater leading to excessive concentrations of Fe and Mn are site specific, which has a great influence on how one approaches the problem. Site specific conditions which may influence high concentrations of Fe and Mn in groundwater is; the contact of groundwater with oxygen, chemistry, microbiological activity, geological formation and pumping regime (Smith, 2006; Du *et al.*, 2018).

1.2 Problem Statement

The occurrence of high Fe and Mn concentrations in groundwater reduces the yield, productivity and quality of existing boreholes in the WCP. This is due to the lack of information and understanding of the site-specific conditions that influence the chemical behaviour of Fe and Mn in groundwater.

1.3 Research Question

What are the spatial variations of Fe and Mn concentrations in groundwater within the WCP? Which site-specific conditions influence/control elevated Fe and Mn concentrations?

What is the likelihood of precipitation of Fe and Mn, based on a detected solution composition?

Which techniques are most suitable for sampling Fe and Mn?

1.4 Thesis Statement

Variations in Fe and Mn concentrations in groundwater in the WCP are controlled or influenced by site specific conditions that result in elevated Fe and Mn concentrations.

1.5 Research Aims and Objectives

The aim of this research project is to investigate and understand the spatial distribution of Fe and Mn in groundwater within the WCP and to delineate the site-specific processes that influence the concentrations of Fe and Mn. The objectives to achieve the above-mentioned aim are:

1. To assess spatial variations in Fe and Mn concentrations.
2. To establish site-specific processes controlling the concentration of Fe and Mn in groundwater.
3. To model the likelihood of precipitation of Fe and Mn based on detected solution composition.
4. To assess the best practice method/techniques for sampling Fe and Mn.

1.6 Motivation for Research

Surface water has become an unreliable source of water as it is currently being overused and stressed. The development of new supplies and subsequent surface water treatments may be expensive or unavailable in rural areas (Robey, 2014).

A study showed the following limitations on Fe rehabilitation treatments in South Africa were identified (Robey, 2014):

- Inadequate monitoring protocol of production boreholes and water quality for early detection of clogging. Once clogging of the production borehole has been identified it is often too late to treat and efficiently rectify the problem.
- Materials that the borehole was constructed from is often incorrect, this is due to the lack of knowledge of this problem when the well field was initially developed which results in reduced recovery yields.
- The National Environmental Management Act No. 107 of 1998 and the National Water Act. 36 of 1998 regulations may cause delays in rehabilitation and re-drilling as well as the costs and skills required, regular cleaning of production boreholes is not implemented.

Previous studies such as the work of (Robey, 2014) focused on the treatment of boreholes affected by Fe related clogging or high concentrations of Fe and Mn as well as monitoring and maintenance of boreholes affected by this problem in the WCP. This research project will draw focus on understanding why Fe-related clogging occurs and where high concentrations of Fe and Mn occurs in selected parts of the WCP. This will help produce information that can be used for the drilling of future production boreholes.

Studies have suggested to stop the pumping of water with high concentrations of Fe and Mn to be used as a potable water supply due to the additional treatment processes that take place once the water has been pumped out. During the treatment processes, Fe or Mn may precipitate onto the equipment, which may cause further clogging or damage. The precipitation of Fe and Mn in equipment results in reduced water supply and the constant maintenance costs for equipment, which is expensive and not ideal for a rural environment who lack the resources. Therefore, if the occurrence of excessive Mn and Fe concentrations can be predicted it can be avoided during the sourcing of new water supplies (Homoncik *et al.*, 2010).

1.7 Contextualization of the Study

In Northern Germany at the Großenkneten water works, there was a case of high concentrations of Fe in the groundwater (Houben G. W, 2010). This resulted in the build-up of Fe encrustation and a decrease in the yield (Houben G. W, 2010). The well field, which was constructed in 1969, had to be abandoned in 2007 due to the repeated iron encrustation problem (Houben G.

W, 2010). This build-up of Fe encrustation in the aquifer was not considered to be natural due to the original lithological log, which consisted of predominantly grey colours (Houben G. W, 2010). It was found that the concentration of Fe content tends to decrease with distance from the well screen, which strongly suggests the presence of pumping-induced incrustations outside of the annulus (Houben G. W, 2010). It is considered irregular for Fe encrustation to form in the deeper parts of the aquifer, which are known to be reducing and as a result Fe-rich and oxygen deficient. It was suggested that the switching on and off the pump and pumping induced drawdown allowed shallow oxygenated water to mix with deep Fe-rich water, this resulted in the formation of Fe incrustation deep in the aquifer (Houben G. W, 2010).

In the WCP of South Africa research on the likelihood of a borehole to have Fe-related clogging in the aquifers within the Table Mountain Group was conducted (Smith & Roychoudhury, 2013). Investigation of the control's aquifer lithology and groundwater conditions (water chemistry and organic acids) has on the mobilization of Fe^{2+} and presence in the abstracted groundwater was considered (Smith & Roychoudhury, 2013). The experimental research showed that the arenaceous Peninsula and Skuweberg formations have the potential to release large amounts of Fe either under oxic conditions with low pH or under anoxic conditions (independent of pH) (Smith & Roychoudhury, 2013). This research concluded that the likelihood of Fe clogging to occur in boreholes requires knowledge of the redox conditions in the aquifer and the source of lithology of the aquifer (Smith & Roychoudhury, 2013). Bodrud-Doza, (2016) found that in Bangladesh, Fe and Mn was found in higher concentrations than other heavy metals in groundwater.

1.8 Study Area

The WCP lies on the southern tip of Africa and represents 10.6% of the total of South Africa's total land area which is 129 462km^2 . The province extends beyond Strandfontein on the West Coast around the Cape Peninsula and Cape Point to Nature's Valley along the Garden Route on the South Coast (Gumbi and van Weele, 2013).

Along the southern coast of the WCP, the Atlantic and Indian Oceans meet, with the cold Benguela current flowing up the west coast and the warm Aghulas current flowing westwards along the southern coast (Gumbi and van Weele, 2013). The Cape Fold Belt extends from east to west for more than 800km along the southern margin of Africa and is part of an extensive orogenic belt of later Paleozoic and earliest Mesozoic age (Lock, Brian, 1980). The Cape Fold

Belt dominates the WCP by extending along the length of it, which is responsible for the L-shaped mountain range (du Plessis and Scholms, 2017).

Three climatic zones identified in the WCP which are the Mediterranean, South Coast and Karoo climatic region are due to the presence of the Cape Fold Belt, Benguela current and the Aghulas current (du Plessis, 2017). The Mediterranean region includes the southwestern and west coast part of the province that typically receives winter rainfall between the months of May to August. This rainfall is supplied form the cyclones which are formed from the South Atlantic Ocean as well as the combination of the cold Benguela current and the northward displacement of high-pressure systems (du Plessis, 2017). The South Coast region stretches eastward from Cape Aghulas which experiences all-year round rainfall due to the moist air from the Indian Ocean (du Plessis, 2017). The Cape Fold belt forms a natural divide between the South Coast and Karoo climate regions, therefore, the extent of the influence of the Indian Ocean are not felt in these regions. As a result, the Karoo region is limited to the inland plateau of South Africa and receives rainfall all year (du Plessis, 2017).

The WCP is responsible for 50% of South Africa's agricultural exports and supplies about 20% of the national agricultural production (du Plessis, 2017). The province hosts a productive wine industry, which is exported internationally as well as provides tourism (du Plessis, 2017). The remainder of the area is recognized for its trade in animal products, such as, sheep (meat and wool), chickens (eggs), cows (dairy), beef and pork (meat) (du Plessis, 2017). The coastline has a large variety of marine life, which supports a profitable fishing sector (du Plessis, 2017).

In terms of water supply, the Table Mountain Group and the Sandveld Group are the two important aquifers that are used for the municipal water supply (Smith & Roychoudhury, 2013). The extensive Table Mountain Group is a fractured, quartzite aquifer, which makes it a suitable water source for both the Western and Eastern Cape Provinces (Smith & Roychoudhury, 2013). In the Cape Town and surrounding areas, the Malmesbury Group is the oldest major rock outcrop (Table 1) that is subdivided into three distinct terrains, Tygerberg, Swartland and Boland (Bargmann, 2003). The Malmesbury Group is generally considered to be a low yielding aquifer (0.5 l/s) with variable water quality (Conrad, Smit, Murray, & van Gend-Muller, 2019). The last important aquifer of importance is the Cape Flats Aquifer of the "Late-Tertiary and Recent Sands", characterised by a flat,sandy subsurface that is underlain by an impervious shaly bedrock aquifer of the Malmesbury Group (Jia, 2007). Table 1 shows the stratigraphy of the WCP.

Table 1: Stratigraphic column of the geology of the WCP (Bargmann, 2003).

Age	Group	Formation	Main Rocktypes
Early Cretaceous (132Ma)			Dolerite
Ordovician - Early Devonian (450-409 Ma)	Table Mountain Group	Rietvlei	Sandstone, Siltstone, Shale
		Skurweberg	Sandstone
		Goudini	Sandstone, Siltstone, Shale
		Cederberg	Shale
		Pakhuis	Diamictite, Sandstone
		Peninsula	Sandstone
		Graafwater	Sandstone, Siltstone, Shale
		Piekenierskloof	Sandstone, Conglomerate
Early - Mid Ordovician (500 - 450 Ma)	Klipheuwel Group	Populierbos	Mudstone, Shale
		Magrug	Conglomerate, Sandstone
Late Proterozoic Early Cambrian (600 - 500 Ma)	Cape Granite Suite		Granite, Mafic, Granodiorite and Alkali Granite Intrusives
Late Proterozoic (~950 - 570 Ma)	Malmesbury Group	Proterville	Shale, Greywacke
		Norree	Greywacke, Quartzite
		Piketberg	Grit, Conglomerate, Greywacke
		Franschhoek	Conglomerate, Quartzite
		Mooreesberg	Greywacke
		Klipplaat	Quartz schist
		Berg River	Mica Schist, Greywacke
		Tygerberg	Greywacke, Shale, Siltstone and Quartzite

1.9 Thesis Structure and Outline

Chapter One: Introduction

Include the background information about the study including a brief review of the current knowledge as well as highlighting the aims and objectives of the research project.

Chapter Two: Literature Review

This chapter will cover the in-depth knowledge of the research project showing how the research topic fits in on a local and international scale. It also covers the methods used around the studying and understanding of this research topic.

Chapter Three: Study Area

This chapter will include information on the climate, geology, land use and hydrological properties of the study area.

Chapter Four: Methods

This chapter will include the various methods of how the objectives of this research project will be achieved. It will highlight the different types of data required for each method, outlining the advantages and the disadvantages of each method chosen.

Chapter Five: Results & Discussion

This chapter will cover the results and discussion of the research project once the data analysis has been completed. It will display the outcomes of each objective using the appropriate maps, tables and graphs. It analyses the results and the interpretation of the results by commenting on what was expected and what was not expected. It will provide detail on the relationships in the datasets and provide information on the impact of these relationships in context to the research topic.

Chapter Six: Conclusions and recommendations?

This chapter will conclude the thesis by covering if the aims and objectives of the study have been achieved. It will cover the significant results, the limitations and make suggestions for future research.

CHAPTER 2: LITERATURE REVIEW

2.1 Introduction

Changes in water quality can result in health, aesthetic and economic impacts (Department of Water Affairs and Forestry, 1996). Often these problems, which result from change in water quality, are associated not only with the presence of a constituent but with the interaction between constituents (Department of Water Affairs and Forestry, 1996). Groundwater is generally characterized by low temperatures (7-10°C), high carbon dioxide concentrations, low redox potentials (absence of oxygen), high mineral content (high alkalinity and hardness) and a very low suspended solid content (El Araby, Hawash and El Diwani, 2009).

2.1.1 Iron and Manganese

Fe oxide concentration in soils naturally vary from 0.1% to 50% (Oppong-Anane *et al.*, 2018). Fe oxide can be found as discrete minerals, nodules or fillings in the cracks and veins of minerals, coatings on clay and sand particles or as major constituent of concretions, mottles and other segregations (Oppong-Anane *et al.*, 2018). Fe oxides minerals vary in crystallinity, stability, solubility, specific surface area, and particle size (Oppong-Anane *et al.*, 2018). Crystallinity is an important differentiating factor for Fe oxides, they range from amorphous forms such as Ferrihydrite Fe(OH)3 to the highly crystalline Goethite (FeOOH) and Hematite (Fe2O3) minerals (Oppong-Anane *et al.*, 2018). Fe oxide minerals undergo an ageing process which causes them to go through a transformation in which the amorphous Fe oxides evolve into a more stable crystalline form (Oppong-Anane *et al.*, 2018). Dissolution of Fe is controlled by multiple parameters in addition to the pH level such as the type of mineral phases present, the degree of crystallinity, levels and type of organic matter and microbial activity (which plays a big role) (Oppong-Anane *et al.*, 2018).

The commonly found and reported Fe oxide minerals are Ferrihydrite, which dominates the low crystallinity oxides and the higher crystallinity Goethite (Houben, 2003). Goethite is found in rocks in various parts of global ecosystems, and it is one of the most thermodynamically stable Fe oxides at ambient temperature, as a result of its nature it is either the first Fe oxide to form or the end member of many transformations (Cornell and Schwertmann, 2007). In large crystal aggregates, Goethite is yellow to brown in colour and is responsible for the colour of many soils and rock deposits. In industries Goethite is an important pigment (Cornell and Schwertmann, 2007). Ferrihydrite is reddish-brown in colour and commonly found in surface environments, it exists only as nano-crystals and if not stabilized it will transform into a more stable Fe oxide (Cornell and Schwertmann, 2007).

The form or state in which Mn and Fe are found within an aquifer is highly dependent on the oxygen balance within the aquifer (Hatva, 1989). There are multiple environmental factors which play a role in the oxygen balance within an aquifer including the geological structure, characteristics of the aquifer, type of soil and bedrock, seasonal cycling, pattern of groundwater flow and the species of Fe and Mn bacteria found in the aquifer (Hatva, 1989). Results from pumping tests indicated that Fe and Mn are non-existent when DO exceeds 4.0 mg/L^{-1}. If the DO falls below this level, the chance of the occurrence of Fe and Mn occurring in its dissolved form rapidly increases (Hatva, 1989).

2.1.2 Iron

Fe is the fourth most abundant element and makes up 5% of the Earth's crust. In its pure form, Fe is silver in colour but usually it appears as greyish black or brown deposits as a result of oxidation (Department of Water Affairs and Forestry, 1996). Fe is an element of multiple valency that can migrate in the form of elementary ions and generate various ionic or colloidal complex compounds with OH^-, HCO_3^-, CO_3^{2-}, SO_3^{2-}, HS_3^-, S_2^- and organic matter. These migration types depend on the state of the thermodynamic system and its parameters. An important role in Fe stability and its speciation forms is played by the occurrence of CO_2, HCO_3, H_2S, organic matter, phosphorus compounds, and Fe bacteria in water, as well as by the temperature and solubility of rocks (Diliūnas and Jurevičius, 2006). Fe commonly occurs in two oxidation states Fe^{2+} and Fe^{3+}. At surface conditions both Fe^{2+} and Fe^{3+} are found to be stable, under reducing conditions Fe^{2+} is soluble and only in the presence of an oxidant does Fe^{2+} oxidize to Fe^{3+} (Smith and Roychoudhury, 2013). At a low pH, Fe^{3+} is soluble and with increasing pH it becomes insoluble however, solubility can increase again at high pH levels As a result, Fe is found in solution in water with a pH greater than 3, in reducing conditions and occurs in the solid phase in all other environments (Smith and Roychoudhury, 2013). Figure 1 below shows the exposure of Fe^{2+} to oxygen resulting in the formation of Fe^{3+} through the process of oxidation (Ahmad, 2012).

Figure 1: Fe oxidation reactions (Ahmad, 2012):

- The oxidation of divalent ferrous ion (Fe2+) to trivalent ferric ions (Fe3+) can be described by (Eq.1.1)
  $$Fe^{2+} = Fe^{3+} + e^- \quad \text{(Eq.1.1)}$$
- In situations where there are high concentrations of dissolved oxygen (DO), the Fe3+ can further react with hydroxyl groups to precipitate into a solid form and is described by (Eq.1.2).
  $$Fe^{3+} + 3OH^- = Fe(OH)_3 \quad \text{(Eq.1.2)}$$
- The entire redox reaction sequence can be written as (Eq.1.3)
  $$Fe^{2+} + 3H_2O = Fe(OH)_3 + 3H^+ + e^- \quad \text{(Eq.1.3)}$$

Fe oxidation is increased by substances that form stable complexes with Fe^{3+} such as fluoride, phosphate, colloidal Fe oxide and natural organic matter (Smith and Roychoudhury, 2013). The rate of Fe oxidation is minimally affected by temperature between 5° and 35°C (Smith and Roychoudhury, 2013). Environments with high DO and pH concentrations, the half-life of Fe^{2+} can be as little as 2 minutes and in low pH environments with no DO, the half-life of Fe^{2+} can be 2700 days (Smith and Roychoudhury, 2013).

The type, concentration, occurrence and distribution of Fe oxides depend on the environmental conditions in soils which vary spatially and temporally (Rossel *et al.*, 2010). Fe oxides have an influence on soil properties, even if present in very small concentrations, they can affect the soil colour, the aggregation of the soil particles, the retention of cations and anions at particle surfaces, as well as electron and proton buffering (Rossel *et al.*, 2010). Fe is an essential micronutrient which is required by all living organisms (Department of Water Affairs and Forestry, 1996). High concentrations of Fe present an aesthetic concern due to ferrous salts being unstable under near-neutral pH conditions in drinking water, therefore, it precipitates as insoluble ferric hydroxide which settles out as a rust-coloured silt (Department of Water Affairs and Forestry, 1996).

Variations in Fe oxide minerals exist in the crystallinity, stability, solubility, particle size and specific surface area (SSA). In terms of the crystallinity, Fe oxides can range from highly crystalline goethite and hematite minerals to amorphous forms such as ferrihydrite. However, Fe oxides go through an ageing process in which it transforms from amorphous Fe oxide to a more stable crystalline form. Fe oxide particle sizes range from 5 to 150nm which results in SSA values as high as 250-400m^2/g. Due to these minerals existing as finely divided and positively charged particles with a high surface area, they absorb inorganic anions such as phosphate, silicate, nitrate and arsenate and organic anions such as citrate (Rossel *et al.*, 2010).

During the production of drinking water, anoxic groundwater containing Fe^{2+} is aerated and Fe-oxyhydroxide precipitates. Though Fe in drinking water may be more beneficial than poisonous, these Fe-oxyhydroxides precipitates may be responsible for clogging distribution systems, stained clothing and sanitary installations, therefore Fe is removed during water treatment. Slimy deposits from Fe^{2+}-oxidizing bacteria can be an issue in hand-pumped wells. Mn applies in similar ways as the above however, Mn-oxides become reduced at a higher pe than Fe-oxides and Mn is much less abundant than Fe in aquifers (Apello & Postma, 2009).

Organic matter of natural origin in natural aquatic ecosystems are associated with high concentrations of Fe (Theis and Singer, 1974). Previous studies have reported that many natural waters such as groundwaters, surface waters and municipal wastewaters which contain humic substances severely retard the oxidation of Fe^{2+} (Theis and Singer, 1974). These findings have a number of consequences when it comes to water quality management, in particular, water treatment plants (Theis and Singer, 1974). Water treatment plants are dependent on the oxidation of Fe^{2+} by oxygen and on sedimentation and filtration of the resultant Fe^{3+} hydroxide when it comes to Fe removal from groundwater, the presence of humic substances in groundwater have been recorded interfering with these processes (Theis and Singer, 1974). Davies (1970), Prakash and Rashid (1968) and Martin et al., (1971) through investigations have demonstrated that Fe in association with humic materials are generally available as a nutrient for the growth of aquatic species, and that these humic substances tend to stabilize the Fe, therefore increasing its nutritive availability (Theis and Singer, 1974). In the aqueous environment, Fe^{2+} and Fe^{3+} can be stabilized by dissolved organic matter in amounts in excess of that predicted by simple thermodynamic and kinetic considerations (Theis and Singer, 1974). In summary, Fe^{2+} is capable of forming complexes with organic matter, therefore it is resistant to oxidation even in the presence of DO (Theis and Singer, 1974).

2.1.3 Manganese

Mn is the 10th most abundant element found in a variety of geological settings and nearly ubiquitous in soils and sediments. The average crustal rock contains about 0.1% of Mn, and it is second to Fe as the most common heavy metal found (Post, 1999).

Mn is a grey-white, brittle, trace metal found commonly in the environment. It is a minor component of most rock types, present in soils from weathering and aerial deposition (Department of Water Affairs and Forestry, 1996; Homoncik *et al.*, 2010). Rock types that contain high concentrations of Mn are mafic, ultramafic, shale, greywacke and limestone. Through weathering processes, these rocks can increase the amount of Mn in the soil (Homoncik *et al.*, 2010). Mn is known as a toxic, heavy metal with a presence that may be lethal if found at elevated levels in the environment (Trollip, Hughes and Titshall, 2013). However, Mn is an important nutrient required by plants, birds, animals and microorganisms (Trollip, Hughes and Titshall, 2013). Terrestrial plants require approximately 10 to 50mg Mn kg^{-1} of tissue with the average amount of Mn in plants ranging from 15 to 1000 $mg.kg^{-1}$ (Trollip, Hughes and Titshall, 2013). However, excessive amounts can be neurotoxic. In usual water concentrations, Mn has more a aesthetic effect than a toxic one (Department of Water Affairs and Forestry, 1996).

Mn exists in several different oxidation states, but the most common forms found in the environment are soluble Mn^{2+} when reduced and insoluble Mn^{4+} when oxidized (Department of Water Affairs and Forestry, 1996; Homoncik *et al.*, 2010). Minerals that contain Mn which are commonly found include; pyrolusite (MnO_2), manganite ($Mn_2O_3 \cdot H_2O$), rhodochrosite ($MnCO_3$) and rhodonite ($MnSiO_3$) (Department of Water Affairs and Forestry, 1996). Mn^{4+} typically precipitates out of solution to form a black hydrate oxide which is responsible for the staining problems that occur with Mn-bearing water (Department of Water Affairs and Forestry, 1996). The average concentration of Mn in fresh water is 8µg/l which can range from 0.02-130µg/l, in soils 1000mg/kg and in sea water it is approximately 0.2µg/l (Department of Water Affairs and Forestry, 1996). Mn concentrations that are in the mg/L range are found in anaerobic, bottom level waters where Mn has been mobilized from the sediments (Department of Water Affairs and Forestry, 1996). Many parameters play a role when it comes to mobilizing Mn and controlling its speciation in water, such as pH, redox potential (Eh), DO, and dissolved organic carbon (DOC) (Homoncik et al., 2010). At a lower pH and Eh value, Mn occurs in its soluble and reduced form of Mn^{2+} and is oxidized to form precipitates in the presence of oxygen and a high pH (Homoncik et al., 2010). At pH > 7 and Eh of 800mV which are equilibrium conditions, Mn is most likely to be in the form of Mn^{2+} (Homoncik et al., 2010). It is observed that the hydrochemistry of Mn is closely related with that of Fe hydrochemistry - both elements behave synergistically in their dissolution from sediments under aerobic conditions and re-precipitate under aerobic conditions (Department of Water Affairs and Forestry, 1996).

Micro-organisms play a vital role in Mn mobilization by either enhancing or inhibiting concentrations in groundwater (Homoncik *et al.*, 2010). The effects of micro-organisms can be direct through enzymatic catalysis of Mn oxidation and reduction and specific binding by cell-associated materials (Homoncik *et al.*, 2010). Micro-organisms indirectly affect Mn mobilization by altering the pH and Eh conditions of the micro-environment, thereby influencing Mn speciation and concentration (Homoncik *et al.*, 2010). The impact of the microbiological activity on the behaviour of Mn in water is often clear in the accumulation of oxidized Mn in biofilms on pipe surfaces (Homoncik *et al.*, 2010).

A significant amount of drinking water in many countries is supplied by alluvial aquifers hydraulically connected to neighbouring rivers (Bourg and Berlin, 1994). Groundwater of a higher quality is provided from well fields located near rivers, however in the case of highly polluted rivers or small communities that cannot afford sophisticated water treatment plants, river banks serve as a mechanical, biological and chemical filtration system (Bourg and Berlin, 1994). The characteristics of alluvial aquifers such as the spatial heterogeneity can aggravate the appearance of unwanted substances, especially the redox sensitive elements, Fe and Mn (Bourg and Berlin, 1994). A groundwater system's distinct annual cycles was observed in Switzerland by Bourg and Berlin in 1994, variations were explained by seasonal changes in the temperature and their incidence on the biological activity in the river and banks on the solubility of minerals (Bourg and Berlin, 1994). In the first few meters of infiltration, during summer, Mn and other trace elements were solubilized (Bourg and Berlin, 1994). Winter brought more oxidizing conditions which precipitated Mn^{2+} in the river water onto the bank sediments and in the aquifer (Bourg and Berlin, 1994). Microbiological activity and the resulting degradation of organic matter is the controlling factor of the seasonal occurrence of Mn in groundwater, caused by the dissolution of solid Mn oxides naturally present in the river bank and aquifer solids (Bourg and Berlin, 1994). The study reported that a threshold temperature of 10°C is necessary in order to start the bacterial activity which will, in turn create the reduced conditions required for the solubilization of Mn (Bourg and Berlin, 1994).

Another influence on the concentration of Mn is Fe. A study done by Homonocik 2010 in Scotland showed that high Fe concentrations only occur with high Mn concentration, but high Mn concentrations can be found across a range of Fe concentrations (Homoncik *et al.*, 2010). The bedrock aquifer unit of the study area was made up of Jurassic to Tertiary, Permo-Triassic, Carboniferous, Devonian, Ordovician/Silurian, Cambrian and Precambrian and Igneous rock formations (Homoncik *et al.*, 2010). Therefore, it was observed that the water chemistry parameter that is the most strongly related to Mn concentrations along with oxygen is Fe (Homoncik *et al.*, 2010). This study performed a regression analysis and observed that the two elements do not behave in the exact same way (Homoncik *et al.*, 2010). Mn concentrations have a strong relationship with Eh, DO and pH and Fe concentrations are significantly related to DOC, SEC and Eh (Homoncik *et al.*, 2010). Therefore, the relationship that Mn and Fe share with Eh suggests that the interaction between the two elements in groundwater is mediated by Eh (Homoncik *et al.*, 2010).

In common groundwaters, beyond the normal redox conditions required for mobilization, there is a close relationship between Fe and Mn oxidation and reduction (Homoncik *et al.*, 2010). The precipitation of Fe oxides at lower Eh values than Mn may lead to the removal of Mn by occlusion and sorption to precipitated Fe, this is due to Mn^{2+} having a high affinity for Fe^{3+} oxides (Homoncik *et al.*, 2010).

In solutions where both Mn and Fe are present and are not strongly reducing and circumneutral, Mn concentrations may be lower at a particular Eh than expected (Homoncik *et al.*, 2010). On the other hand, when Fe oxides are reduced, Mn^{2+} is released (Homoncik *et al.*, 2010). With the occurrence of pH and Eh conditions which both contribute towards the mobilization of Fe and Mn, this process may assist in explaining why elevated Fe concentrations often occur with high Mn concentrations (Homoncik *et al.*, 2010). Fe^{2+} is more likely to adsorb or form complexes with DOC than Mn which results in high concentrations of Fe^{2+} occurring than what would be expected at a particular Eh (Homoncik *et al.*, 2010).

In a sandy aquifer, the distribution of Fe occurs through coatings of Fe oxides covering light fractionation of quartz and feldspars (Apello & Postma, 2009). Theses fractionations primarily contain Fe^{2+} bearing silicates such as amphiboles, pyroxenes or biotite and the final fraction contains Fe oxide minerals made of magnetite and ilmenite (Apello & Postma, 2009).

Dissolution of Fe^{2+} bearing silicates such as amphiboles, pyroxenes and magnetite release Fe^{2+} into the groundwater under anoxic conditions (Apello & Postma, 2009). The dissolution rate of these minerals are generally very low which results in low concentrations of Fe^{2+} (Apello & Postma, 2009). During oxic conditions, the Fe^{2+} released via dissolution precipitates as an Fe oxyhydroxide coating which will inhibit further dissolution from taking place (Apello & Postma, 2009). The red colour observed in sandstones is due to a thin coating of hematite covering the sediment grains (Apello & Postma, 2009). Areas of groundwater discharge, the Fe^{2+}-rich groundwater contacts atmospheric oxygen which facilitates the precipitation of Fe oxy-hydroxides that forms deposits in stream beds and bog Fe ores (Apello & Postma, 2009)

Micro-organisms such as *Gallionella* or *Lepthothrix* are important mediators in the precipitating of Fe and Mn and are commonly found in groundwater environments (Houben, 2003). Boreholes provide an excellent breeding ground for these bacteria since they are sedentary organisms that require their nutrients to flow past them (Houben, 2003). Mixed waters in boreholes are commonly oxic and therefore contain some reduced Fe or Mn at the same time (Houben, 2003). The micro-organisms are able to gain energy from the reduced Fe (“iron breathing”) by catalyzing the oxidation process and the resulting metal oxides often become attached to the sticky bacterial exopolymer (Houben, 2003).

2.1.4 Iron Oxides

Fe oxides are common compounds which are often found in the natural environment and can be easily synthesized in a laboratory (Cornell and Schwertmann, 2007). In the natural environment, they are present in almost all of the different sections of the global systems such as the atmosphere, pedosphere, biosphere, hydrosphere and lithosphere where they participate in the manifold interrelationships between these sections (Cornell and Schwertmann, 2007). The formation of Fe oxides involves aerobic weathering of magmatic rocks in both terrestrial and marine environments followed by the redistribution process between different global sections (Cornell and Schwertmann, 2007). Some of the processes involve erosion from the pedosphere into the hydrosphere or atmosphere, mechanical transport by wind/water and most importantly reductive dissolution followed by migration of Fe^{2+} and oxidation re-precipitation in a new section (Cornell and Schwertmann, 2007). Important examples of redistribution are Fe ore formation and Fe oxide precipitation in biota (Cornell and Schwertmann, 2007). Man plays a role in these processes as a consumer of Fe metal and Fe oxides for various industrial processes and not only as a living organism (Cornell and Schwertmann, 2007). Therefore, the general result of all these processes is a continuous increase in Fe oxides in the global system at the cost of Fe in a magmatic rock which is the primary source rock (Cornell and Schwertmann, 2007).

There are 16 Fe oxides which are either oxides, hydroxides or oxide-hydroxides (Cornell and Schwertmann, 2007). These Fe oxides are a combination of Fe with O and/or OH. Fe oxide compounds are commonly found in the trivalent state; three compounds – FeO, $Fe(OH)_2$ and Fe_3O_4 which contain Fe^{2+} (Cornell and Schwertmann, 2007). Fe oxides are made up of close packaged arrays of anions, usually in hexagonal (hcp) or cubic close packing (ccp) where the interstices are partially filled with divalent or trivalent Fe primarily in octahedral (VI) – $Fe(O,OH)_6$ – although in some cases in tetrahedral (IV) – FeO_4 coordination (Cornell and Schwertmann, 2007). Different oxides vary in the way in which the basic structural units, $Fe(O,OH)_6$, $Fe(O)_4$, are arranged in space (Cornell and Schwertmann, 2007). At times, a small concentration of anions such as Cl^-, SO_4^{2-} or CO_3^{2-} may also be part of the structure (Cornell and Schwertmann, 2007).

Other characteristics that should be noted about Fe oxides include the low solubility of Fe^{3+} which results in high stability, the bright colours, partial replacement of Fe in the structure by other cations and the catalytic activity (Cornell and Schwertmann, 2007). Fe oxides often form minute crystals in both the industrial and natural environments due to their high energy of crystallization (Cornell and Schwertmann, 2007). As a result, they have a high specific surface area, often > $100 m^2 g^{-1}$, resulting in them being effective sorbents for a large range of dissolved molecules, ions and gases (Cornell and Schwertmann, 2007).

The Fe oxides, hydroxides and oxide hydroxide are crystalline, the most commonly found Fe oxides are goethite, lepidocrocite, ferrihydrite, hematite and magnetite (Cornell and Schwertmann, 2007). The conditions under which the crystals are formed determine the degree of structural order and the crystal size, although this may be highly variable (Cornell and Schwertmann, 2007). Fe oxides can be differentiated into low and high crystallinity. The low crystallinity Fe oxides are dominated by the mineral Ferrihydrite and higher crystallinity Fe oxides are dominated by goethite and at times smaller amounts of lepidocrocite (Houben, 2003). All Fe oxides show a variety of crystallinities except for ferrihydrite and schwertmannite which have a poor crystal structure (Cornell and Schwertmann, 2007).

Table 2: List of all Fe oxides and description (Cornell and Schwertmann, 2007)

Fe Oxide Name	**Description**

Goethite (α – FeOOH)	Goethite is found in rocks and the different sections of the global ecosystem. It has a diasphere structure that is based on hexagonal close packing (hcp) of anions. It is the most thermodynamically stable Fe at ambient temperatures, this results in goethite being the first oxide to form or the end member after many transformations. Goethite is dark brown or black in massive crystal aggregates unlike the powder which is yellow and the reason for the colour of many rocks, soils and ochre deposits, therefore making goethite an important pigment industrially.
Lepidocrocite (γ – FeOOH)	Lepidocrocite has an orange colour and named after its platy crystal shape (lepidos = scale) and its orange colour (Krokus = saffron). It is often an oxidation product of Fe^{2+} that is found in rocks, soils, biota and rust. It contains the boehmite (γ-AlOOH) structure which is based on the ccp of anions.
Ferrihydrite	Ferrihydrite is a reddish-brown colour that is commonly found in surface environments and is often erroneously termed as "amorphous iron oxide" or "hydrous ferric oxide (HFO)". It is different from other Fe oxides because it exists exclusively as nanocrystals unless stabilized in some way or transforms with time into more stable Fe oxide. Therefore, Ferrihydrite is a vital ancestor of more stable and better crystalline Fe oxides. Ferrihydrite structurally consists

	of hcp anions and is a combination of defect-free and defective structural units. This is a variable composition, especially with respect to OH and H_2O.
Hematite (α – Fe_2O_3)	Hematite is commonly found in rocks and soils and is known as the oldest Fe oxide mineral. It is a blood-red colour (Greek haima mean blood) if finely divided and in coarsely crystalline material it is black or a sparkling grey colour. Hematite has the corundum (Al_2O_3) structure that is centred around on the hcp anion packing. It has similarities to goethite in that it is extremely stable and is commonly the end member of transformations of other Fe oxides. It is a major member of the bonded Fe formations and is an important pigment and a valuable ore.
Magnetite (Fe_3O_4)	Magnetite contains both Fe^{2+} and Fe^{3+}, black in colour and is a ferromagnetic mineral. Magnetite is a vital Fe ore with an inverse spinal structure and together with titanomagnetite is responsible for the magnetic properties of rocks. It is formed in different organisms where it serves as an orientation aid.

2.1.5 Manganese Oxides

Mn is easily oxidized which produces more than 30 known Mn oxide/hydroxide minerals. They can be found as fresh grained aggregates, veins, marine and fresh-water nodules and concretions, crust, dendrites and coatings on other mineral particles and rock surfaces (Post, 1999). The major minerals found in soils are lithiophorite, hollandite and birnessite (Post, 1999). Mn found in soils and sediments easily participate in a range of oxidation-reduction and cation-exchange reactions (Post, 1999). Mn has been extensively studied for the past several decades but identifying the particular mineral(s) in a Mn oxide specimen is still a challenge and as a result scientists report “Mn oxide” instead of a particular mineral (Post, 1999).

Mn geochemically behaves like Mg, Fe, Ni and Co and has the tendency to partition into minerals that form in the early stages of the magmatic crystallization (Post, 1999). Mn can be found in significant quantities in late-stage deposits such as pegmatites (Post, 1999). Mn is highly mobile at Mn^{2+} in acidic aqueous systems and readily depleted from igneous and metamorphic rocks by interaction with surface water and groundwater (Post, 1999).

Mn oxide/hydroxide usually have high adsorption capacities and scavenging capabilities, therefore it provides one of the primary controls of heavy metals and other trace elements in soils and aquatic sediments (Post, 1999). Understanding these controls is key for maintaining and improving fertility of soil, mitigating health affects in humans and animals, and for water treatment for consumption and industrial use (Post, 1999). Due to Mn oxide minerals commonly occurring as coatings and fine-grained aggregates with large surface areas, the chemical influence these oxides have is far out of proportion of their concentrations (Post, 1999). Therefore the presence of tiny amounts of Mn oxide minerals might be acceptable to control the distribution of heavy metals between earth, materials and associated aqueous systems (Post, 1999). Major Mn minerals found in soils are lithiophorite, hollandite and birnessite (Post, 1999). The strong presence of Mn oxides in soils and sediments allows them to easily participate in a range of redox and cation-exchange reactions (Post, 1999). Mn occurs in natural systems in three oxidation states: Mn^{2+}, Mn^{3+} and Mn^{4+}, allowing for a range of multivalent phases (Post, 1999). Mn oxides also show a diverse range of atomic structures of which many can easily be accommodated in a wide collection of other metal cations (Post, 1999). Temperature and chemical conditions as well as biological interactions allow Mn minerals to form and become abundant in most geological systems (Post, 1999). Many Mn oxide minerals are brown to black in colour and mainly found as closely mixed fine-grained, poorly crystalline masses or coatings (Post, 1999).

2.2 Cycling of iron and manganese in an aquifer

In many aquifers, there is a distinct redox zoning with the redox potential becoming increasingly more anoxic the further down you go (Houben, 2003). A fully screened borehole does not only cause a change in the flow field but also a vertical hydro-chemical “short-circuit” for all the hydro-chemical zones (Houben, 2003). In addition, the borehole exposes the water column to atmospheric conditions, therefore, the dissolved Fe and/or Mn mix with dissolved O_2 and NO_3^- which will result in oxide precipitation as seen in Figure 2 (Houben, 2003).

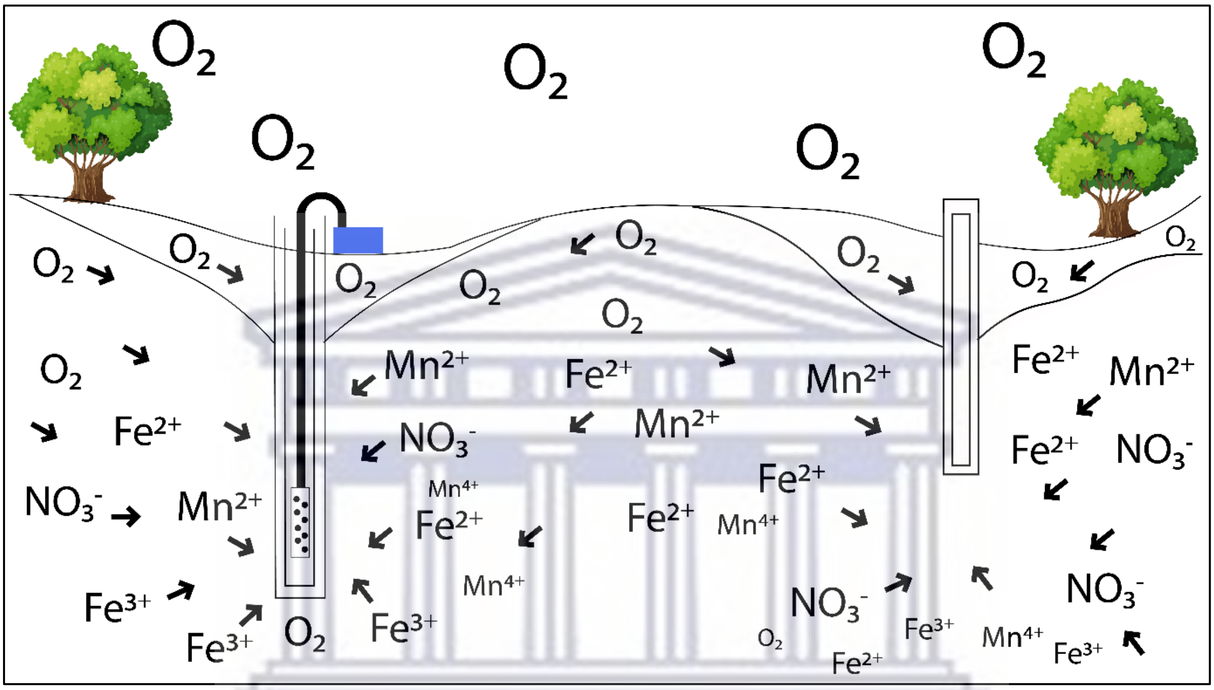

Figure 2: Borehole exposure to atmospheric conditions

Mixing is enhanced by the turbulent flow conditions inside the borehole when pumping takes place (Houben, 2003). Degassing of CO_2 increases the pH which will increase the oxidation of Fe^{2+} and the precipitating oxides have an auto-catalytic effect on the oxidation processes (Houben, 2003). Micro-organisms, especially Fe bacteria such as *Gallionella spp*. play a big role in the natural way of cycling of Fe which takes place between dissolved and precipitated phases at the water sediment interface (Department of Water Affairs and Forestry, 1996). The co-precipitation of trace metals such as arsenic, copper, cadmium and lead can also result in the natural cycling of Fe (Department of Water Affairs and Forestry, 1996).

Pump inlets and screen slots are zones with high velocities which is where the highest rates of scale deposition are commonly found (Houben, 2003). A change in the redox equilibrium between the aquifer and the borehole results in the oxidation of Fe^{2+} and Mn^{2+} and the precipitation of Fe^{3+} and Mn^{4+} in the borehole gravel pack and surrounding aquifer or it forms coatings on the production borehole screen and pump (Smith, 2006). These coatings on the screen and pump will result in the eventual decrease in water quality and quantity (Smith, 2006; Du *et al.*, 2018; van Beek, Hofman-Caris and Zweere, 2020). Figure 2, below, indicates the clogging of a borehole screen and head (van Beek, Hofman-Caris and Zweere, 2020). When concentrations of Fe^{2+} are as low as 0.1 mg/L it may be oxidized in the presence of oxygen to form an oxide coating on water pipelines which may later slough off and subsequently clog geysers, pumping fixtures or even sprinklers (Robey K, 2014).

The amount of incrustation that is found in a borehole varies and this is determined by the hydro-chemical zoning of the aquifer (Houben, 2003). Through camera inspections of the borehole interior, it shows that in most cases incrustations begin to form at the top of the filter screen which is where most of the oxygen enters the well and as time goes on this incrustation will spread to deeper segments, this is indicated by Figure 3 (Houben, 2003).

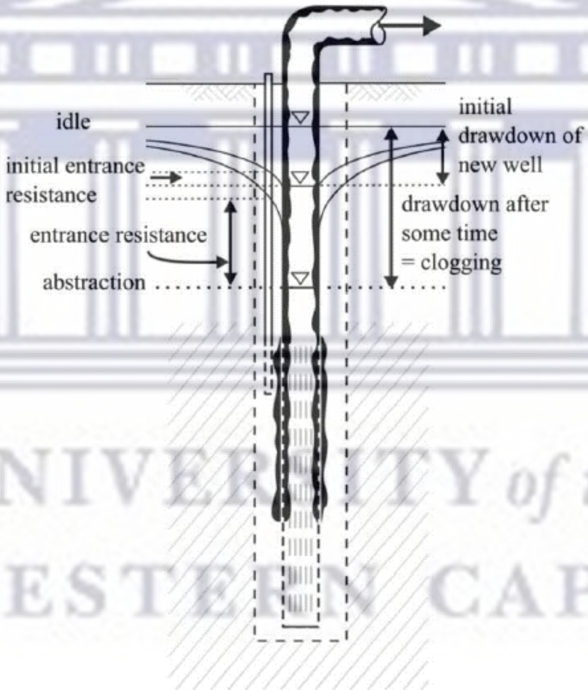

Figure 3: Diagram indicating the clogging of a borehole screen and head (van Beek, Hofman-Caris and Zweere, 2020).

In bank filtrate boreholes the reserve is seen due to the oxic water entering in the deeper parts of the well screen (Houben, 2003). Looking at microscopic thin sections of Fe oxide samples, it shows that the structures resemble annular rings, this indicates that precipitation is repeated continuously with the older layers behaving as a starting point for newer ones to form on (Houben, 2003).

As seen in the German study by Houben (2003) Fe and Mn oxide incrustations can be told apart with Fe being much more abundant than Mn, as a result, they rarely occur together in one well (Houben, 2003). This is due to the various redox potentials required for the formation of these oxides (Fe: ca. 0,0-0,5 V, Mn ca. 0,6-1,2 V) and often the concentration of oxidants mixed in the well is not enough to promote Mn oxidation (Houben, 2003). Another possible reason for Fe and Mn not occurring in the same well is that precipitation of either Fe or Mn occurring in the aquifer itself so that the water entering the well has a deficiency of one of them (Houben, 2003).

A study in Serbia characterized an alluvial setting where oxic and anoxic groundwater blend (Majkić-Dursun, Petković and Dimkić, 2015). High concentrations of DO from the upper, unsaturated part of the aquifer and anoxic groundwater featuring elevated Fe concentration from the deeper saturated part of the aquifer meet and mix (Majkić-Dursun, Petković and Dimkić, 2015). Thorough precipitation of Fe hydroxides found is due to the saturated parts of the aquifer creating a redox front within the borehole screens (Majkić-Dursun, Petković and Dimkić, 2015). Chemical oxidation of Fe^{2+} to Fe^{3+} by oxygen followed by precipitation is a complex process and the oxidation of dissolved Fe^{2+} present in the groundwater to Fe^{3+} has a tendency to be a gradual process (Majkić-Dursun, Petković and Dimkić, 2015). There is a variety of partially oxidized low-crystalline $Fe^{2+} – Fe^{3+}$ intermediate species present in the aqueous solution which is involved in the over-all process (Majkić-Dursun, Petković and Dimkić, 2015). During the time the Fe intermediates could re-crystallize into a range of stable Fe hydroxide end products such as goethite (Majkić-Dursun, Petković and Dimkić, 2015).

The rate of oxidation is directly dependent on the amount of oxygen available in the groundwater (Majkić-Dursun, Petković and Dimkić, 2015). The concentration of dissolved groundwater varies over a wide range due to events that may introduce or remove oxygen, such as river water flowing into the aquifer, removal of oxygen may occur through oxidation of organic matter or adjacent sediments (Majkić-Dursun, Petković and Dimkić, 2015). Other reasons for the variation in oxygen content is due to; the setting of submergible pumps into the screen slot, the declining of static and dynamic groundwater levels into the casing interval, an unsuitable pump work scheme, aquifer recharge mode and the introduction of the piezometric heads into the screen slots which further leads to the groundwater being exposed to atmospheric conditions. (Majkić-Dursun, Petković and Dimkić, 2015). The concentration of Fe present in groundwater is the most important factor for the formation of encrustations (Majkić-Dursun, Petković and Dimkić, 2015). Therefore, groundwater from the deeper parts of the aquifer is anoxic and Fe is present as Fe^{2+} which comes into contact with oxygen which will rapidly oxidize to Fe^{3+} (Majkić-Dursun, Petković and Dimkić, 2015).

Unconsolidated Aquifers - Thick sediments associated with rivers and coastal regions are unconsolidated sediments which include many of the world's most important aquifers (Morris *et al.*, 2003). Due to large volumes of groundwater being stored in them, large quantities of water are pumped from these aquifers for water supply and irrigation (Morris *et al.*, 2003). Unconsolidated aquifers are almost invariably stratified, with permeable layers (sand or gravel) separated by less permeable layers (silty or clayey strata) and some in discontinuous layers or lenses (Morris *et al.*, 2003). There is great potential for dilution to take place as both the aquifers and intervening aquitards in these systems have high porosities (Morris *et al.*, 2003). These aquifers may have complex flow patterns because the stratification can produce significant vertical head gradients which facilitates movement from one layer to the next, once pumped (Morris *et al.*, 2003). However, the flow velocities both vertically and laterally are usually low which generally makes the microbiological quality excellent, unless at very shallow depths and where the contaminant load is very high, such as beneath cities (Morris *et al.*, 2003). The slow travel time implies a long contact time with the sediment and in certain aquifers it can result in mineralization of water due to increased dissolution of the rock matrix taking place (Morris *et al.*, 2003). In summary the solute content is variable and dependent on the residence time, composition of the aquifer matrix, physiochemical processes and these formations may also be susceptible to problems caused by pumping (Morris *et al.*, 2003).

Clay, Sandstone and Sedimentary Aquifers (Potentially Fractured) - One of the most important sources of Fe in groundwater is from clayey and carbonate deposits (Diliūnas and Jurevičius, 2006). The concentration of Fe in water with a low oxygen content is determined mainly by the solubility of Fe carbonate (Diliūnas and Jurevičius, 2006). Around 40 – 60% of Fe migrates through aquifers as Fe^{2+} ions, which are usually in equilibrium with the Fe carbonate system (Diliūnas and Jurevičius, 2006). Along with Fe^{2+} other compounds and ions that take part in this equilibrium system are CO_2, H_2CO_3, H^+, HCO_3^-, CO_3^{2-} (Diliūnas and Jurevičius, 2006).

The following carbonate equilibrium can describe their state of occurrence (Diliūnas and Jurevičius, 2006):

CO_2 (atmospheric)

$\updownarrow$

CO_2 (in water) + $H_2O \longleftrightarrow H_2CO_3 \longleftrightarrow H^+ + HCO_3^- \longleftrightarrow 2H^+ + CO_3^{2-}$

$FeCO_3$ (in sediments) + CO_2 (in water) + $H_2O \longleftrightarrow Fe^{2+} + CO_3^{2-}$

$\updownarrow$

$FeCO_3$ (in rocks, deposits)

In closed hydrogeological systems, with increasing the confinement level of aquifers the reductive conditions gradually develop resulting in the content of CO_2 and organic matter as well as the number of Fe bacteria to increase (Diliūnas and Jurevičius, 2006). Organic matter is rapidly consumed by oxygen during oxidation, making its residual content in water below 0.5 mg/L, i.e. 3-7 times lower than the Fe concentration (Diliūnas and Jurevičius, 2006). A chain reaction takes place when there is a change in a component of a system (Diliūnas and Jurevičius, 2006). Groundwater is separated from the Fe source during abstraction, as a result, the carbonate equilibrium is disrupted and Fe is partly precipitated as $FeCO_3$ (Diliūnas and Jurevičius, 2006). Consolidated sedimentary aquifers are vital aquifers and are found worldwide within consolidated sedimentary strata (principally sandstone and limestone) (Morris *et al.*, 2003). Certain sandstones maintain a primary porosity and are normally of low to moderate permeability (Morris *et al.*, 2003). Older formations contain cemented sandstones where the primary porosity is highly variable and depending on the degree of cementation, the rocks can range from friable to highly indurated (Morris *et al.*, 2003). However, in the latter, it is the secondary or fractured porosity that provides the aquifer permeability and storage (Morris *et al.*, 2003).

Pumping Regime - Unsuitable and unsustainable pumping scheme produces a general decline in groundwater levels and causes a disturbance to the geochemical conditions of the initial system (Majkić-Dursun, Petković and Dimkić, 2015). During such conditions the anoxic groundwater becomes oxidized, while the groundwater composition and microbial ecology are changed and the rate of precipitation of low-crystalline Fe hydroxides have a catalytic effect on the oxidation of Fe^{2+} (Majkić-Dursun, Petković and Dimkić, 2015). Over exploitation is defined as the situation in which the average rate of aquifer abstractions is greater than or close to the average recharge rate of the aquifer (Majkić-Dursun, Petković and Dimkić, 2015). Over-exploitation of groundwater implies intensive use of groundwater which has multiple results such as the declining groundwater levels in then wells and the extended area of the source, changes in hydraulic gradients, changes in aquifer recharge regime, reduced discharges of natural springs and variations in the oxic state and groundwater quality (Majkić-Dursun, Petković and Dimkić, 2015).

A case study in Lithuania on the formation of Fe compounds in the quaternary groundwater indicated that the main factors determining the formation and stability of Fe compounds in groundwater is the aquifer-atmosphere interaction, i.e. the degree of confinement of a water-bearing system (Diliūnas and Jurevičius, 2006). There are three identified types of hydrogeological systems: open, semi-opened and a closed system (Diliūnas and Jurevičius, 2006). Open hydrogeological systems are made up of shallow sand, gravel aquifers, aquifer complexes in river valleys and watershed areas (Diliūnas and Jurevičius, 2006). Lithuania is dominated by calcium-magnesium-bicarbonate water type in all of its hydrogeological systems (Diliūnas and Jurevičius, 2006). With the increase in confinement of the aquifer there is an increase in the salinity, the concentration of dissolved chemical components and the number of Fe bacteria, however, the concentration of DO goes down (Diliūnas and Jurevičius, 2006). As a result, in closed hydrogeological systems the oxidation conditions deteriorate with Fe concentrations increasing (Diliūnas and Jurevičius, 2006). Based on Fe speciation and its stability in groundwater, three characteristic hydrogeological and hydrogeochemical groups can be categorized:

(1) Aquifers made of marine sediments which are rich in organics.

(2) Aquifers in watershed areas made of fluvial glacial deposits which are recharged by atmospheric precipitation.

(3) Alluvial aquifers which abstract water therefore mainly being recharged by river water.

2.2.1 Iron in aquifers

As pH and redox conditions change in an aquifer Fe is cycled between sources and sinks (Smith and Roychoudhury, 2013). The Fe is sourced from minerals within the aquifer and under reducing conditions or low pH it is mobilized (Smith and Roychoudhury, 2013). By introducing oxygen or an increase in pH in the system it will cause Fe to precipitate within the aquifer (Smith and Roychoudhury, 2013). The source minerals of Fe in groundwater is dependent on the rock-type of the aquifer (Smith and Roychoudhury, 2013). In crystalline rocks, Fe^{2+} is present in mafic minerals such as amphiboles, pyroxenes, olivine and biotite (Smith and

Roychoudhury, 2013). Mafic materials weather incongruently to form clay minerals such as kaolinite because they are not in equilibrium with earth surface conditions (Smith and Roychoudhury, 2013). Fe^{2+} present in mafic minerals is oxidized and precipitates Fe hydroxide during the weathering reaction (Smith and Roychoudhury, 2013). Sedimentary rocks are where Fe is present as Fe^{2+} bearing oxides (magnetite, ilmenite), sulphides (pyrite) and carbonates (siderite), or Fe^{3+}- bearing oxides (e.g. haematite, goethite, ferrihydrite, lepidocrocite), which is dependent on the redox environment of deposition of the sedimentary rock (Smith and Roychoudhury, 2013). Fe is also found to be present in clay minerals, chlorite and glauconite contain Fe as part of their structural formula, but Fe can be substituted into clay minerals such as smectite and illite (Smith and Roychoudhury, 2013). In certain cases, Fe in the silicate minerals has been found to be a more important source of Fe than Fe oxide minerals such as ilmenite and magnetite (Smith and Roychoudhury, 2013).

For controlling Fe concentrations in groundwater Fe sinks are more important than the source mineral of Fe (Smith and Roychoudhury, 2013). Fe^{2+} oxidized during the weathering of unstable silicate minerals precipitates as amorphous Fe hydroxide which will recrystallize and "ages" to more stable phases over time (Smith and Roychoudhury, 2013). The order that Fe oxide increases in its stability are from amorphous (ferrihydrite) to lepidocrocite, magnetite, goethite and finally hematite (Smith and Roychoudhury, 2013). In reducing conditions the Fe^{2+} containing minerals such as siderite and Fe sulphide control Fe solubility (Smith and Roychoudhury, 2013). Where the sulphate concentrations are low, siderite is expected to be important (Smith and Roychoudhury, 2013). Sulphate reduction can occur in aquifers with available organic carbon and sulphate which results in the initial formation of H_2S and later in the precipitation of Fe sulphide minerals, such as marcasite or pyrite (Smith and Roychoudhury, 2013).

The degree of oxygenation of the groundwater is another controlling factor of the cycling of Fe between sources and sinks (Smith and Roychoudhury, 2013). Water recharging the aquifer is oxygenated although oxidation of organic carbon in the water and organic carbon encountered along the flow path consumes the oxygen in the water (Smith and Roychoudhury, 2013). Oxygen is consumed during weathering reactions (Smith and Roychoudhury, 2013). Organic carbon oxidation reactions require alternate electron acceptors once the oxygen is depleted, electron acceptors are used in order of decreasing energy released, i.e. NO_3, MnO_2, $Fe(OH)_3$, SO_4, CO_2 and H_2 (Smith and Roychoudhury, 2013).

Dissimilatory Fe-reduction is a process where a reduction of Fe^{3+}-bearing minerals to release Fe^{2+} into groundwater is generally coupled with the oxidation of dissolved organic carbon by bacteria (Smith and Roychoudhury, 2013). Zones of different reactions that are not mutually exclusive can shift with time due to a redox gradient developing away from the recharge zone (Smith and Roychoudhury, 2013). A redox zonation develops at the discharge point in the aquifer where oxygen diffuses into it to a limited extent (Smith and Roychoudhury, 2013). Soluble Fe^{2+} oxidizes to Fe^{3+} and precipitates as $Fe(OH)_3$ in the presence of oxygen (Smith and Roychoudhury, 2013). Over short time intervals in a redox boundary, cycles of mobilization and immobilization of Fe can take place, this determines the spatial pattern of Fe distribution (Smith and Roychoudhury, 2013).

2.2.2 Manganese in aquifers

Differences in the concentration of Mn found in groundwater can be caused by various geology, nature of Mn present in the aquifer geology and the physicochemical conditions found in the aquifer (Homoncik *et al.*, 2010). More investigations need to be done on this theory by using sufficient rock chemistry data (Homoncik *et al.*, 2010). The natural background of Mn in soils ranges from <1 to 4000 $mg.kg^{-1}$ with mean values of 200 to $600mg.kg^{-1}$ (Trollip, Hughes and Titshall, 2013). Soil is not the only source of Mn in the aquifer, Mn can enter from direct atmospheric deposition, wash-off from plants and other surfaces, leaching from plant tissue and the decomposition of organic material (Trollip, Hughes and Titshall, 2013). The solubility of Mn is controlled by two major variables which are similar to Fe, pH and the redox potential (Trollip, Hughes and Titshall, 2013). Mn is found in soil in three common valence states Mn^{2+}, Mn^{3+} and Mn^{4+} (Trollip, Hughes and Titshall, 2013). Mn leaches into groundwater, particularly Mn^{2+}, as it is a primary plant micronutrient and the concentration increases in the soil as the pH drops below 5.5 (Trollip, Hughes and Titshall, 2013).

2.3 Iron encrustation and iron-related clogging

Different encrustations occur in boreholes, these include Fe hydroxides, Fe sulphides, Fe carbonates and Mn oxides (Smith and Roychoudhury, 2013). The most common form of encrustation is Fe hydroxide which differs according to their mineralogy, crystallinity and chemistry (Smith and Roychoudhury, 2013). The solution from which the oxide precipitates from, particularly the Fe^{3+} and Fe^{2+} concentrations, temperature, ionic strength, pH, Eh and ionic composition affect the crystallinity, chemistry, particle size, morphology, colour and surface properties of natural Fe oxides (Smith and Roychoudhury, 2013). The commonly found

Fe hydroxide minerals responsible for encrustation are ferrihydrite, goethite and haematite. Fe oxides found in the natural environment are less crystalline than synthetic Fe oxides (Smith and Roychoudhury, 2013).

2.3.1 Borehole iron encrustation

Introduction of oxygen into groundwater via a borehole forms an anoxic-oxic boundary which facilitates Fe encrustation (Smith and Roychoudhury, 2013). This introduction of oxygen into groundwater results in the oxidation of Fe^{2+} to Fe^{3+}, which usually takes place within the sub-oxic zone of the aquifer (Smith and Roychoudhury, 2013). Fe^{3+} in near-neutral pH conditions (6.3-6.8) is insoluble and precipitates as an Fe oxide mineral, these Fe oxide minerals fill pore spaces surrounding the borehole, in the aquifer (Smith and Roychoudhury, 2013). Fe precipitation is further enhanced by the increase of pH, this takes place through boreholes exposing the water column to atmospheric conditions, resulting in penetration of DO into the well and diffusion into groundwater as well as degassing of CO_2 leading to an increase in pH (Smith and Roychoudhury, 2013). Boreholes form a “short-circuit” between the oxidized water in the upper formations of an aquifer, which may result in the mixing and aeration by physical cascading of water from the upper and lower formation of the aquifer (Smith and Roychoudhury, 2013). Cycling of Fe and sulphur are interlinked, therefore, changes in sulphate concentrations are commonly associated with borehole encrustations, possibly due to Fe sulphides minerals in the aquifer being oxidized (Smith and Roychoudhury, 2013). Fe oxidation occurs in the sub-oxic zone of the redox gradient in an aquifer, while sulphide oxidation will take place in the adjacent anoxic zone (Smith and Roychoudhury, 2013). It has been observed in borehole cores from the Table Mountain Group (TMG) that joints and fractures are filled with Fe sulphide minerals (Smith and Roychoudhury, 2013). Borehole conditions with low DO concentrations are expected to have a rate of chemical Fe oxidation far slower than what has been previously observed (Smith and Roychoudhury, 2013). Biological oxidation/precipitation of Fe oxides is 1000 times faster than chemical oxidation/precipitation (Smith and Roychoudhury, 2013). Fe encrustation is closely linked to the process of biofouling which is the formation and deposition of mineral sessile bacterial colonies, also known as biofilms, within the borehole (Smith and Roychoudhury, 2013). Biofouling is believed to be responsible for the Fe encrustation in the TMG and the Atlantis aquifers (Smith and Roychoudhury, 2013; Robey, Tredoux and Chevallier, 2014).

2.3.2 Iron and manganese biofouling

Biofouling is the clogging of a borehole which is caused by the accumulation of bacterial cell bodies, formations of extra-cellular polymers (ECP, slimes) and microbial catalysed oxidation (Smith and Roychoudhury, 2013). This leads to the precipitation of Fe oxides, in the boreholes and the pore spaces of the aquifer (Smith and Roychoudhury, 2013). A biofilm layer is where microorganisms attach to submerged surfaces, it is a complex heterogeneous assemblage of cell clusters, extra-cellular polymers, pores and conduits (Smith and Roychoudhury, 2013). The biofilm lifecycle starts with the colonization of surfaces by non-filamentous bacteria, this provides an organic substrate for the growth of filamentous Fe bacteria (Smith and Roychoudhury, 2013). This is followed by the maturation of the biofilm into a group of species of bacteria (Smith and Roychoudhury, 2013). Different bacterial species are arranged within the biofilm so that different metabolic types contribute optimally to the whole ecosystem (Smith and Roychoudhury, 2013).

Fe biofouling of boreholes is favoured in conditions with high concentrations of Fe^{2+}, phosphorus, other nutrients, organic substrate and pH values in the near-neutral range (Smith and Roychoudhury, 2013). Water velocities of about 1 mls enhance nucleation and precipitation of Fe and nutrient uptake, also limiting scouring of the biofilm (Smith and Roychoudhury, 2013). Another favourable condition is the presence of a steep redox gradient and a boundary between the oxic and anoxic water as found within boreholes (Smith and Roychoudhury, 2013). Fe oxidizing bacteria are commonly found where anoxic water containing elevated concentrations of Fe^{2+} approaches an area with higher DO concentrations, such as the outflow of a spring or a borehole (Smith and Roychoudhury, 2013).

Three main groups are involved in biofouling which are Iron Related Bacteria (IRB), Slime Forming Bacteria (SFB) and Sulphate Reducing Bacteria (SRB) (Smith and Roychoudhury, 2013). SFB are commonly found and produce large amounts of ECP (Smith and Roychoudhury, 2013). In more reducing areas of an aquifer which is further away from oxygen sources, SRB are found (Smith and Roychoudhury, 2013). If organisms catalyse the oxidation of Fe^{2+} or change the water chemistry of the borehole to favour Fe oxidation, it can be considered to be IRB (Smith and Roychoudhury, 2013).

Two major components which have been given a large amount of attention dur to their dominant and observable presence in slimes is Fe and Mn (Cullimore, 1999). Environments that are relatively rich in DO are exposed to transient amounts of Fe and Mn present in the water and therefore commonly form slimes that are orange, red and brown in colour

(Cullimore, 1999). IRB is the dominant group of bacteria found in this slime (Cullimore, 1999). The bacteria found within this slime has unique properties which allow them to take up Fe and Mn in excessive amounts (Cullimore, 1999). The excess Fe or Mn is either deposited around the cell, within the slime or in special structures protecting or extending from the cells (Cullimore, 1999). Thereafter they are further deposited as different oxides and/or hydroxides (Cullimore, 1999). The precise combination of the oxides and hydroxides will determine an orange, red or brown slime as the bio-accumulated concentration increases (Cullimore, 1999). Deposits rich in Fe and Mn appear to perform a few roles from being protective against predation and physical disruption to serving as a nutrient reserve (Cullimore, 1999). Due to these slimes forming sites that consume large amounts of oxygen it may allow anaerobic bacteria to survive and grown within those parts of the slime where oxygen is absent (Cullimore, 1999). Consequently, when these slimes shift to a black phase it is indicative that there is an oxygen depletion in the environment (Cullimore, 1999).

Water that is exposed to this slime suffer from a great disadvantage in that bacteria will slough off from the slime into the water in an irregular manner (Cullimore, 1999). These events of sloughing off occur in a random pattern from the slime which causes a variable population to be recorded in the water over a period of sampling (Cullimore, 1999). Water generates a very distinct pigmentation when shearing occurs which can be easily seen (Cullimore, 1999). Field experiments conducted to date indicate that iron tends to accumulate in biozones 1 and 2, close around the well (Cullimore, 1999). However, Mn tends to be more diffusively distributed through all of the active biozones (Cullimore, 1999). Sites of Mn and Fe bioaccumulation appear to be around and in microbial cells which is relatively defined (Cullimore, 1999). These sites of bioaccumulation can either be (Cullimore, 1999):

(1) Extruded in an ECP substance forming a twisted ribbon from the cell (i.e., *Gallionella*).

(2) Accumulation occurs inside a defined sheath formed around a group of microbial cells.

(3) Accumulation occurs on the outside of the sheath which forms a tube around a few microbial cells.

(4) Accumulation occurs randomly in and around the polymeric slimes which encompasses a few microbial cells.

(5) Accumulation takes place into the microbial cells directly.

Borehole clogging due to biofouling is caused by the biofilm occupying a sufficient volume within the interstitial spaces to cause a restriction in the flow to water into the well (Cullimore, 1999). These restrictions can take place in three ways (Cullimore, 1999):

(1) The interstitial spaces can be filled with the biofilm formation which can directly restrict flow.

(2) The biofilms surface sloughing off can cause shearing of polymerics from the biofilm which increase the resistance to hydraulic flow.

(3) Gas which evolves may remain entrapped which can form a barrier.

(4) Water may additionally accumulate and become entrapped within the biofilm which may cause a radical increase in the volume of the biofilm, therefore, initiating and occlusion of the interstitial spaces.

As a result of a combination of the above mechanisms the restriction of hydraulic flow may occur which can either result in partial or complete clogging of the borehole (Cullimore, 1999).

Biofouling is influenced by groundwater temperatures, however, the variance in groundwater temperature is at a much lower order of magnitude than for surface waters (Cullimore, 1999). Surface temperatures can experience significant daily shifts in temperature (e.g., > +1 / -2°C per 24-hour period) and radical seasonal variations, especially in temperate zones (Cullimore, 1999). However, when looking at groundwater, the seasonal variations may range from as little as 0.5 to 1°C (Cullimore, 1999). In shallower wells the fluctuations can be as high as 5°C, seasonally (Cullimore, 1999). Therefore, microorganisms that can grow efficiently at ambient temperatures without experiencing major daily changes will dominate the type of microbial colonization likely to occur within a groundwater system (Cullimore, 1999). The act of pumping, it is likely that the cause of temperature shifts, this moves water towards the well from different depths where a temperature gradient may cause an elevation of the water temperature arriving at the well. In addition, the heat that is generated by pumping may itself be the cause for the temperature increase (Cullimore, 1999). Psychrotrophic bacteria (able to grow at below 15°C) or mesotrophic bacteria (able to grow within temperatures of 15 - 45°C) are most likely to be continuously supported throughout the year due to the narrow range of operating temperature which occurs in groundwater (Cullimore). Seasonal fluctuations reported for surface-waters are therefore not applicable to the microbial activities which take place in groundwater (Cullimore, 1999).

Organic material is also involved in biofouling and may arrive at the sites where biofouling takes place in one or two forms (Cullimore, 1999). The first form is the dissolved form and the second is suspended in a particulate mass moving through the water system (Cullimore, 1999). Assimilation occurs through the shifting of the dissolved organics into the mobile particulate state as the groundwater moves closer to the zone of influence that the well is generating in the surrounding groundwater (Cullimore, 1999). A few interactions begin to take place once the organic material arrives in the biozones surrounding the well (Cullimore, 1999). This can either result in the adsorption of the materials into the biofilm known as bioaccumulation or the degradation of the compounds from the aqueous phase known as biodegradation (Cullimore, 1999). There are a few ways that organic materials can enter the biological systems after entering the biozones resulting from influences in the water well (Cullimore, 1999). This may include:

(1) Passive accumulation of organic material within the polymeric matrices of the biofilm.

(2) Active accumulation of organic material within the viable cells with subsequent degradation.

(3) Utilizing synthetic and energy-generating functions.

2.3.3 Management strategies

Aquifer clogging has been an issue frequently raised as early as the 1970's (van Halem *et al.*, 2010). Iron oxidation requires the presence of oxygen and due to this, most wellfield management strategies are developed to reduce oxygenation of groundwater (Smith and Roychoudhury, 2013). Redox reactions of groundwater are done through different methods such as minimizing drawdown by reducing pumping rates and extending pumping times (Smith and Roychoudhury, 2013). The reduced pumping rate also limits the supply of nutrients to organisms, this can deplete oxygen in water if organisms are using oxygen as an electron acceptor (Smith and Roychoudhury, 2013). Prevention of oxic and anoxic water mixing from two different horizons within the well by sealing off oxygenated water strikes (Smith and Roychoudhury, 2013). Avoiding the water level to drop below the top of the screen through pumping, by correct screen placement and not over-pumping of the borehole (Smith and Roychoudhury, 2013). Installation of systems to prevent oxygen entering the borehole entirely, an example of this is keeping the borehole filled with nitrogen gas (Smith and Roychoudhury, 2013). The accurate placement of screens is vital in minimizing oxygen introduction into the borehole (Smith and Roychoudhury, 2013). Borehole construction material, PVC or steel, can influence the rate of encrustation as well as how easily the borehole can be cleaned (Smith and Roychoudhury, 2013).

Part of the management of Fe oxide encrustation is monitoring parameters which can predict the onset of biofouling, such as the concentrations of Fe and nutrients in the borehole (Smith and Roychoudhury, 2013). In Europe anticipated Fe oxidation is used by pumping oxygenated water into the well or into the boreholes surrounding the main production borehole (Smith and Roychoudhury, 2013). Fe oxidation and precipitation occurs in the aquifer away from the main borehole that will be pumped, once this is done, Fe-free water is pumped from the borehole (Smith and Roychoudhury, 2013). It has been found that the permeability of the aquifer reduces slightly due to the volume of aquifer being affected by injected oxygenated water is large (Smith and Roychoudhury, 2013). Once a borehole is clogged, the management of pumping rates or monitoring of well chemistry will not improve the condition of the borehole, this calls for the implementation of rehabilitation procedures (Smith and Roychoudhury, 2013).

2.3.4 Rehabilitation methods

Clogged boreholes or biofilms are hard to treat, both mechanical and chemical methods are currently being used as rehabilitation methods but there is still no 100% effective rehabilitation method (Smith and Roychoudhury, 2013). Conventional methods of removing Fe from water supplies includes applying common water treatment processes of coagulation with line or alum, followed by settlement and filtration (Department of Water Affairs and Forestry, 1996). Another way of removing Fe from water is by using the oxidation process which converts Fe into an insoluble hydroxide or hydrated oxide which is removed through filtration (Department of Water Affairs and Forestry, 1996). The following various treatment approaches are used, addition of lime to water which will raise the pH of it, thus facilitating the oxidation of Fe by the air in the water which is followed by settlement of Fe oxide (Department of Water Affairs and Forestry, 1996). Chemical oxidation of water can be done by dosing the water with chlorine, hydrogen peroxide, ozone or other strong oxidants. Industrially, chlorine is commonly used as the chemical oxidant although after the treatment, high levels of residual chlorine should be avoided as it may interfere with the quality of water (Department of Water Affairs and Forestry, 1996). Aeration of water by devices such as fountains, cascades or mechanical aeration (Department of Water Affairs and Forestry, 1996). Industrial scale removal of Fe requires close monitoring due to the consequences of incomplete treatment which may be severe (Department of Water Affairs and Forestry, 1996). For efficient iron removal and treatment, it is important to determine both the total and dissolved iron species and their relative concentrations (Department of Water Affairs and Forestry, 1996).

Mechanical rehabilitation involves the physical breaking down of Fe oxide precipitates from the borehole walls (Smith and Roychoudhury, 2013). This can be done by wire brushing, water jetting to wash off loose deposits, surge and purge procedures using water or gases like carbon dioxide, steam cleaning to obtain well temperatures of 60° -70°C, using a sonar jet, or a vibratory explosive (Smith and Roychoudhury, 2013). In certain extreme cases calcium hypochlorite is placed in the borehole followed by throwing in a stick of dynamite (Smith and Roychoudhury, 2013).

Chemical rehabilitation is focused on controlling bacterial populations within the borehole by using chemicals to sterilize the borehole and dissolve the Fe encrustations in the well (Smith and Roychoudhury, 2013). To mineralize organic matter, strong oxidizing agents are used, e.g. hydrogen peroxide: $C(H_2O) + 2H_2O_2 = CO_2 + 3H_2O$ (Smith and Roychoudhury, 2013). Some other examples are sodium hypochlorite, calcium hypochlorite, chlorine dioxide, chlorine gas and potassium permanganate (Smith and Roychoudhury, 2013). Disadvantages of using these chemicals are that they will oxidize Fe^{2+} and Cl containing oxidizers e.g. hypochlorite and combine with dissolved organics to form chlorinated hydrocarbons (Smith and Roychoudhury, 2013). Organic and inorganic acids such as hydrochloric, citric, acetic, sulphamic and sulphuric acids dissolve Fe oxide minerals by the process of assisted dissolution: $Fe\ OOH + 3H^+ = Fe^{3+} + 2H_2O$ (Smith and Roychoudhury, 2013). Acid dissolution reactions are optimal at $pH<<2$ values (Smith and Roychoudhury, 2013). The acids used require neutralization after rehabilitation has occurred in order to prevent corrosion (Smith and Roychoudhury, 2013). Complexing agents, example oxalate, by the process of ligand-controlled dissolution (Smith and Roychoudhury, 2013). The disadvantage of organic molecules is that they can lead to secondary microbial pollution (Smith and Roychoudhury, 2013). Reducing agents such as ascorbic acid, sodium dithionite bring insoluble Fe^{3+} into solution through the process of reduction: $2FeOOH + NaS_2O_4 + 4H^+ = 2Fe^{2+} + 2Na^+ + 2HSO_3^- + 2H_2O$ (Smith and Roychoudhury, 2013). Effective reducing agents which are able to dissolve ferrihydrite and goethite quickly are Na-diothionite and oxalic acid (Smith and Roychoudhury, 2013). A combination of reducing and complexing agents increase how effective the rehabilitation is (Smith and Roychoudhury, 2013). Many chemicals can successfully dissolve ferrihydrite but are unsuccessful with dissolving goethite (Smith and Roychoudhury, 2013). It is believed by certain authors that regular bacterial disinfection of boreholes can slow down biofouling by retarding bacterial growth (Smith and Roychoudhury, 2013). None of the above-mentioned methods are effective in all cases, therefore, it is vital to understand the causes and types of encrustation before rehabilitation is attempted (Smith and Roychoudhury, 2013).

Since the 1970’s in Europe, subsurface Fe removal has been implemented, however, the technology has not yet been widely applied elsewhere (van Halem *et al.*, 2010). A common method, in-situ iron removal (ISIR) takes place in the aquifer, therefore not as visible and as conventional as aboveground rapid sand filtration, which is a cause for concern when it comes to long-term sustainability (van Halem *et al.*, 2010). Despite Fe clogging being an issue that has been frequently raised, the literature agrees that clogging of the aquifer does not pose a serious threat to subsurface iron removal (van Halem *et al.*, 2010). The lack of aquifer clogging has been proposed to be caused by:

(1) The decreasing of porosity with time which leads to further infiltration of injected water into the aquifer.

(2) Fe precipitating at different infiltration distances which may vary depending on the size of the oxidation zone.

(3) Fe deposits are most formed in dead-end pores or stagnant zones.

(4) The transformation of voluminous amorphous Fe hydroxides to less voluminous crystalline hydroxides.

ISIR is a strong and sustainable Fe and Mn removal method because it is fast, simple and, cost-effective processes (Robey, 2014). ISIR can increase production borehole longevity, reduce the application for ex-situ treatment which may be costly, generate sludge and use large amounts of water and electricity (Robey, 2014). ISIR can be easily applied to wellfields both large and small as well be designed to be mobile (Robey, 2014). Several different ISIR designs may be implemented but four main methods are used which are, the Vyredox method, single borehole method, two-production borehole method and the combination of the Vyredox and single borehole method (Robey, 2014). The Vyredox method which is commonly used consists of a production hole being surrounded by a ring or semi-circle of multiple injection well-points (e.g., between 2 – 23) which provides an oxidation screen that Fe and Mn-free groundwater is drawn to and pumped from the production borehole (Robey, 2014). The Netherlands typically makes use of the single borehole method where a production borehole is modified to alternation between production and injection (Robey, 2014). The two-production borehole method makes use of two modified production boreholes which are equipped for both injection and abstraction, the one borehole produces water for recharge for the borehole being treated (Robey, 2014). In ISIR the raw groundwater and injected water quality dictate the involvement of cation exchange, for example it will increase with higher sodium ions present in the water being injected but decreases in the presence of other cations in the groundwater (Robey, 2014). For cation exchange to work in ISIR it depends on the exchangeable Fe^{2+} on the aquifer sediment grains, this in turn is dependent on sorption capacity of the aquifer, which in turn is dependent of the presence of organic matter, oxides and clay (Robey, 2014).

The application of ISIR requires the understanding of hydraulic parameters within the study area because a setting with high transmissivity is best-suited for only in-situ treatment (Robey, 2014). This is necessary because the mounding effect is caused by the injection of a volume of water that is smaller (i.e., the water dissipates faster into the aquifer), unlike in a low transmissivity aquifer which could limit the injection volume or rate of injection by pressure build-up (Robey, 2014). The hydraulic conductivity is another important hydraulic parameter as it provides information on the aquifers ability to “accept” a certain volume of water at a given injection rate (Robey, 2014). Having information on the sustainable yield is important as it provides estimates of the rate of injection that the ISIR test can be conducted at (Robey, 2014).

ISIR methodologies have been proven to be the most effective technique when it comes to the removal of high concentrations of Fe and Mn accumulates in groundwater (Robey, 2014). When it comes to the removal efficiency (V/Vi) the ISIR is a great disadvantage over normal ex-situ treatments as it is estimated by the volumetric ratio of abstracted volume (V) over the injected volume (Vi) (Robey, 2014). ISIR efficiency ratios can range from 2 to 5 depending on the hydrogeological conditions, water quality and set threshold concentration values (Robey, 2014).

Boester and Martinell (1988) investigated the Fe hydroxide deposits near subsurface treatment wells and were unable to microscopically identify any severe precipitation at the oldest Swedish build plant in 1971 (van Halem *et al.*, 2010). The adsorptive-catalytic oxidation mechanism would suggest that the formation of neatly ordered Fe hydroxides, rather than voluminous amorphous Fe sludge (van Halem *et al.*, 2010). Processes such as cation exchange, recrystallization and interfacial electron transfer have been proposed to occur during subsurface Fe removal, therefore resulting in different hypotheses on Fe precipitation with time (van

Halem *et al.*, 2010). After 12 years of the plant being used, Fe was found to accumulate at specific depths near the subsurface Fe removal wells (van Halem *et al.*, 2010). It is unknown if it was due to preferred flow paths, or geochemical/mineralogy conditions or if subsurface Fe removal favoured certain soil layers (van Halem *et al.*, 2010). Most of the Fe accumulated was characterized as crystalline which suggests that precipitated amorphous Fe hydroxides have transformed to Fe hydroxides of higher crystallinity (van Halem *et al.*, 2010). These crystalline and compact Fe hydroxides have not noticeably clogged the investigated well and/or between the years 1996 and 2008 (van Halem *et al.*, 2010). As drawdown increases slower than in normal production wells the subsurface Fe removal wells need even less frequent rehabilitation (van Halem *et al.*, 2010). Along with iron, other groundwater constituents such as Mn, As and Se were found to accumulate (van Halem *et al.*, 2010).

2.4 Methods used for sampling iron

2.4.1 Measuring iron and manganese

Cases which investigate Fe clogging as a problem or groundwater affected by acid mine drainage look at the measurement of difference redox states of Fe separately (Fe^{2+} and Fe^{3+}) (Weaver *et al.*, 2004). These cases also require the Eh and pH data for further understanding of the problems being investigated (Weaver *et al.*, 2004). Due to Fe^{2+} oxidizing to Fe^{3+} in the presence of oxygen it is important to conduct the analyses as soon as possible after sample collection or preferably to analyse the Fe species in the field, if the equipment is available (Weaver *et al.*, 2004). Supplies such as Hach or Merck have test kits available for Fe^{2+} and Total Fe determination at different concentration ranges and levels of accuracy (Weaver *et al.*, 2004). The colormetric technique which is the common analysis used is based on using reagents that form a coloured complex with Fe^{2+} (Weaver *et al.*, 2004). Two samples are used, one that is analysed directly for Fe^{2+} and the second sample that is digested and treated with a reducing agent followed by the analysis for Total Fe. Fe^{3+} is calculated by subtracting Fe^{2+} from Total Fe (Weaver *et al*., 2004). To directly determine Fe^{3+} a method has been determined which uses a selective complexing agent called acetohydroxamic acid that provides a more accurate speciation result (Weaver *et al*., 2004). To determine the colloidal and dissolved fraction of each redox species of Fe, filtered or unfiltered samples may be used (Weaver *et al.*, 2004)

2.4.2 Importance of Field Determinants

Chosen determinants are analysed at the well head during the sample run for three reasons:

1. To obtain reliable values of those determinants that will change in the bottle once sampling has finished.
2. To check the effectiveness of purging.
3. To provide values that may be needed to decide on the sampling sequence immediately during the sample run or to decide on the sampling procedure. (Weaver *et al.*, 2004)

Once groundwater is removed from its natural environment and brought to the surface, several water quality related determinants undergo changes due to oxygen, aeration and degassing which takes place (Weaver *et al.*, 2004). These determinants are:

- pH
- Electrical Conductivity (EC)
- Temperature
- Eh
- DO
- Alkalinity

To measure these determinants it is advised that a flow-through cell is to be used so that the sample is not subjected to the chemical or physical changes caused by exposing the groundwater to atmospheric conditions (Weaver *et al.*, 2004).

pH and EC - pH and EC are continuously measured in or to check the efficiency of purging with the standing water being replaced with fresh water. If the determinants are stable during purging for one well volume, then the sample collection may begin, although it is best practice to wait until three volumes of water is removed from the well before the sample is collected (Weaver *et al.*, 2004). Degassing or adsorption of CO_2 takes place when groundwater is brought to the surface which changes the value of the pH, in some samples the change in pH in order of 2 units have been recorded. Information of the in-situ pH is important to understand the potential mobility of constituents, chemical equilibria, encrustation and the corrosion potential of the groundwater (Weaver *et al.*, 2004).

Temperature - Chemical, biological reaction rates and equilibria are mostly affected by temperature. Temperature is easy to measure and by measuring the phreatic water temperature it reflects the groundwater recharge conditions and for confined water it can reflect the depth of flow (Weaver *et al.*, 2004).

Eh - When it comes to monitoring groundwater pollution it is advised to use a flow-through cell particularly as in-situ polluted groundwater often has Eh values of below zero (Weaver *et al.*, 2004). Before being brought to the surface, groundwater with a negative Eh when exposed to atmospheric conditions will rapidly absorb oxygen causing oxidation and precipitation of some constituents (Weaver *et al.*, 2004). The measurement for Eh potential of groundwater is misleadingly easy to perform and the values may seem reliable as the measurement method gives stable values (Hatva, 1989). However, several researchers have proven that the use of Eh potential measurements involves many problems associated with the hydrogeochemical interpretation of both the measurement techniques and results obtained (Hatva, 1989).

Electrical Conductivity - Electrical conductivity indicates the concentration of salts in solution, therefore changes in physical and chemical changes caused by the exposure of the groundwater sample to atmospheric conditions can affect the EC value (Weaver *et al.*, 2004).

Dissolved Oxygen - DO concentrations are directly impacted by the aeration of water, therefore,DO needs to be measured using a flow-through cell (Weaver *et al.*, 2004). The DO measurement is important for groundwater pollution studies due to DO along with Eh concentration regulating the valence state of trace metals and this constrains the bacteriological metabolism or organic compounds (Weaver *et al.*, 2004).

Alkalinity - Measuring alkalinity is done in the field since degassing of CO_2 may cause precipitation of carbonates (Weaver *et al.*, 2004). Precipitation of carbonates will cause the laboratory analytical results to show a lower alkalinity than is actually found in the groundwater that was sampled (Weaver *et al.*, 2004). Measuring field alkalinity is necessary for carbonate rock hydrogeochemical studies and essential for water stabilization investigations (Weaver *et al.*, 2004).

Well Construction - To reduce bias to water samples and insure that screen opening is not reduced by the build-up of corrosion products or by compression, selecting the correct casing and screen materials which retain their integrity in the subsurface environment is important, the use of iron and steel should be avoided (Kerr Environmental *et al.*, 1989). These impacts can be frequently checked through repeated tests of in-situ hydraulic conductivity of the well over time (Kerr Environmental *et al.*, 1989). If a noticeable change in hydraulic conductivity is observed or there is deterioration of the well, redevelopment and replacement of the well should be considered (Kerr Environmental *et al.*, 1989). Inconsistent water level readings, abrupt changes in turbidity or purging behaviour of the monitoring wells before sampling takes place are warning signals of possible loss of material integrity (Kerr Environmental *et al.*, 1989).

Purging and Sampling - Water remaining in the well casing between periods of sampling is found to be unrepresentative of water in the formation of the screened interval (Kerr Environmental *et al.*, 1989). This water must be removed through the process of purging or isolated from the sample collected through using a packer arrangement prior to the collection of the sample (Kerr Environmental *et al.*, 1989). By properly purging the borehole and filtering the sample it prevents previously precipitated Fe^{3+} hydroxide from entering the sample bottle (Weaver *et al.*, 2004). When using the dip meter to take water level readings it should be noted to use caution as to avoid disturbance of fines or precipitates which may enter or have formed in the interior walls of the well casing or found at the bottom of the well due to chemical reactions or microbial processes (Kerr Environmental *et al.*, 1989). When removing the stagnant water from the wells it is important to use low flow rates so as to not cause damage to the well, further development of the well, disturbance to corrosion or cause products via reactions inside the well (Kerr Environmental *et al.*, 1989). Using certain sampling devices such as bailers and air-lift arrangements should be discouraged to avoid the entrainment of suspended materials that are not representative of mobile chemical constituents in the formation of interest (Kerr Environmental *et al.*, 1989). In conclusion, when sampling it is recommended that the sample is to be pumped slowly to minimize turbidity and the sample should collected in a particular manner to avoid carbon dioxide and oxygen exchange with the atmosphere (Kerr Environmental *et al.*, 1989). The container used to sample can either be glass or plastic, in order to prevent previously Fe and Mn from becoming soluble, use either new bottles or prepare acid-washed bottles in advance (Weaver *et al.*, 2004). The sample should be filtered using a 0.45 micron filter as soon as it is discharged and sample needs to be kept cool with no preservation required (Weaver *et al.*, 2004). In scenarios where it may be necessary to know the concentration of precipitated Fe or Mn which is present in the form of colloids in the groundwater, unfiltered samples are collected and the results are reported as Total Fe (Weaver, Cave and Talma, 2004). Filtered samples are reported as Fe^{2+} and the difference between the Total Fe and the Fe^{2+} will produce the concentration of Fe^{3+} as stated earlier (Weaver, Cave and Talma, 2004).

Hydrogeological Setting - Hydrogeological conditions of the site being investigated must be monitored and evaluated for possible impacts the setting may have on developing the monitoring program and quality of the resulting data (Barcelona *et al.*, 1985). Various factors should be taken into consideration such as the distribution of geological materials, the movement and occurrence of groundwater through the formation, the location of the site in the regional groundwater flow system, the relative permeability of the materials and potential exchange between contaminants and the geochemical and biological constituents of the formation of interest (Barcelona *et al.*, 1985).

The three basic types of geologic materials which are normally encountered when it comes to groundwater monitoring programs: 1) porous media, 2) fractured media and 3) fractured porous media (Barcelona *et al.*, 1985). Porous media allows the water and contaminants to move through the pore spaces of the individual grains of media (Barcelona *et al.*, 1985). Porous media is made up of either sand, gravel, silt, loess, clay, till or sandstone (Barcelona *et al.*, 1985). Fractured media allows water and contaminants to move through both the intergranular pore spaces and the cracks or crevices in the soil or rock (Barcelona *et al.*, 1985). This movement or occurrence of the water moving through the pores and cracks or solution crevices is dependent on the relative porosity and degree of channelling from cracks or crevices (Barcelona *et al.*, 1985). Fractured media is made up of fractured tills, fractured sandstone and some fractured shales (Barcelona *et al.*, 1985). The distribution of porous, fractured and porous fractured media is heterogeneous and is rarely homogenous or uniform (Barcelona *et al.*, 1985). In most geological settings, two or more types of material will be found (Barcelona *et al.*, 1985). If one type of material is found at a specific site there may be large differences encountered with the hydrologic characteristics (Barcelona *et al.*, 1985). Therefore, the location of the site within the regional groundwater flow system must also be investigated (Barcelona *et al.*, 1985).

To determine the horizontal and vertical groundwater flow paths at the site of interest, piezometric surface data or water level information for each geologic formation at properly selected vertical and horizonal locations are required (Barcelona *et al.*, 1985). In order to design a proper monitoring program the groundwater flow direction is not the only required information but it is essential to determine the approximate rates of groundwater movement (Barcelona *et al.*, 1985). To estimate the bulk groundwater flow rates, hydraulic conductivity and gradient data is needed (Barcelona *et al.*, 1985). Slug or pump test data from field tests can provide the hydraulic conductivity data required (Barcelona *et al.*, 1985).

2.4.3 Sample Collection Protocols

It is important information such as equipment used, weather conditions, documentation of adherence to the protocol and unusual observations, three basic elements of the sampling protocol are to be recorded:

1. (1) Prior to sampling, water level measurements
2. (2) Purging of the well information such as the volume and rate at which water is removed.
3. (3) Actual sample collection information including sample preservation, well-purging parameters, sample handling and chain of custody.

Water level measurement is taken to establish the non-pumping water level (Barcelona *et al.*, 1985). Purging of the well is done to remove the stagnant water to capture a representative sample. It is recommended to pump water until well purging parameters stabilize to +-10% which should require two successive well volumes to be pumped (Barcelona *et al.*, 1985). Sample collection should take place at land surface or in the borehole with minimal disturbance of the groundwater chemistry (Barcelona *et al.*, 1985). Low flow sampling is recommended therefore the pumping rate should be limited to ~100ml/min for volatile organics and gas-sensitive parameters (Barcelona *et al.*, 1985). Filters are used determine soluble constituents and is a form of preservation, it should be done immediately after sample collection (Barcelona *et al.*, 1985). Analyses done in the field will avoid bias, especially for parameters which do not store well such as gases, alkalinity and pH, therefore it is recommended that they should, if possible, be analyzed in the field (Barcelona *et al.*, 1985). Field blanks and standards will allow for the correction of analytical results for changes which may occur after sample collection, preservation, storage and transport (Barcelona *et al.*, 1985). It is recommended that at least one blank and one standard for each sensitive parameters should be made in the field on each day of the sampling run as well as spiked samples for good QA/QC (Barcelona *et al.*, 1985). Refrigeration of samples should allow for the minimization of chemical alterations which can take place prior to sample analyses (Barcelona *et al.*, 1985). Documentation of the holding periods should be carefully noted in order to observe maximum sample holding and storage periods recommended by the agency (Barcelona *et al.*, 1985)

A study in Finland looked at sampling techniques of groundwater (Hatva, 1989). While purging, stabilized readings were generally reached within 10-15 minutes in groundwaters containing DO (Hatva, 1989). In most cases, with respect to Fe, groundwaters which are reducing reached stabilized readings within 30 minutes (Hatva, 1989). pH values were measured partly in the laboratory due to water quality changes which inevitably occur during transportation as a result of carbon dioxide being released (Hatva, 1989). Therefore, pH values measured in the laboratory are slightly higher than the pH values measured directly after sampling for the same sample (Hatva, 1989). However, the precipitation of Fe may result in the lowering of pH in samples which contain high Fe content (Hatva, 1989). Major errors lie in the Eh potential measurements, the cause in aerobic conditions is traceable to the platinum electrode, the surface builds up an oxide layer and together with the dominating pair of H_2O/O_2 in water makes the electrode behave like a pH electrode (Hatva, 1989). During the study it was found that measurement results are also affected by fine-grained soil in the groundwater (Hatva, 1989). It was found that in turbid groundwater which have high DO content the measured results may be several hundreds of mV smaller than those obtained from the same tube after it being cleaned through pumping (Hatva, 1989). Eh values remaining below the theoretical limit of reduction of water have been detected in turbid groundwaters, this could be due to over-voltage and slowness of some reactions (Hatva, 1989). These reasons can be combined with the assumptions that:

(1) With the platinum electrode in the water, an electrode-active redox pair such as Fe^{2+}/Fe^{3+} is capable of electron transfer.

(2) There is a sufficiently high exchange current density in the redox reaction.

(3) No DO exists in the water, Eh measurement results will represent the Eh potential of the redox pair (Fe^{2+}/Fe^{3+})

Only when the concentrations of Fe^{2+} or Fe^{3+} in water is at least 10^{-5} mol^{-1} or $0.56mgl^{-1}$ respectively, will sufficient accuracy in measurements be achieved. However, as the concentration decreased the exchange current density in a redox reaction will decrease. There are no exact limits for the concentration, above which the Eh measurement would automatically be reliable is given (Hatva, 1989). When the measured Eh potential is representative of a “mixed potential” not representative of a certain single redox pair, it may produce unreliable results (Hatva, 1989). A case of when mixed potentials occur, is when Fe and oxygen are in a dissolved form in water (Hatva, 1989). Eh potential measurements represent mixed potentials in many natural waters, which makes the measurements unusable for quantitative interpretation (Hatva, 1989).

According to Wikberg and Axelsen (1987), the actual Eh potential corresponding to e.g. the Fe/Fe redox pair, may be called the effective Eh potential of water (Hatva, 1989). To indicate the Eh-pH conditions in which specific ionic species dominate, the fields of soluble and insoluble forms of Fe and Mn can be delineated in the diagram on the basis of thermodynamic computation (Hatva, 1989). The equation that determines the boundary between oxidized and reduced forms of an element is the Nernst Equation:

$$Eh = E^0 + \frac{\mathrm{RT}}{\mathrm{nf}} \ln \frac{\alpha 10}{\alpha\, red}$$

Where: Eh = electrochemical potential measured using the Standard Hydrogen Electrode (V)

E^0 = temperature-dependent constant, standard potential (V)

R = universal gas constant (J mol^{-1} K^{-1})

T = temperature (K)

n = number of electrons transferred in half reaction

F = Faraday constant ($Cmol^{-1}$)

α ox = activity of oxidizing agent (mol^{-1})

α red = activity of reducing agent (mol^{-1})

$\ln \frac{\alpha ox}{\alpha red}$ = activities of reducing agents in half-reaction, in mass law form(Hatva, 1989)

Several solute may be present in groundwater which are involved in the precipitation or solution of Mn and Fe (Hatva, 1989). Activities of ions derived from dissolved carbon dioxide and from Sulphur have important effects on the precipitation and solution of Fe and Mn (Hatva, 1989). The occurrence of Fe and Mn is influenced by major factors such as aquifer characterization which requires information on the geological structure and prevailing flow pattern during the course of the study (Hatva, 1989) Categorizing the aquifer also takes into consideration the morphology and genesis of the aquifer as well as its original location (Hatva, 1989).

2.4.4 Data Analysis Interpretation of Fe and Mn

Mean values should be used to compare with the criteria given. Turbidity and pH must be considered in the interpretation of Fe concentrations (Department of Water Affairs and Forestry, 1996). Mean values should be used to compare with the criteria given. The occurrence of elevated Mn concentrations in surface waters is typically cyclic unless directly due to pollination by Mn-bearing effluents. Transient episodes of elevated Mn concentrations in pipelines can result in long-standing Mn problem through precipitation followed by gradual release. In the investigation of consumer complaints of Mn staining, point of use analyses should be done in conjunction with that of the source water (Department of Water Affairs and Forestry, 1996).

Data analyses methods, multivariate statistical analysis such as principal components analysis (PCA) and cluster analysis (CA) can be used for the characterization of groundwater (Bodrud-Doza, 2016). The PCA was used for the extraction of principal components to evaluate spatial variations and the possible sources of heavy metals in groundwater by Bodrud-Doza, 2016. CA can be performed to classify the elements of different sources based on the similarities of their chemical properties (Bodrud-Doza, 2016).

Ashley, (1978) applied a factor analysis and a cluster analysis to two differing sets of hydrochemical groundwater data. The factor analysis and cluster analysis were moderately successful as statistical tools for revealing the patterns of groundwater flow, hydrochemical and hydrogeochemical features (Ashley, 1978). The factor analysis and cluster analysis provide advantages over the traditional graphical methods used to solve similar problems due to their systematic nature and they can generate inter-parameter relationships that may be overlooked in more traditional methods (Ashley, 1978). However, there is a disadvantage which is that they are easily prone to misuse and misinterpretation due to their complexity which requires the user to have adequate knowledge of it (Ashley, 1978).

2.5 Factors impacting iron precipitation

In inorganic, organic and biochemical reactions, electrons are the essential reactants (Husson, 2013). Chemistry of living organisms rely more on redox reactions (electron transfers) than it does on acid-base reactions which are more focused on proton transfers (Husson, 2013).

2.5.1 Fe

Fe solubility is strongly influenced by both Eh and pH (Husson, 2013). Plants absorb Fe as Fe^{2+} (Husson, 2013). At low Eh values the concentration of Fe^{2+} is high in the soil solution, a rapid decrease is observed when the Eh rises above a pH5, in relation to the formation of Fe oxides and hydroxides (Husson, 2013). Therefore, Fe deficiency can take place at high pH and Eh and Fe^{2+} toxicity is common at low pH and Eh (Husson, 2013). Fe strongly influences the Eh-pH characteristic in natural environments and Fe redox reactions delineate an important redox-threshold in pedogenesis (Husson, 2013).

2.5.2 Micronutrients

Other micronutrients availability such Mn, Cu or Zn are strongly influenced by the Eh and pH in soil (Husson, 2013). Proof is available for the direct or indirect biological alterations in the solubility, availability or the redox start of the above elements as well as others (Husson, 2013). The Pourbaix diagram indicates that Mn^{2+} is both a function of Eh and Ph (Husson, 2013). Mn deficiency can occur under aerobic conditions in alkaline soil (Husson, 2013). With low pH, Mn toxicity is a common occurrence and a decrease in Eh is related to a higher Mn bioavailability (Husson, 2013).

2.5.3 Plants impacts on soil Eh and pH

In the rhizosphere of plants, there is the ability to dramatically alter the Eh and pH (Husson, 2013). Plant roots are able to create conditions that allow for the development of unique microbial communities in the rhizosphere, to an extent that evolution has shaped soil life to adapt to this specific ecological niche (Husson, 2013). The alteration either directly affects root exudation or have an indirect effect through preferential development of specific microorganisms which alter the pH and Eh (Husson, 2013). Essential oxygen is obtained through a system of air-filled intercellular space for roots or plants adapted to highly reduced environments (Husson, 2013). Plants that live in wetlands such as rice have the ability to raise the Eh in their rhizosphere by oxygen transport through the aerenchyma (Husson, 2013). The ability that plants have to raise the Eh in their rhizosphere helps to protect themselves against phytotoxic concentrations of reducing substances (Husson, 2013).

2.5.4 Dissolved Oxygen

DO found in groundwater normally originates from the contact with the atmosphere before it recharges the aquifer (Boghici, 2003). The solubility of oxygen in the water is dependent on a few factors such as the partial pressure of oxygen in the atmosphere, the dissolved solid contents of the groundwater and the temperature within the aquifer (Boghici, 2003). Contrary to what is generally believed, the presence of DO in groundwater is a common occurrence and this is found to be particularly evident in hydrologically stressed systems (Husson, 2013). DO is able to exist at great depths in aquifers which have little to no oxidized material in the water flow path and it may also be present in any aquifer where the residence time of the water is short compared to the rate of oxygen being consumed (Husson, 2013). The amount of DO measured is used to determine the Eh which can be used for geochemical studies (Boghici, 2003).

CHAPTER 3: STUDY AREA

3.1 Introduction

The Western Cape Province covers 129370 km^2 (Figure 4) and is situated in the south-western part of South Africa (van Niekerk and Joubert, 2011). The eastern and northern parts of the province are bounded by other provinces in South Africa and the rest is seaward bordered by the Indian Ocean in the south and Atlantic Ocean in the west (van Niekerk and Joubert, 2011). The main area for this study is the City of Cape Town and surrounding towns of Paarl, Sonstraal and Kraaifontein (Figure 4). The City of Cape Town has a population of 3.75 million people in just over 1 million households (van Niekerk and Joubert, 2011). The municipality covers an area of 2500 km^2 as well as just over 300 km of coastline (van Niekerk and Joubert, 2011). The City of Cape Town alone requires 1000 million litres of water per a day and this water is mostly supplied from a variety of dams (van Niekerk and Joubert, 2011).

3.2 Climate

The Western Cape Province is made up of three distinct climatic regions which are, the Mediterranean, the South Coast and Karoo regions (van Niekerk and Joubert, 2011). The Mediterranean region is in the Western and South-Western parts of the province and receives most of its rainfall during winter (van Niekerk and Joubert, 2011). The reason for this is due to the influence of the cold Benguela current of the Atlantic Ocean and the northward

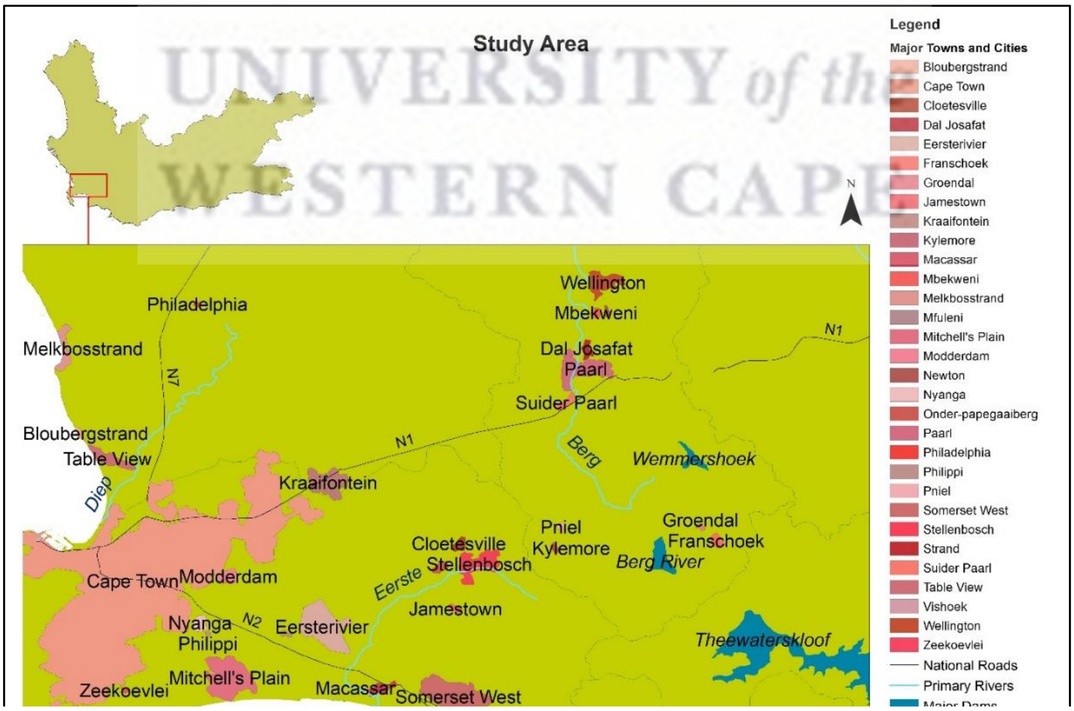

Figure 4: Map of the study area highlighting major towns and cities, damns, rivers and national roads in selected areas of the WCP

displacement of high-pressure systems during winter which allow westerly winds to introduce cold polar air to the region (van Niekerk and Joubert, 2011). While the winters are mild to cool, the summers are warm to hot (van Niekerk and Joubert, 2011). Rainfall variability in the region is high due to heavy orographic rainfalls despite most of the rainfall being received as prefrontal rain and postfrontal showers (van Niekerk and Joubert, 2011).

However, in the South Coast region, which extends eastward from Cape Agulhas, there is rainfall throughout the year (van Niekerk and Joubert, 2011). This rainfall is as a result of the movement of moist, warm air from the Indian ocean and orographic influences which results in the northern facing slopes receiving less rainfall than the southern mountain slopes which generally receives more rainfall (van Niekerk and Joubert, 2011). Despite the weather being warm during the summer and mild during the winter, there is a noted decrease in temperature with an increase in altitude (van Niekerk and Joubert, 2011). The mountain ranges in the province form a natural divide between the South Coast and Karoo climate regions therefore the effect of the Indian Ocean doesn’t extend further than the mountain ranges (van Niekerk and Joubert, 2011). The Karoo region is situated in the inland plateau of South Africa and receives most of its rainfall in the form of thundershowers during late summer (van Niekerk and Joubert, 2011). The temperatures vary considerably from summer to winter (Figure 5 and Figure 6) and the rainfall in this semi-arid region is unreliable and low (Figure 7) (van Niekerk and Joubert, 2011). According to Figure 5, the research project average max annual temperature fall within the first 3 ranges from 0°C to 29°C. In Figure 6, the study area is resembled by the last category where the average min annual temperature is greater than 8°C. Figure 7 highlights the mean annual rainfall between 201mm and > 1000mm where the last 4 ranges categorise the sites in the research project. The Cape Flats area has a typical Mediterranean climate where the summers are hot and relatively dry, and the winters are cold and wet (Adelana, Xu and Vrbka, 2010). However, the mountainous nature of the Cape Fold Belt causes the climate of the region to fluctuate (Adelana, Xu and Vrbka, 2010). The Cape Flats area is characterised by frequent strong winds with prevailing southeast trade winds in summer which are replaced by the northwest anti-trade wings in winter which results in rainy conditions (Adelana, Xu and Vrbka, 2010). Historical precipitation data of 165 years (1841-2006) has shown that the mean annual precipitation during this period is 619mm and there are strong fluctuations between 229 and 1037mm of precipitation (Adelana, Xu and Vrbka, 2010). Temperatures during summer are mild with the average maximum being 26ºC and the winter months are cool with an average minimum of 7ºC (Adelana, Xu and Vrbka, 2010). Winter is when 80% of the annual precipitation occurs with the maximum downpour taking place in June and minimum precipitation in February (Adelana, Xu and Vrbka, 2010).

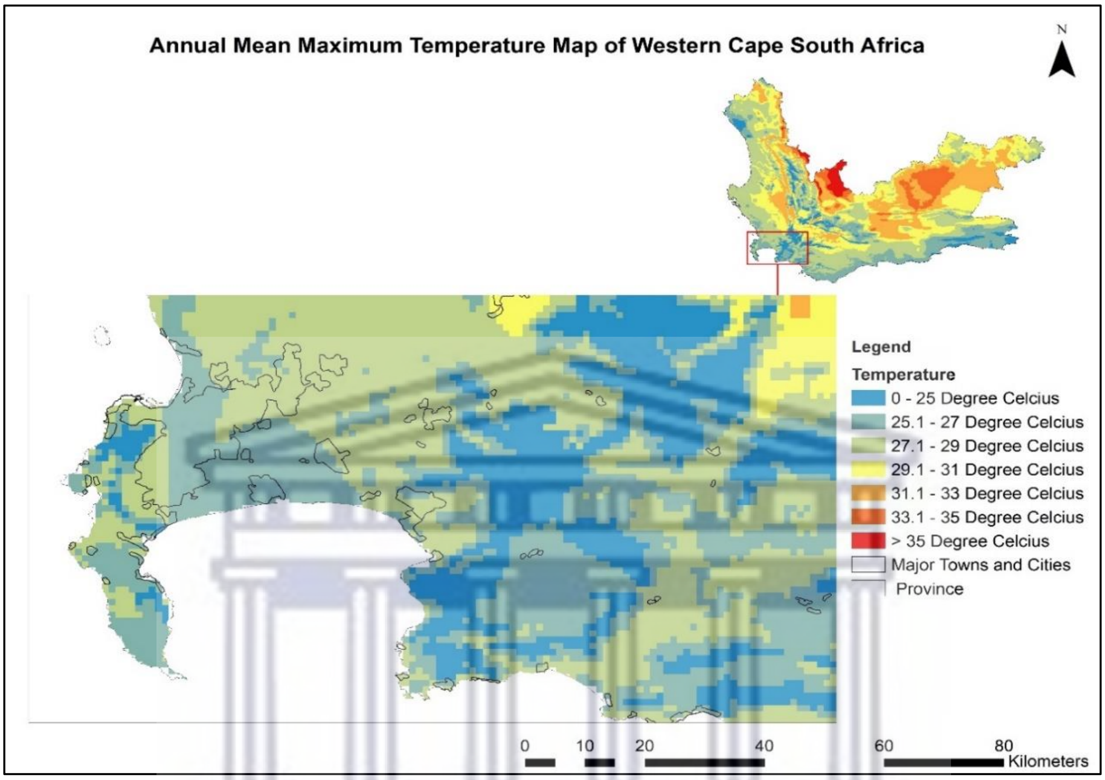

Figure 5: Map showing the annual mean maximum temperatures of the major cities and towns in the WCP.

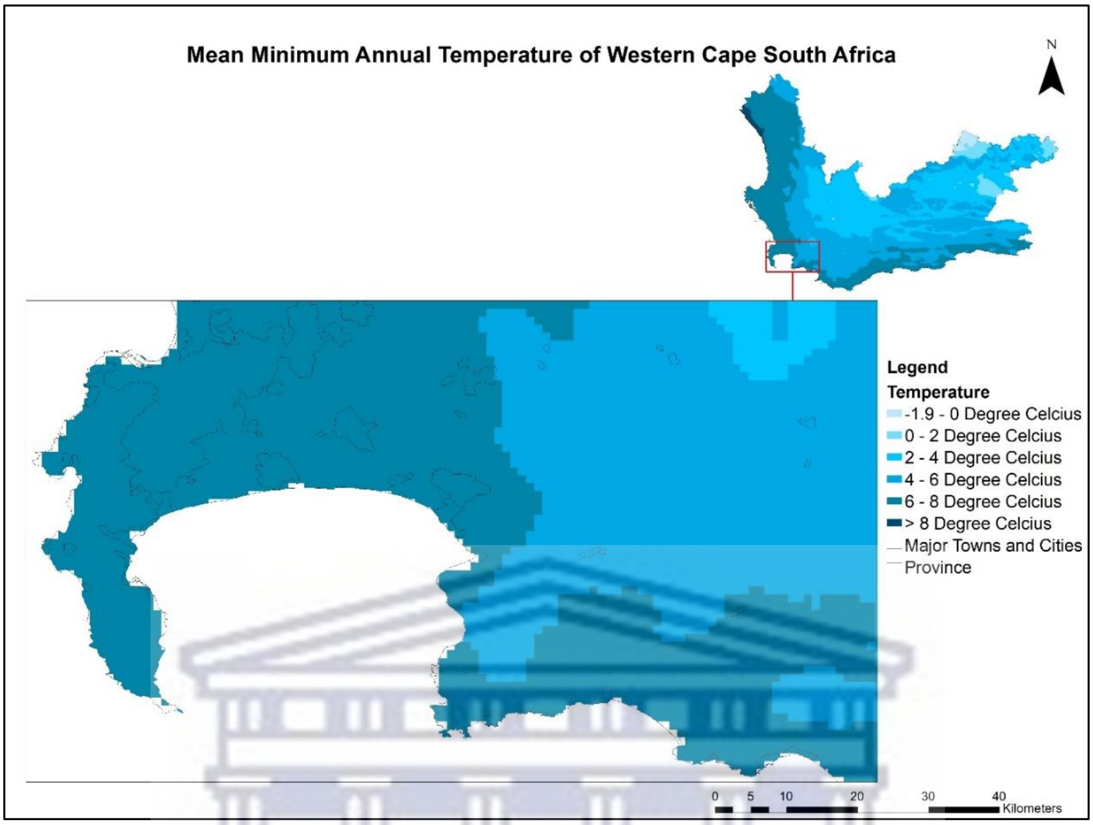

Figure 7: Map showing the mean minimum annual temperature of the major cities and towns in selected areas of the WCP.

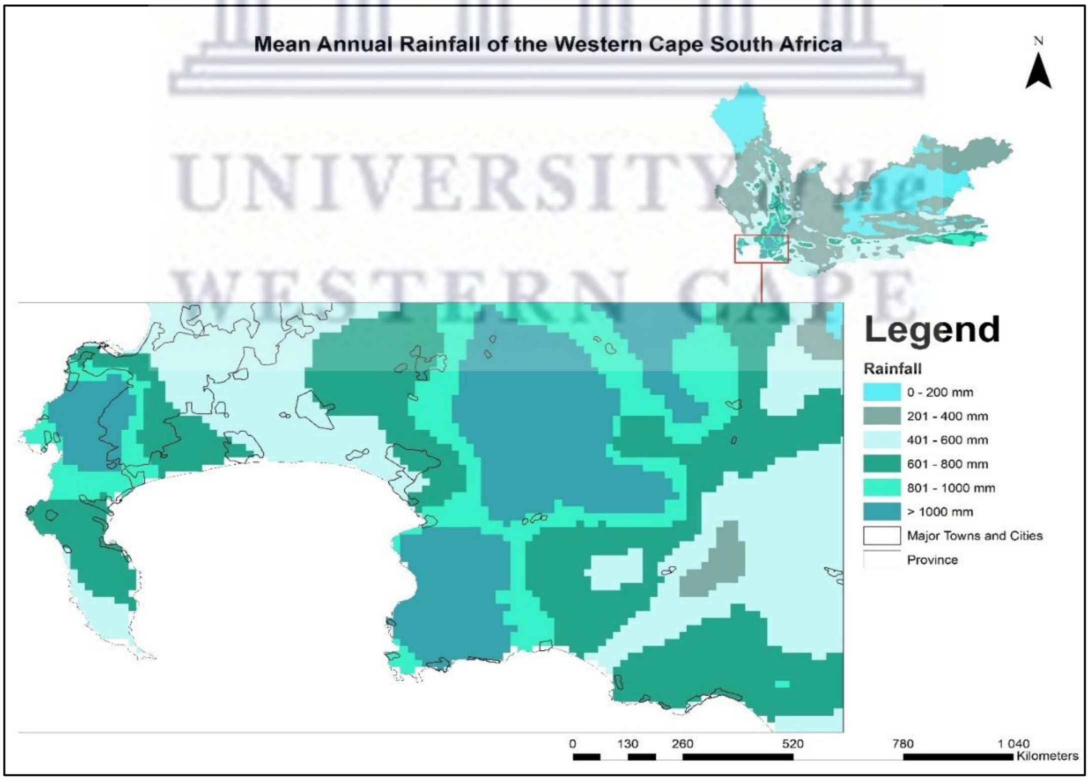

Figure 6: Map showing the mean annual rainfall in the major cities and towns in selected areas of the WCP.

3.3 Land Use

The Western Cape region covers approximately 12.4% of the total agricultural land available in South Africa which is an area of 11.5 million hectares (ha) of agricultural activity (Pegram and Baleta, 2014). The Western Cape province is the strongest contributor to South Africa's national agricultural exports as it makes up more than half of the country's exports (Pegram and Baleta, 2014). The province produces between 55% and 60% of South Africa's agricultural exports, which is valued at more than R7 billion per year (Pegram and Baleta, 2014). About half of these exports are made of wine and a large portion is made up of processed and unprocessed fruit (Pegram and Baleta, 2014). In South Africa the commercial agriculture of the Western Cape contributes 22.4% to gross farming income (Pegram and Baleta, 2014). Due to the physical geographic features of the Western Cape, which differs from the rest of South Africa, the agriculture is distinguished in several ways (Pegram and Baleta, 2014). The crop mix and the productive potential is different due the winter rainfall of the Cape Winelands area and the year-round rainfall of the Southern Cape region (Pegram and Baleta, 2014). The production stability of the agricultural regions depends on the adequate winter rainfall and the support of well-developed infrastructure for both input supply and output processing (Pegram and Baleta, 2014). There is a diverse production capacity which is made up of 11 commodities that greatly contribute to agricultural production (Pegram and Baleta, 2014). Together, this crop production made up of fruit, poultry and eggs, winter grains such as barely, wheat and hops, viticulture and vegetables contribute to more than 75% of the total output and as a result the diversity of the agriculture also contributes to the sector's general stability (Pegram and Baleta, 2014). With fruit and wine making up the core commodities of the agricultural output, horticulture products contribute 53% (Pegram and Baleta, 2014). Important areas which contribute towards agricultural production are the Cape Winelands, Cape Metro, West Coast and Overberg (Pegram and Baleta, 2014). Animal products and animals contribute 42%, ranging from poultry, cattle, sheep, ostriches and pigs in descending size contribution (Pegram and Baleta, 2014). Other key producing areas are Paarl, Worcester, Goodwood, Malmesbury, Swellendam and Oudtshoorn (Pegram and Baleta, 2014). Field crops contribute 7% of production which is made up of maize and barely with wheat being the dominant crop (Pegram and Baleta, 2014). Malmesbury, Mooreesburg, Piketberg (West Coast region) and Celdon and Bredasdorp (Overberg region) are responsibly for 70% of the wheat crop production (Pegram and Baleta, 2014). Forestry and fishing contribute 1% although forestry is limited and mainly state-owned (Pegram and Baleta, 2014).

The service sector in the Western Cape is concentrated in the Cape Metropolitan area and is broken down into different sub-sectors which are: retail and wholesale, catering and accommodation, transport and storage, communication, finance and insurance, business and services, and government services (Pegram and Baleta, 2014). The agriculture sector is not the only sector that heavily depends on the water, but it is needed for the tourism, manufacturing (both agriculturally based and industrial) and the tertiary sectors (Pegram and Baleta, 2014). Compared to the agriculture sector, the tertiary sector may use little water volumetrically and a large proportion of the services rendered are related to the agricultural sector (Pegram and Baleta, 2014). The quality and assurance of water supply in the Western Cape economy needs to be higher in comparison to the agriculture industry as our export economy is dependent on water (Pegram and Baleta, 2014).

3.4 Geology

The present-day Western Cape resulted from the Pan African Saldanian orogeny and a passive margin basin of the supercontinent of Gondwanaland (Dippenaar, 2016). In the geological record there are three main subdivisions which are preserved, the Table Mountain, Bokkeveld and Witteberg Groups (Dippenaar, 2016). Later, the Cape Orogeny deformed significantly into the Cape Fold Mountains (Dippenaar, 2016). In the Ordovician to Early Devonian age, shallow marine to fluvial conditions deposited mainly sandstones which makes the Table Mountain Group (TMG) the oldest of the subdivisions (Dippenaar, 2016). This was followed by fossiliferous shale and sandstone of the Bokkeveld due to delta environments between Early and Middle Devonian age (Dippenaar, 2016). Lastly comes the Witteberg Group during the Late Devonian to Early Carboniferous age and it comprises of sandstone and mudrock that got deposited in a shallow marine to delataic environments (Dippenaar, 2016). The Western Cape's topography ranges from coastal plains to complex mountain ranges and valleys (van Niekerk and Joubert, 2011). The Cape Fold Belt forms an L-shaped mountain range oriented in a north to south and east to west direction which dominates the topography (van Niekerk and Joubert, 2011).

3.4.1 Malmesbury Group

The pre-Cambrian Malmesbury Group is the oldest rocks in the Western Cape made up of mainly meta-sedimentary and meta-volcanic rock forms part of the western branch of the Saldania belt (Adelana, Xu and Vrbka, 2010) (Conrad, Smit, Murray, & van Gend-Muller, 2019). The Malmesbury Group is mainly made up of greywacke, schist, shale, phyllite, limestone, conglomerate, commonly highly lineated and foliated, and further sub-divided into three distinctly different terrains (Adelana, Xu and Vrbka, 2010) (Conrad, Smit, Murray, & van Gend-Muller, 2019). The three terranes are the north-eastern Boland terrane which is separated by the Piketberg – Wellington fault zone from the central Swartland Terrane and the Swartland is separated by the Colenso (Saldanha – Stellenbosch) fault from the Piketberg – Wellington fault zone (Dippenaar, 2016). Within the south-western Tygerberg terrane falls Cape Town with the Tygerberg Formation forming the only subdivision of the Malmesbury Group in the area (Dippenaar, 2016). Due to immense changes in pressure and temperature during the geological past it changed rock types resulting in most of the terrane rock being metamorphic rock (Dippenaar, 2016). The change in conditions resulted in mineral change, change in orientation and recrystallization which resulted in the formation of a new suite of rock types (Dippenaar, 2016). Underlaying the Malmesbury Group is the Namaqua-Natal basement which puts the age of the Malmesbury Group to no older than 1000 Ma (Conrad, Smit, Murray, & van Gend-Muller, 2019).

The Malmesbury Group is intruded by the Cape Granite Suite which is dated at 632 Ma, this could be the youngest possible age of the Malmesbury Group during the Pan African Saldania Belt event (Conrad, Smit, Murray, & van Gend-Muller, 2019) (Dippenaar, 2016). The Cape Supergroup overlies the Malmesbury Group and is made up of mainly bedded quartzites with bed thickness ranging from one to four meters (Conrad, Smit, Murray, & van Gend-Muller, 2019). During the formation of the Cape Fold Belt, deformation took place which caused the sediments of both the Malmesbury Group and TMG to have a metamorphic overprint (Conrad, Smit, Murray, & van Gend-Muller, 2019). This resulted in the sandstones as quartzites of the TMG and sedimentary rocks of the Malmesbury Group being tightly folded in places (Conrad, Smit, Murray, & van Gend-Muller, 2019). The Cape Granite Suite has a highly variable composition which ranges between olivine grabbro to leucogranite with granites and granodionites being the most abundant throughout it (Dippenaar, 2016). Most of the granites are undeformed and subdivide into plutons, the eastern (around George), southwestern (around Cape Town) and northern pluton (around Richtersveld) (Dippenaar, 2016). All of Cape Town rocks fall within the Malmesbury Batholith and more specifically the Cape Peninsula Granite of the Cape Granite Suits (Dippenaar, 2016).

3.4.2 Table Mountain Group

From early Ordovician to early Carboniferous times, between 500 and 340 million years ago, the sediments of the Cape Supergroup were deposited (Pietersen and Parsons, 2002). The Cape

Fold Belt (CFB), between 280 – 220 million years old, which straddles the west and south coasts of South Africa and has a predominantly siliclastic sequence that is exposed across the entire length of the orogenic belt (Pietersen and Parsons, 2002). TMG, Bokkeveld and Witteberg Groups are made up of a succession of quartz, siltstones, shales, with minor conglomerate and thin diamictite units (Pietersen and Parsons, 2002). The Cape Supergroup maximum thickness is 5300m for Western Cape and 9600m for the Eastern Cape (Pietersen and Parsons, 2002). In shallow marine environments under tidal, storm and wave conditions as well as in non-marine, braided fluvial environments the sediments that make up the Cape Supergroup was deposited (Pietersen and Parsons, 2002). A combination of factors such as medium to coarse grain size, relative purity of some of the quartz arenites and their well-indurated nature and fracturing, due to the faulting and folding in the fold belt, enhances both the quality of the groundwater and its exploitation potential (Pietersen and Parsons, 2002). The lowermost part of the Cape Supergroup, made up of cratonic sheet sandstones of the TMG forms the basis of the CFB from Port Elizabeth in the east to Vanrhysdorp in the west (Pietersen and Parsons, 2002). Along the West Coast and in the Southwestern Cape, most of the stratigraphic research on these rocks were done due to the low deformational intensity (Pietersen and Parsons, 2002). The TMG is further divided into eight formations Rietvlei, Skurweberg, Goudini, Cederberg, Pakhuis, Peninsula, Graafwater and Piekenierskloof where the common rocktypes are sandstone, siltstone and shale (Bargmann, 2003).

The Cape Flats area is the large sandy area connecting the mainland with the hard-rock Cape Peninsula (Adelana, Xu and Vrbka, 2010). The Cape Flats falls under the City of Cape Town Water Management Area (WMA), covering an area of 630 km^2 and an extensive area of approximately 2159 km^2 (Adelana, Xu and Vrbka, 2010). The current land use is made up of urban and industrial. Intense land use for agricultural and for waste disposal makes the Cape Flats sand more susceptible to pollution (Adelana, Xu and Vrbka, 2010). The Cape Flats makes up the "Late-Tertiary and Recent sands" unit of the Western Cape which overlies the Malmesbury Shale and that can be up to 50m thick in places (Adelana, Xu and Vrbka, 2010). The Sandveld Group makes up an extensive sand aquifer which is hydrogeologically divided into 4 main units: The Cape Flats aquifer unit, The Silwerstroom Witzand unit (in the Atlantis area), the Grootwater unit (in the Yzerfontein region) and the Berg River unit (in the Saldanha area) (Adelana, Xu and Vrbka, 2010).

3.5 Hydrogeology

When it comes to groundwater development in the Western Cape Province the target is often the TMG, in favour of the Malmesbury Group, as a potential source of groundwater (Conrad, Smit, Murray, & van Gend-Muller, 2019). A study by Meyer (2001) concluded that TMG is preferred over the Malmesbury Group due to the "largely argillaceous and thus incompetent nature of many of the lithological units" in the Malmesbury Group, compared to the "largely competent and brittle-natured arenaceous unit" of the TMG (Conrad, Smit, Murray, & van Gend-Muller, 2019). The TMG or commonly known as the "sand" aquifers is often considered to be more favourable for groundwater target zones (Conrad, Smit, Murray, & van Gend-Muller, 2019). The TMG aquifer is made up 95% of sandstone, quartzite units and shale, variable amounts of feldspar and clay minerals which is extensively exploited for agricultural purposes (Pietersen and Parsons, 2002). In 2015, 2016, 2017 and 2018, extensive borehole drilling took place in the TMG due to the onset of a severe drought (Conrad, Smit, Murray, & van Gend-Muller, 2019). This drilling of boreholes took place on the owner's property, and due to the urgency, it took place irrespective of whether the geology was favourable or not (Conrad, Smit, Murray, & van Gend-Muller, 2019). From this groundwater supply project in response to the drought, several of these projects demonstrate that in certain geographical areas, the Malmesbury Group was a favourable aquifer (Conrad, Smit, Murray, & van Gend-Muller, 2019). This resulted in higher aquifer yields with acceptable water quality (Conrad, Smit, Murray, & van Gend-Muller, 2019).

It is commonly known that the Malmesbury Group is a low-yielding (<0.5 l/s) aquifer with variable water quality (Conrad, Smit, Murray, & van Gend-Muller, 2019). The electrical conductivity (EC) ranges from <100 mS/m TO > 1000 mS/m (Conrad, Smit, Murray, & van Gend-Muller, 2019). An assessment done on the ground water resources in the Berg region considered the Malmesbury Group to be an aquidance on a regional scale, that "consists dominantly of geochemically weak slates and phyllites, which are incapable of supporting open features below the near-surface weathered zone." (Conrad, Smit, Murray, & van Gend-Muller, 2019).

Contrary to previous estimates, the Malmesbury Group does contain groundwater, based on yield tests of one to three days, and this can be abstracted at high flow rates (Conrad, Smit, Murray, & van Gend-Muller, 2019). These abstraction rates are associated with specific geological conditions which result in large fracture networks that are not representative of the bulk rock properties of the Malmesbury Group (Conrad, Smit, Murray, & van Gend-Muller, 2019).

CHAPTER 4: METHODS

4.2 Methods

This research project made use of quantitative and qualitative research methods. This was chosen as it is appropriate in understanding and achieving the objectives of this research project. The data required in order to achieve the first objective data was sourced from the National Groundwater Archive. The second objective also required historical data, which was sourced from when the boreholes were drilled. This borehole data for Sonstraal Hospital, Kraaifontein Community Health Clinic and Paarl Hospital was sourced from L2K2 Consultants, DP Marais Hospital data was sourced from Umvoto Africa and Brooklyn Chest Hospital from GEOSS South Africa. This included groundwater chemistry data, pumping test data and geological data of the WCP. In addition to the historical data being used there was sampling done at selected sites to understand the current groundwater chemistry.

4.2.1 Fieldwork

In order to obtain the data required for the fourth objective, field measurements were required to be taken. This included forming a sampling program, which included the collecting of samples from the various sites in the study area. During the sampling, a closer investigation of the pumping regimes was assessed in terms of when the boreholes are switched off and on and site maintenance, groundwater use and quality through interviews. By visiting the sites and collecting samples, this information was used to understand if the Fe being pumped was in the Fe^{2+} or Fe^{3+} form.

It was necessary to take samples from all different major aquifer systems in the WCP, which are the Cape Flats Aquifer, Table Mountain Group Aquifer and Malmesbury Aquifer. This was required to understand the rock water interaction, which covers the hydrogeochemistry section of this research project.

4.2.2 Desktop Study

- In order to achieve the first objective, which is to assess spatial variations in Fe and Mn concentrations, the concentration of Fe and Mn at each site of the study was required. This made use of the groundwater chemistry data that was previously recorded as well as collected data through fieldwork. ArcGIS was used, which is, Geographical Information System used for the creation of maps, compiling geographic data, analysing mapped information and sharing and discovering geographic information.

The ArcMap component of ArcGIS was used to view, edit, create and analyse geospatial data to produce geochemical maps through the exploring of data within a data set to symbolize features accordingly that showed the spatial variation of Fe and Mn concentrations in the WCP.

- In order to achieve the second objective, which is to establish the site-specific processes that control the concentration of Fe and Mn in groundwater, it required the use of the groundwater chemistry data, geological data, lithological logs, site interviews and land use images. This data was collated and analysed using correlation and regression analysis tools, which assisted in the understanding of the site-specific processes and relationships that control the concentration of Fe and Mn in groundwater.

- The third objective is to model the likelihood of Fe and Mn precipitating from the detected solution composition. Once the field work and lab analysis were conducted this data was used through Geochemist Workbench and PHREEQC to characterise the aquifer type and likelihood of Fe and Mn precipitating. Geochemist Workbench software helped in producing piper plot diagrams to classify the groundwater in the different types of aquifers. PHREEQC is a computer program which can be used for speciation and saturation (index calculations, reaction-path and advective transport calculations involving specified irreversible reactions, mixing of solutions, mineral and gas equilibrium, surface-complexation reactions and ion-exchange reactions, and inverse modelling) which finds sets of mineral and gas mole transfers that account for composition differences between the waters, within specified compositional uncertainties. From the above abilities of the PHREEQC program, geochemical was well equipped to provide a thorough understanding of the processes that control the concentration of Fe and Mn in groundwater.

- The final objective which is the to assess the best practice methods/techniques for sampling Fe and Mn was achieved through the field sampling. Immediate analysis of Fe and Mn took place on site using the DR900 (Figure 8) and samples were collected and sent to a lab to analyse the Mn and Fe after storage and transportation.

4.3 Field work measurements and analysis

4.3.1 Parameters to be measured

At each borehole the following physicochemical parameters will be taken.

- pH
- EC
- DO
- OSat
- Temperature
- Iron
- Manganese

Figure 8: Image of handheld HACH DR900 measuring device.

4.3.2 Periodate Oxidation Method

The Periodate oxidation method was used for the analyses of soluble Mn in water and wastewater. This method was applied using the DR900 HACH handheld device. The samples were not preserved and analysed immediately. The interference substances are:

Calcium	700 mg/L
Chloride	70,000 mg/L
Iron	5 mg/L
Magnesium	100,000 mg/L

Highly buffered samples or extreme sample pH can prevent the correct pH adjustment of the sample by the reagents. Sample pre-treatment may be necessary.

Materials required to prepare the standard solution:

- Manganese standard solution 1000 mg/L
- 1-L volumetric flask, Class A
- 10-mL volumetric pipet, Class A and pipet filler safety bulb
- Deionized water

A 10.0 mg/L manganese standard solution was prepared by using a pipet to add 10.0 mg/L of 1000 mg/L manganese standard solution into the volumetric flask. The solution was diluted to the mark with deionized water after which it was mixed well. This was followed by using the test procedure to measure the concentration of the prepared standard solution. The result from the test procedure was compared to the expected result.

Materials to carry out the sample analyses:

- 10-mL sample cell
- 10-mL volumetric pipet

The samples were prepared by filling a sample cell with 10mL of sample. The contents of one Buffer Powder Pillow, Citrate Type for Manganese were added to the sample cell. The stopper was then inserted into the sample cell and inverted to mix until the powder pillow contents had completely dissolved. The contents of one Sodium Periodate Powder Pillow was added to the sample cell. The stopper was inserted into the sample cell and inverted to mix the contents of the powder pillow until dissolved. The colour of the sample changed to a violet colour if Mn was present in the sample. A 2-minute reaction time was set. A blank sample was prepared by filling a second sample cell with 10 mL of sample. When the timer expired the blank cell was cleaned with a dry cloth and inserted into the machine cell holder. Zero was pushed and the display showed 0.0 mg/L Mn. The sample cell was cleaned with a dry cloth and inserted into the machine cell holder and the read button was pushed after which the results were in mg/L Mn.

4.3.3 FerroVer Method

The FerroVer method used for water, wastewater and seawater for determining Total Fe. This method was applied to the DR900 HACH handheld device. The samples were analysed immediately and not preserved. The interference substances are:

Calcium, Ca^{2+}	No effect at less than 10,000 mg/L as $CaCO_{3-}$
Chloride. Cl^-	No effect at less than 185,000 mg/L
Copper, Cu^{2+}	No effect, masking agent is contained in FerroVer Reagent
High iron level	Inhibit colour development. Dilute sample and re-test to verify results.
Iron oxide	A mild, vigorous or Digesdahl digestion is necessary. After digestion, adjust the sample pH to 3-5 with sodium hydroxide, then analyse.

Materials used to prepare the standard solution:

- Fe standard solution, 100 mg/L
- 100-mL volumetric flask, Class A
- 2-mL volumetric pipet, Class A and pipet filler
- Deionized water

A 2.00 mg/L Fe standard solution was prepared by using a pipet to add 2 mL of the 100-mg/L Fe standard solution into the volumetric flask. This solution was diluted by filling the volumetric flask with deionized water until the mark. This was followed by inserting a stopper and mixing it well. The test procedure was used to measure the concentration of the standard solution prepared after which the actual results were compared with the expected results.

Materials for total Fe analyses:

- Ferrover iron reagent powder pillows, 10-mL
- Sample cells

The sample was prepared by filling a cell with 10 mL of sample. The contents of a FerroVer Iron Reagent Powder Pillow were added to the sample cell. A stopper was inserted into the sample cell and swirled to mix the contents. It should be noted that the undissolved powder did not influence the accuracy. A 3-minute reaction time was set. It is noted that an orange colour appeared in the sample if Fe was present and that samples which contain rust react for 5 minutes or more. A blank sample was prepared by filling a second sample cell with 10 mL of sample after which the cell was cleaned with a dry cloth. After the timer expires the blank cell was inserted into the machines cell holder and the zero button was pushed, the display showed 0.0mg/L Fe. This was followed by the cleaning of the prepared sample cell with a dry cloth and inserting into the machine cell holder. The read button was pushed, and the results were displayed in mg/L Fe.

4.3.4 Sample collection method

To assist with achieving the 4th objective of this research project different sampling and preservation techniques were explored. This was also done in order to understand which method provides the most accurate information. The following sampling techniques were practiced:

1. Flow through cell sample
2. Preserved sample
3. Filtered sample
4. Pipe outlet sample

On arrival at each site, an interview with each site manager was conducted to understand the management of the boreholes. At the boreholes, the diameter of the borehole and collar height was measured, thereafter, the depth to water level was measured. These measurements along with the entire depth of the borehole were used to calculate the volume of water purged from the boreholes, this amounted to three volumes of the borehole. The pump was then inserted to an appropriate depth based on the depth to water level. As purging commences any changes in colour and smell were noted.

Flow through cell:

Once three volumes of the borehole was pumped out, the purging was complete. The pipe outlet was then connected to the flow through cell where handheld probes were inserted to collect temperature, pH and EC. Once the parameter stabilised the Hach DR900 was used to measure Total Fe and Dissolved Fe and Mn once the chemical parameters stabilised. Thereafter the flow through cell sample was collected.

Preserved sample:

The next sample collected was the preserved sample where 2ml of nitric acid per 500ml sample was added into the bottle after the sample was collected. The samples were then refrigerated until taken to the lab for analysis.

Filtered sample:

A 0.45micron and syringe was used to take water from the outlet of the flow through cell and filter to collect the filtered sample.

Pipe outlet sample:

The last sample to be collected was the standard sample taken directly from the pump outlet pipe.

After this the samples were packed into the cooler box with ice to preserve the samples and transported to a fridge for storage. For this study there were sites where the submersible pump was not used as most of the sites where the samples were collected had boreholes fitted with pumps due to the circumstances under which the boreholes were drilled.

4.4 Sampling Sites

Table 3: List of all sampling sites and number of boreholes.

Name of Sites	No. of Boreholes
Sonstraal Hospital	2
Paarl Hospital	4
Kraaifontein	2
UWC Boreholes	2
Brooklyn Chest Hospital	2
DP Marais Hospital	4

Sampling for this study will be once off as this is not a temporal study.

4.4.1 Sampling Equipment

- Sampling bottles 500ml or 1L (x83)
- Iron and Manganese reagents
- DR 900
- Cooler Box
- Ice
- Bucket
- Measuring tape
- Submersible pump
- Electrical contact water level meter
- HACH mustimeter probe for chemical parameters.

4.5 Modelling & Statistics

PHREEQC modelling was done to understand how the change in chemical behaviour influences the concentration of Mn and Fe in groundwater. The following parameters were modelled using incremental reaction modelling through step changes of Fe, Mn, pH, temperature and redox potential. The selected sample was based on the concentration of Fe and Mn. Fe was modelled in 10 steps from 0.01mg/L to 0.91mg/L with 0.10mg/L incremental increases. Mn was modelled in 11 steps from 0.05mg/L to 1.05mg/L with 0.10mg/L increments. The pH levels was modelled increasing from 3 to 9 in 13 steps in increments of 0.5. The redox potential was modelled between -1 and 6 in 8 steps. Finally, temperature will be modelled between 18°C and 28°C in 11 steps. Fe and Mn minerals was selected in the output file where the saturation indices were looked at to understand the precipitation of combined Fe and Mn minerals as well as carbonate minerals with change in chemical conditions. This was further broken down in excel by graphing these outputs to understand the data further in a visual aid.

The results were evaluated using correlation statistics. The correlation between variables were analysed. This was used to determine whether the variables (Fe, Mn, pH, temperature and redox potential) are related to one another. Following this, the ranges and averages of the variables were analysed to determine the extent to which the variables change by changing the independent variables (Fe and Mn minerals). Together these metrics helped to determine whether relationships exist and the extent of the relationship between the independent (Fe and Mn minerals) and dependent variables (Fe, Mn, pH, temperature and redox potential).

Correlation Methodology - The Statistical software "R" was used to determine the correlations. The following methodology was used:

1. Importing the raw data set into the R software
2. Using the "corr" function in R to determine the correlations between parameters
3. The resultant correlation matrix was then exported to excel
4. The final summary table was drawn up by referencing the relevant cells in the excel sheet using the "vlookup function"
5. Steps 1-3 were repeated for each of the data sets in question.

4.6 Limitations of the Study

4.6.1 Sampling Errors

Oxygenation/aeration of the water in the sample or during sampling will cause sampling errors which may occur in different ways. Boreholes behave as vertical hydrochemical "short-circuits" and expose the water column to atmospheric conditions, the DO and NO_3^- mix with dissolved Fe and/or Mn which results in oxide precipitation. During pumping, mixing of anoxic and oxic groundwater takes place when high concentrations of DO from the upper, unsaturated part of the aquifer and anoxic groundwater featuring elevated Fe or Mn concentration from the deeper, saturated part of the aquifer meet. Turbulent flow conditions present in the borehole enhance mixing. Degassing of CO_2 increases the pH which will increase the oxidation of Fe^{2+} and the precipitating oxides have an auto catalytic effect on the oxidation process. The borehole screens create a redox front which causes the precipitation of Fe hydroxides found in the saturated parts of the aquifer. Variation of oxygen content are caused by setting of submergible pumps into the screen slot, the declining static and dynamic groundwater levels into the casing interval, an unsuitable pump work scheme, aquifer recharge mode and the introduction of the piezometric heads into the screen slots which further leads to the groundwater being exposed to atmospheric conditions. Sample bottles that have oxygen/air can cause precipitation of Fe and/or Mn to take place as the CO_2 and oxygen will dissolve into the water and increase the pH which will cause the dissolved Fe and/or Mn to precipitate. Another limitation to the study was the Covid-19 global pandemic that delayed obtaining access to the sampling sites as well as the sampling activity that took place in this research project.

For this study there will be little use of the submersible pump as most of the sites where the samples were collected had boreholes fitted with pumps due to the circumstances under which the boreholes were drilled.

CHAPTER 5: RESULTS AND DISCUSSION

5.1 Spatial variation of Fe and Mn in the Western Cape Province

Data acquired from the National Groundwater Archive was used to generate two spatial distribution maps (Figure 9 and 11) of Fe and Mn. Figure 9 shows the locations of boreholes listed in the database, made up of 28 years of data with a total of 6345 points. The sites that had multiple data points which were collected over time were averaged and displayed on the maps. Fe^{2+} (Figure 9) and Mn^{2+} (Figure 11) concentrations were used to generate these maps. Five concentration ranges are displayed for the Fe^{2+} and Mn^{2+} data based on the database used. These distribution maps assist in understanding the background levels of Fe and Mn in the WCP.

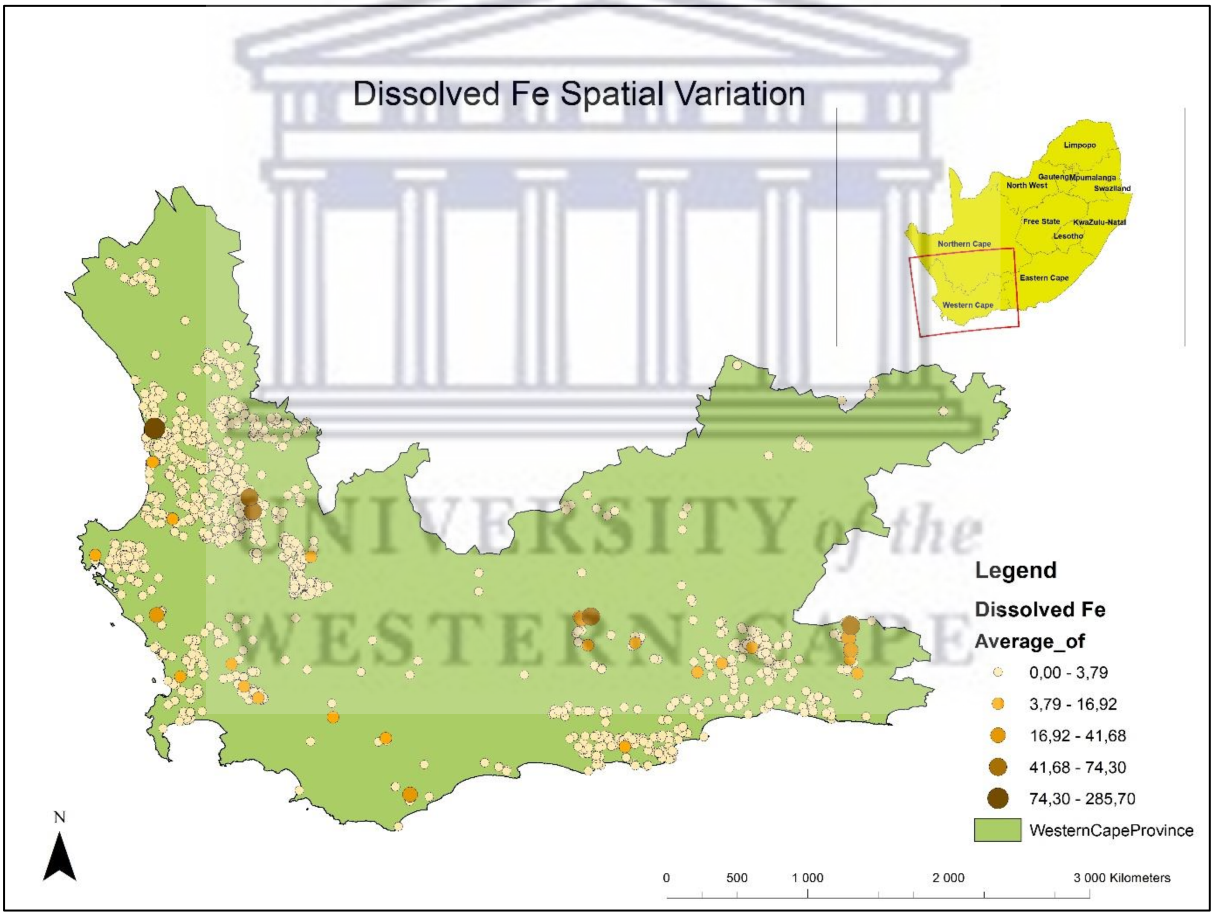

Figure 9: Spatial distribution map of Fe^{2+} in the WCP.

As seen in Figure 9 many data points are concentrated towards the north-western, south-western, and south-easterly parts of the province. These concentrations are mainly made up of a range between 0.00mg/L and 3.79mg/L as indicated in Figure 10. The points between 3.79mg/L and 16.92mg/L are spread from the south-western to south-eastern parts of the province. Ranges between 16.92mg/L and 41.68mg/L are mainly found at the lower south-easterly area of the province. Higher concentrations between 41.68mg/L and 74.30mg/L are found closer to the areas where there are concentrations between 16.92mg/L and 41.68mg/L. There was only one point of a range between 74.30mg/L and 285.70mg/L found on the western side of the province.

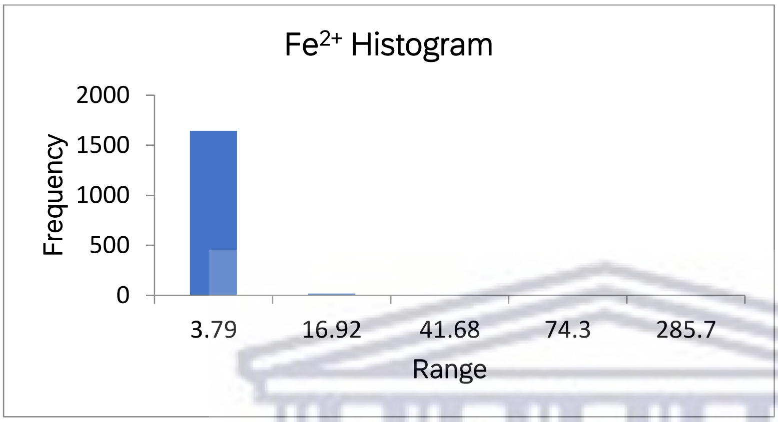

Figure 10: Histogram indicating the frequency of points per Fe2+ range.

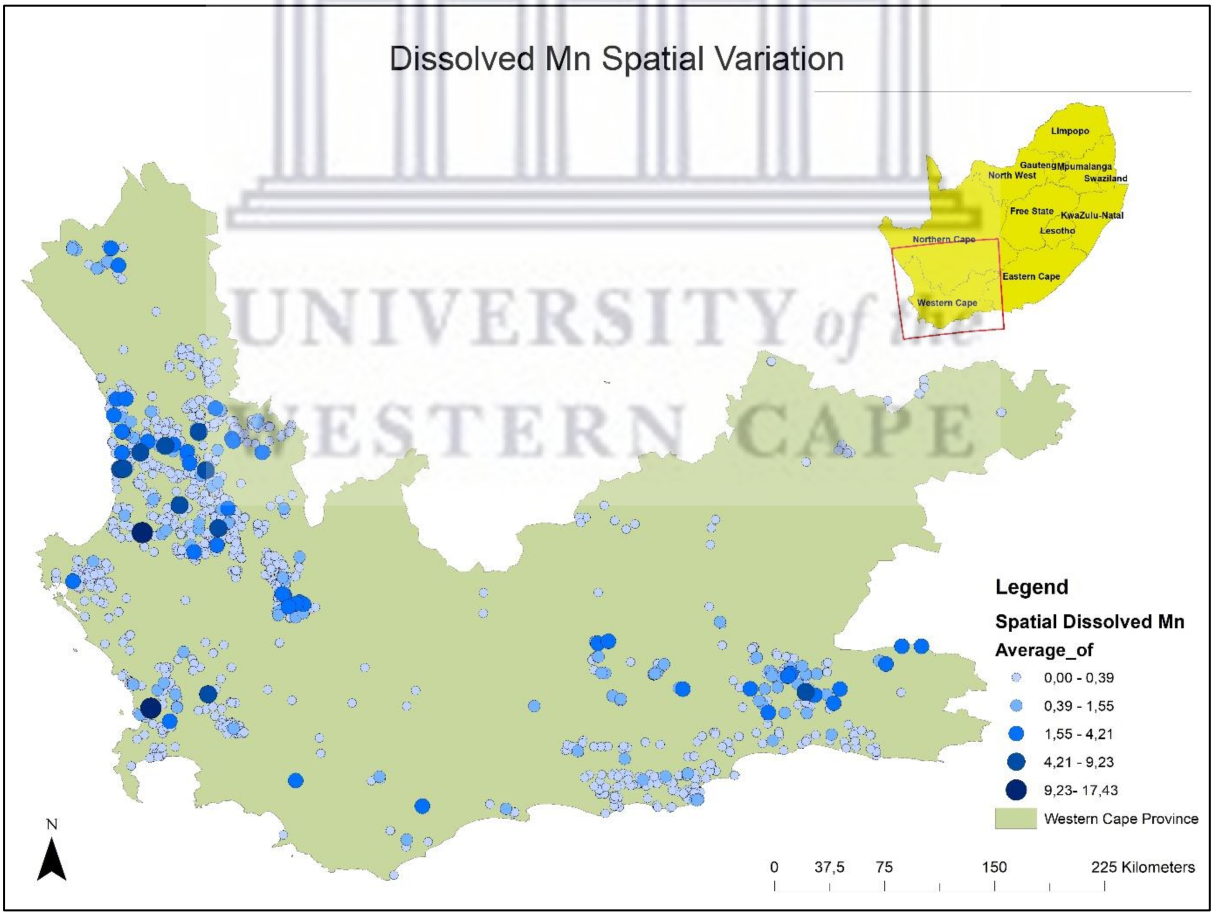

Figure 11: Spatial distribution map of Mn2+ in the WCP.

The concentrations of Mn^{2+} in Figure 11 are significantly lower than Fe^{2+} concentrations. The highest concentrations of Fe^{2+} are 285.70mg/L whereas the highest concentrations of Mn^{2+} are 17.43mg/L. Most of Mn^{2+} are concentrated towards the north-western, south-western, and south-easterly part of the province. Concentrations between 0.39mg/L and 1.55mg/L are also found in the north-western and south-eastern parts of the province. Points between 1.55mg/L and 4.21mg/L mirror the previous range of concentrations. The concentrations of 4.21mg/L and 9.23mg/L are mainly found at the north-western part of the province. The points between 9.23mg/L and 17.43mg/L are both found on the western part of the province.

The study by (Rossel *et al.*, 2010) states that the most abundant metallic oxides in soils are Fe oxides, oxyhydroxides and hydrated oxides and are found in various mineral forms. This can be seen in Figure 9 and Figure 11 for both Fe^{2+} and Mn^{2+} distribution across the WCP. (Smith and Roychoudhury, 2013) observed that locally Fe encrustation takes place when Fe^{2+} exceed 0.1mg/L and on a global scale, Fe encrustation problems are associated with unconsolidated aquifers with low concentrations of DO. China has increased Fe and Mn concentrations in more than 20% of its groundwater resources according to (Kang *et al.*, 2022). Therefore, these maps show the commonality of Fe and Mn occurring in the WCP.

5.2 Site specific processes that control the concentrations of Fe and Mn in groundwater

This section will consider the site-specific or local geological settings, borehole maintenance and water type for the sites sampled at where Fe and Mn was detected in the WCP as part of the business continuity project established at hospitals during the drought period in Cape Town.

5.2.1 Geology and lithology of boreholes of the selected sites

The stratigraphic column of the geology of the WCP is made up of firstly the Malmesbury group, Cape Granite Suite, Klipheuwel Group and lastly followed by the Table Mountain Group (Bargmann, 2003). The basement geology is characterized by shale, greywacke, conglomerate and quartzite and the Table Mountain Group made up of sandstone siltstone and shale (Bargmann, 2003). The business continuity project required geology which contained aquifers that could supply the sites with a continuous water supply. Major water supply aquifers are the Table Mountain Group and the Sandveld Group which are commonly used for municipal supply (Smith and Roychoudhury, 2013). This section makes use of geological maps and lithological logs of the sites sampled at to assess the influence of geology on the concentration of Fe and Mn in groundwater. A total of 5 sites from the business continuity project were sampled that are situated in Cape Town and the surrounding areas. Out of the 5 sites sampled, Brooklyn Chest Hospital (Figure 12), Kraaifontein Community Health Clinic (CHC) (Figure 14) and Paarl Hospital (Figure 15) were drilled into the basement geology called the Malmesbury Group. DP Marais Hospital (Figure 13) was drilled into the TMG. Sonstraal Hospital (Figure 16), which falls in the Kalahari Craton, is made up of weathered granite from the nearby Paarl Pluton and the basement Malmesbury group.

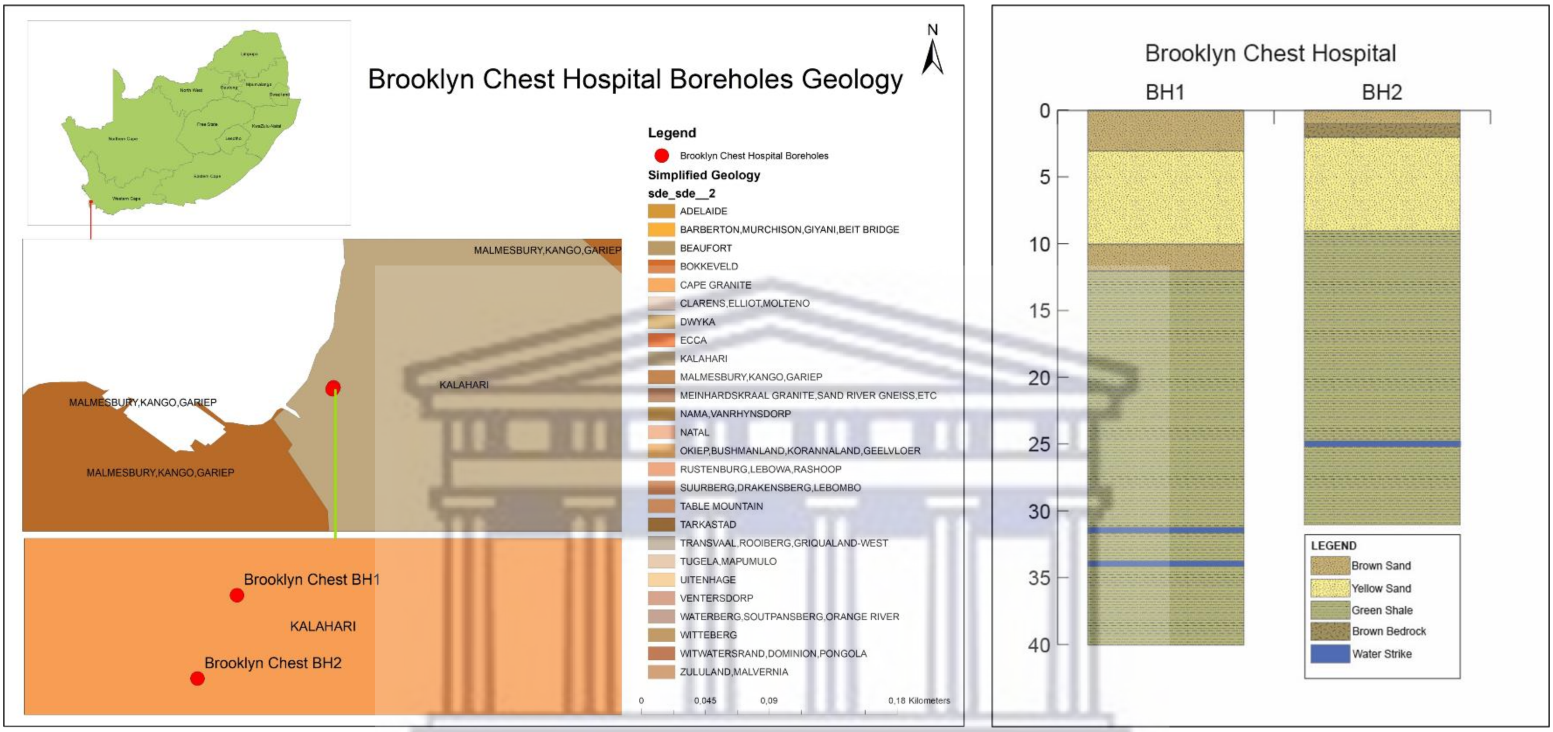

Figure 12: Geological map and lithological log of Brooklyn Chest Hospital boreholes drilled during the drought.

The Brooklyn Chest Hospital did not have a sample as the submersible pump was removed. However, the yellow and brown sand/bedrock lithology (Figure 12) is indicative of the presence of Fe minerals such as Goethite which is commonly found in earths geology (Cornell and Schwertmann, 2007). The yellow soil can be as a result of profile saturation for short periods of time which results in the formation of the mineral Goethite (Rossel *et al.*, 2010). It can be concluded that the yellow soil seen in the lithological logs have Goethite present as it is found in the upper layers near the surface of the boreholes. Due to the water strikes being present below the yellow and brown sand/bedrock it can be assumed that when pumping the anoxic groundwater encounters oxic water in these layers which results in the redox reaction taking place leading to the precipitation of Fe and Mn. This interaction was found in a study done in Germany that concluded on the incrustations found being due to the redox conditions of the aquifer (Houben, 2003). Another study in South Africa (Smith and Roychoudhury, 2013) also concluded that the dissolution of Fe from aquifer lithologies are effected by the redox reaction.

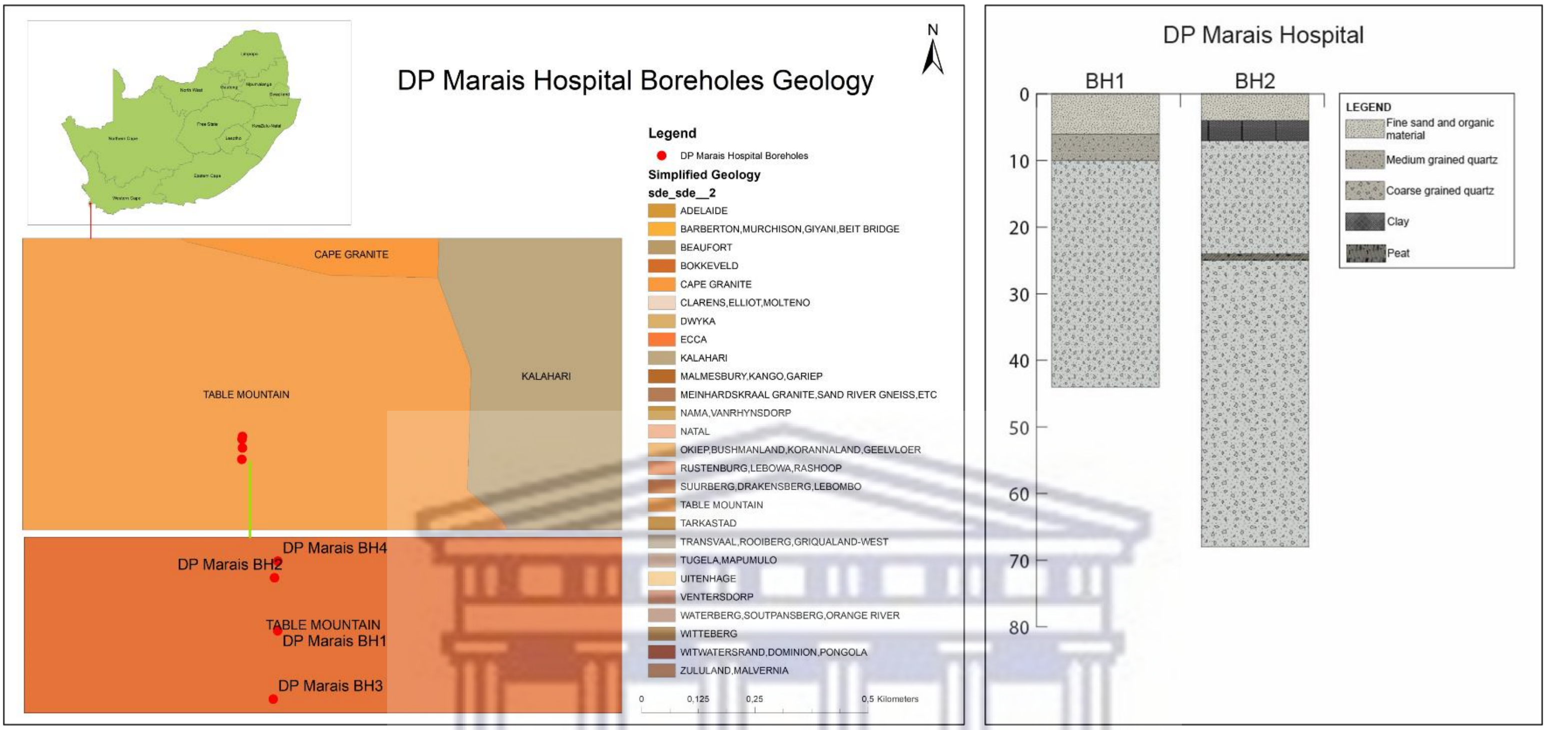

Figure 13: Geological map and lithological log of DP Marais Hospital boreholes drilled during the drought.

The DP Marais Hospital BH1 and BH2 (Figure 13) upper formations are made up of fine sand and organic material, medium grained quartz, coarse grained quartz, clay and peat. DP Marais Hospital had one of the highest Fe and Mn concentrations despite the characteristics of the TMG aquifer which is known to have better water quality than the other major aquifers in the WCP. A potential source of Fe in groundwater can be from carbonate and clayey deposits which are present in DP Marais Hospital BH2, a study in Lithuania by (Diliūnas and Jurevičius, 2006) made a similar observation. The capacity for the TMG aquifer to store water due to its sandstone nature therefore easily allowing the possibility for anoxic groundwater to mix with oxic groundwater allowing for redox reactions to take place (Department of Water Affairs and Forestry, 1996). Unfortunately, the drilling report did not state the level of where the water strikes took place so there is no mention of this information. In the Goudini Formation the lithology is made up of reddish brown quarzitic sandstone and siltstone which is a characteristic of Fe minerals Ferrihydrite, Hematite and Maghemite which was found during the purging of the boreholes (Figure 12) and in the samples collected (Figure 35 and Figure 36).

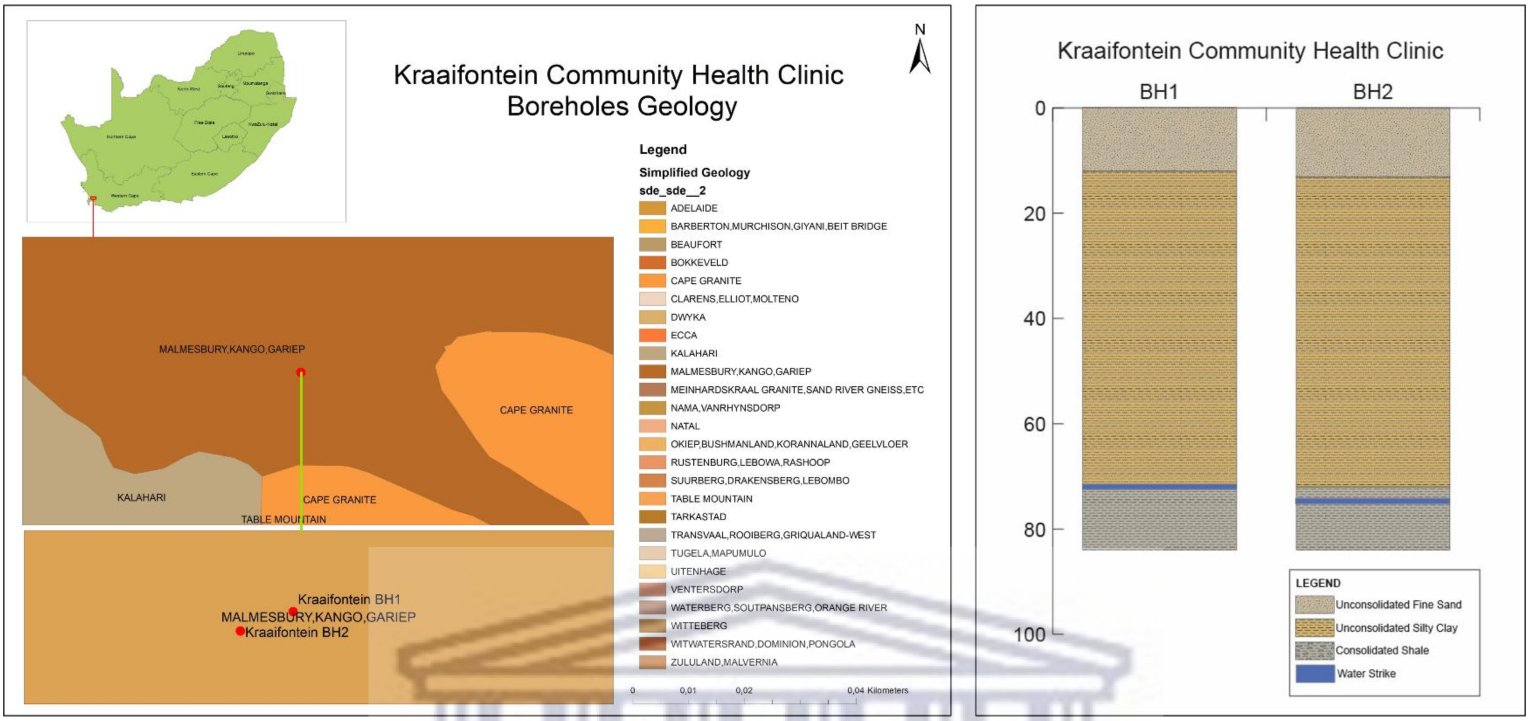

Figure 14: Geological map and lithological log of Kraaifontein Community Health Clinic boreholes drilled during the drought.

For the Kraaifontein CHC the pump was removed so no samples were collected to understand the relationship between the site geology/lithology log (Figure 14) Fe and Mn concentrations. According to the lithological log the unconsolidated fine sand, unconsolidated silty clay and consolidated shale are representative of the Tygerberg Formation where the clay layers are Fe stained. This can contribute to the brown water that came out of the tap as reported in the interview (Table 4).

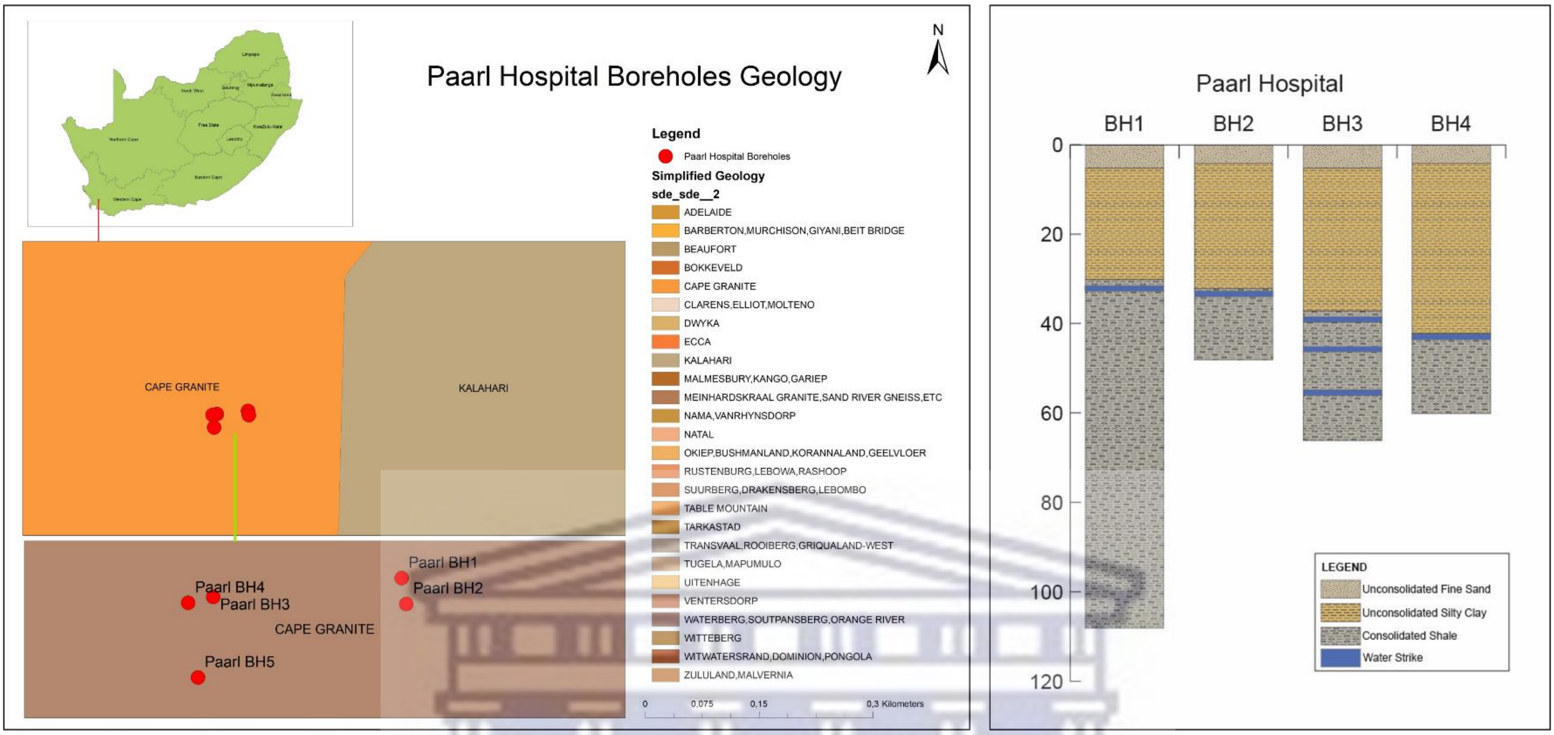

Figure 15: Geological map and lithological log of Paarl Hospital boreholes drilled during the drought.

The Paarl Hospital site has one of the clearest samples with low concentrations of Fe and Mn despite storage and transportation, which can be noted in Table 8 through the comparison of sampling techniques. The lithology of the Paarl Hospital, (Figure 15) is that of the Cape Granite Suite which has similar lithology to the Malmesbury Formation. The Paarl site is one of the more inland sites sampled at and close to a recharge zone of the Paarl mountain range.

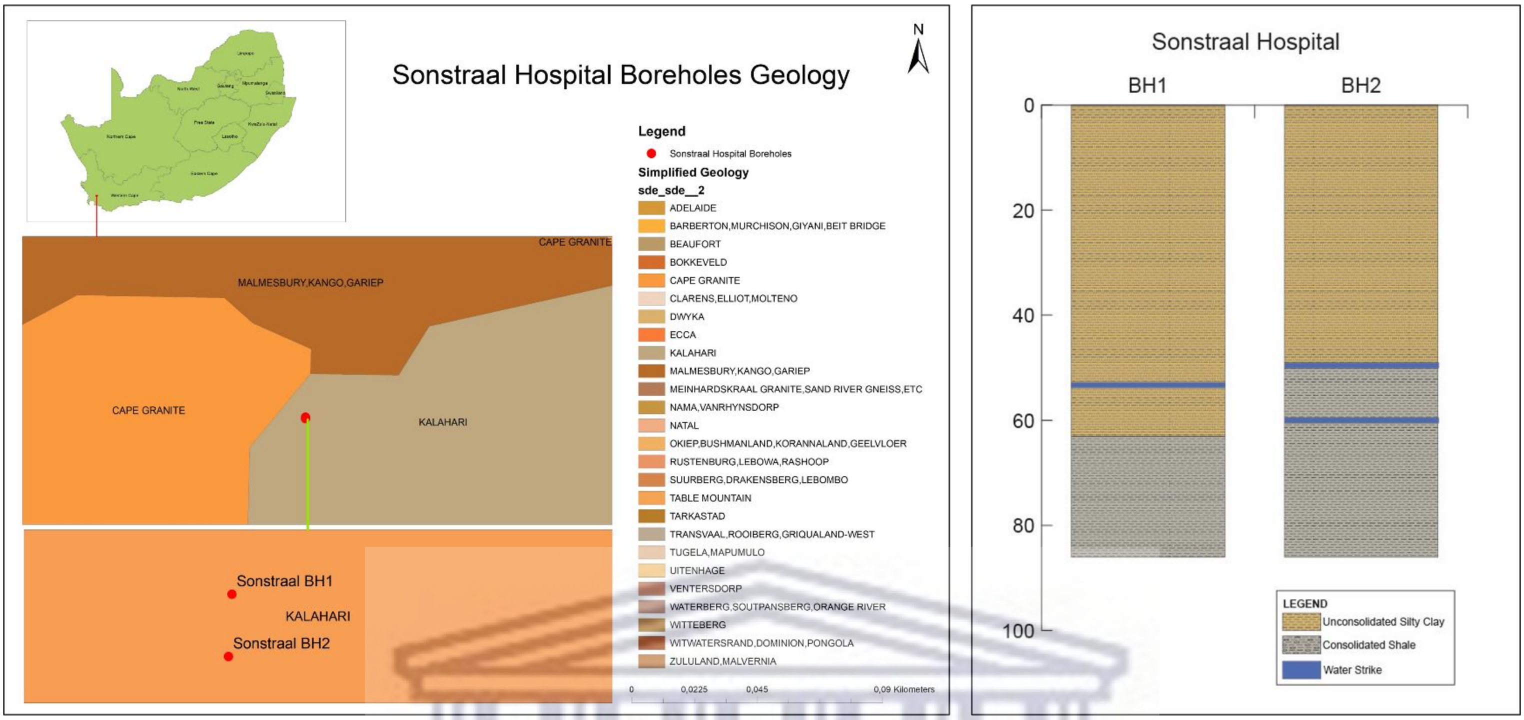

Figure 16: Geological map and lithological log of Sonstraal Hospital boreholes drilled during the drought.

The lithology of the Sonstraal Hospital (Figure 16) is made up of unconsolidated silty clay and consolidated shale. From the Fe and Mn immediate and lab analysed samples, the results show that Sonstraal had one of the lowest concentrations compared to the other sites, Table 7 reflect this information despite the patients in the hospital experiencing taste and water pressure issues.

From the project that was initiated to secure groundwater during the drought that threatened to interrupt the City of Cape Town municipal water supply, it was found that elevated Fe^{2+} concentrations between 2.5mg/L and 4.5mg/L was found in the Malmesbury Group (Conrad, Smit, Murray, & van Gend-Muller, 2019). The geology of DP Marais Hospital (Figure 13) where the boreholes were drilled are made up of the Table Mountain Group consisting of basement rocks of the Cape Granite Suite (Cape Peninsula Batholith) that is characterised by large alkali feldspar crystals in a finer grained quartz matrix.

The impact of recharge and infiltration was considered through the land use at all sites sampled at. The sites are all present in built up urban areas, no agricultural areas are present in the immediate surrounds. This may rule out pollution of groundwater through diffusion of pesticides. None of the hospital sites are located within a 0.5km radius of an industrial area or landfill which indicates that there is a small chance for point source contamination of the groundwater. The Paarl Hospital is placed close to the recharge zone of the nearby Paarl mountain range which could impact the boreholes as groundwater travels far distances before being discharged or pumped (Lerner and Harris, 2009). The land use of DP Marais Hospital is an urban built-up area as the other sites sampled at, except for the Keyser River. According to (Adelana, Xu and Vrbka, 2010), Cape Town groundwater recharge is attributed to water main leakage as well as irrigation water and man-made impacts on quality are a result from urbanisation and changes in land use, however in the case of Fe and Mn concentrations these do not pose a threat to groundwater quality and use. Pollutants move from point of infiltration at the land surface to the point of discharge which can be measured over years, decades or centuries (Lerner and Harris, 2009). This timeline is dependent on the characteristics of the aquifer and the length of the flowpath (Lerner and Harris, 2009). This process allows for the interaction between rock and water which influences the water quality, however this may not be a significant process when looking at its influence on Fe and Mn concentrations as the reaction is highly influenced by a more turbulent processes.

5.2.2 Borehole maintenance and management

All sites in this research project are maintained differently, and this has a direct impact on how the boreholes are managed. The person in charge of the site maintenance was interviewed and questioned and the information in Table 4 is supplied by this person. The water quality of the groundwater pumped from boreholes can reflect the management of the boreholes. An unsuitable and unsustainable pumping regime can result in the disturbing the geochemical conditions of the aquifer system (Majkić-Dursun, Petković and Dimkić, 2015). Knowing the purpose of what the water is used for suggests how much water is required and the required pumping regime.

Table 4: Summary of sampling site interviews.

Questions	**Paarl Hospital**	**Kraaifontein CHC**	**Sonstraal Hospital**	**DP Marais Hospital**	**Brooklyn Chest Hospital**
What is the water used for?	Drinking and domestic use	Drinking and domestic use	Drinking water	Drinking and domestic use	Domestic water use
How often is sampling conducted?	Monthly	Sampled twice a month	Sampled twice a month	Monthly	Monthly
Are heavy metals analysed if sampling is done?	Report sent away	Did not see sampling report	Did not see sampling report	Unsure	Unsure
Has there been any iron clogging issues?	Issues with iron clogging or iron build up on elements	No issues with clogging	Taste issues and water pressure issues	Patients complained about clay taste	
How long is the borehole pumped for?	Pumps for 24 hours and pump until reservoir 200000 kl is filled. But use municipal water now.	Pump switched on at 4pm and off at 7pm	Stays on	Not sure, did not have ownership	
Is the pump switched off and on?	It depends on the use	Yes	No	Yes	Yes
Is the water treated before use?	Treatment plant		Treatment plant	No	
Has a pump test been conducted after drilling?			No		
Comments		Couldn't sample because all pumps were removed and borehole entrances blocked Noticed the water was brown at first and had to wait a few minutes for the colour to change No complaints about taste from those drinking Currently using municipal water			Only been in use for 3 months and then the project was shutdown Noticed brown water and patients are complaining and getting sick

All sites in Table 4 used the water for drinking and domestic use. The pumping regime differed from site to site with some of them staying on as well as switching on and off and other sites not having ownership so they could not comment. Samples were collected between once and twice a month; however, all the site maintenance managers did not know if heavy metals were analysed as the reports were sent away.

When asked about Fe clogging and build-up of Fe, only Paarl Hospital reported that elements of the system had build-up of Fe as Sonstraal and DP Marais Hospitals had patients complain about the taste of the water. Sonstraal Hospital reported on the reduced water pressure which could be attributed to the build-up of Fe that can lead to reduced water pressure, this compares to the work of (Smith and Roychoudhury, 2013). Kraaifontein CHC was not sampled as the pumps were removed and borehole entrances were blocked, however, it was noticed that the water colour would be brown at first and after a few minutes the colour would change and clear up. Brooklyn Chest Hospital was only in use for 3 months before the project was shut down but the same issue of water coming out brown from the tap was reported as Kraaifontein CHC and patients complained about the taste and got sick.

5.2.3 Water Quality

Determining the water type to understand the water quality is considered to be an important factor when assessing the site-specific conditions that may influence the concentration of Fe and Mn in groundwater. Figure 16 shows a trilinear pipe diagram characterising the water types of the 3 sites sampled during this research project.

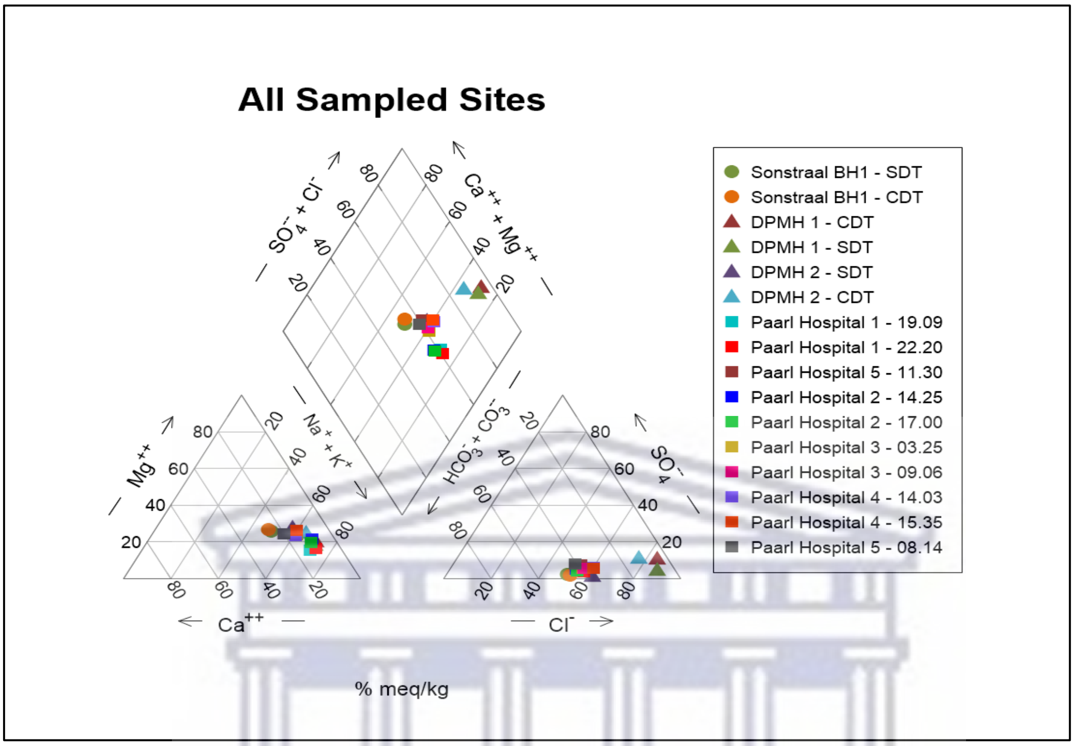

Figure 17: Piper diagram indicating water types of 3 different sampling sites.

The piper diagram represents 3 of the sampling sites. This chemistry data is from drilling reports taken at different times and constant drilling test or step drawdown test conducted by (Gaffoor and Pietersen, 2018).

Sonstraal Hospital water is representative of all four water quality types, calcium sulfate, sodium chloride, sodium bicarbonate and calcium bicarbonate. This indicates that mixing between different water types has taken place which may be attributed to the bedrock and recharge zone near the hospital. The Sonstraal Hospital boreholes are drilled, as seen in Figure 16, into materials consisting of weathered granite from nearby Paarl granite pluton and the water strikes are in the weathered upper portion of the Malmesbury Group consisting of shales. The sources of bicarbonate may be due to the presence of organic matter in the aquifer that is oxidized to produce carbon dioxide that enhances the dissolution of minerals. The Malmesbury shale may have been a source for sulfate by the dissolution of sulfur bearing minerals. The sodium in groundwater may be as a result of the weathering of halite and silicate minerals like feldspar and calcium may also be sourced from the same feldspar as well as pyroxenes. The further surrounding land use is agricultural land which may contribute towards the sodium and calcium in the groundwater.

DP Marais Hospital water is representative of sodium chloride at both BH1 and BH2 and could be as a result of groundwater residence time within the clay-rich weathered Cape Peninsula Batholith. This is found to agree with the comments from the patients of the hospital that complained about the water having a clay taste (Table 4). This is supported by the high EC that can be as a result of the quartz layers which have dissolved that resulted in a more acidic water.

Paarl Hospital has 5 boreholes which are each sampled twice and representative of a mixed water type of sodium bicarbonate and sodium chloride. According to the Paarl Hydrocensus report, it was observed that places surrounding the hospital did not report any water quality issues. The high concentration of sodium chloride can be attributed to the unconsolidated silty clay geology. As sodium is one of the most abundant members of the alkali metal group of studied groundwater, it may be sourced from alkali granite intrusive which is part of the Cape Granite Suite which is the where the Paarl Hospital boreholes are drilled into (Figure 15).

5.3 Likelihood of precipitation of Fe and Mn based on detected solution composition through PHREEQC modelling.

PHREEQC modelling was used in two ways for this research project. It was used to analyse the samples collected from all sites to show the saturation of mineral phases. It was also used to for the prediction of mineral saturation under different conditions by changing the Fe concentrations, Mn concentration, pH levels, temperature and the redox potential incrementally.

5.3.1 Saturation Indices of points sampled

Saturation indices are a method used to predict the relative mineralogy of the lithological unit from groundwater without collecting a solid sample to analyse the mineralogy (Kaliammal and Udayanapilai, 2018). In this research project PHREEQC, the modelling software, was used to calculate the saturation indices of the minerals from all sites sampled at in Table 5. Saturation indices that are greater than zero indicate that the mineral is precipitated and in an oversaturated state, if it is zero the mineral is at an equilibrium state and if less than zero it in the under saturated state therefore the mineral is in dissolved in solution (Kaliammal and Udayanapilai, 2018).

Table 5: Saturation Indices of collected groundwater samples for all sampled sites.

Saturation Indices of Sampling Points							
Mineral Phase	**Chemical Composition**	**DPMH01 - SI Log**	**DPMH02 - SI Log**	**Paarl - SI Log**	**Sonstraal - SI Log**	**UWC BH4 - SI Log**	**UWC BH5 - SI Log**
Calcite	CaCO3	-3.73	-2.15	-0.92	-0.94	0.08	-1.06
Dolomite	CaMg(CO3)2	-7.37	-3.69	-1.66	-1.71	-0.63	-1.98
Fe(OH)3(a)	Fe(OH)3	-3.09	0.00	-0.18		-1.27	-0.73
Gibbsite	Al(OH)3	1.82	0.63		0.61	0.17	0.01
Goethite	FeOOH	2.65	5.74			4.46	5.00
Hausmannite	Mn3O4	-34.15	-18.40	-18.57	-24.32		5.00
Hematite	Fe2O3	7.29	13.47			10.91	11.99
Jarosite-K	KFe3(SO4)2(OH)6	-12.51	-10.41			-14.14	-14.72
Manganite	MnOOH	-12.94	-7.20	-7.06	-9.28		-6.39
Melanterite	FeSO4:7H2O	-6.09	-8.67			-10.80	-10.90
Pyrochroite	Mn(OH)2	-12.08	-7.76	-8.31	-10.10		-7.26
Pyrolusite	MnO2:H2O	-20.38	-13.24	-12.35	-14.69		-12.14
Rhodochrosite	MnCO3	-5.02	-1.53	-2.66	-3.89		-1.10
Siderite	FeCO3	-2.75	-1.90			-4.15	-3.02

Table 5 shows the saturation indices for each sampling site and the minerals found in the saturated (shaded in grey) and unsaturated state. The saturation indices of BH1 at DP Marais Hospital for Fe-bearing minerals were majority in the unsaturated state except for Gibbsite, Goethite and Hematite that are found in the saturated state. The saturated conditions of these three minerals are expected as they are commonly found in rocks and soils in various parts of the earth according to (Cornell and Schwertmann, 2007). From the PHREEQC modelling it indicated that these three minerals can precipitate from solution based on the concentrations present in the sample analysed at the lab. All Mn bearing minerals are in the unsaturated state. This indicates that weathering of these minerals will continue to take place from the surrounding geology. Carbonate minerals (Calcite and Dolomite) are also mainly in an unsaturated state which indicates that these minerals will remain dissolved in solution.

The saturation indices for BH2 at DP Marais Hospital for Fe bearing minerals Goethite and Hematite from the PHREEQC modelling are in a saturated state whereas the remaining minerals are in an unsaturated state. This indicates that these minerals will be in a precipitated form. Fe(OH)3(a) and Gibbsite minerals are found in a near-neutral state. The remaining Fe, Mn and carbonate bearing minerals are in an unsaturated form indicating that weathering of these mineral will take place from the surrounding geology. From the above results it was expected that the mineral $Fe(OH)_3$ would be in the precipitated form or at higher saturation indices as stated by (Lin, Jia and Xu, 2007) since it is drilled into the TMG geology.

From the Paarl Hospital sample the following minerals, Gibbsite, Goethite and Hematite did not appear in the selected output file. The Fe, Mn and carbonate minerals are all found, through the PHREEQC modelling, in an unsaturated state except for Calcite and Fe(OH)3(a) which are found in a near-neutral state.

The Sonstraal Hospital sample is very similar to the Paarl sample as there were no minerals in the saturated state. Calcite and Gibbsite were all found in a near neutral state. This indicates that no precipitation of Fe and Mn is found. Therefore, the chance of borehole clogging at the Sonstraal hospital is insignificant. Fe(OH)3(a), Goethite, Hematite, Jarosite-K, Melantite and Siderite did not appear in the selected output file.

At UWC BH4, the minerals Goethite and Hematite, which are two of the most popular Fe bearing minerals, are found in the saturated state, through PHREEQC modelling, indicating that these minerals will be found in the precipitated form. Carbonate and the Fe mineral Gibbsite are found in an equilibrium state. The Mn bearing minerals in the selected output file did not appear in the unsaturated, equilibrium or saturated state. Therefore, the sample only reflects Fe precipitation.

In BH5 at UWC, Goethite and Hematite are in saturated state, found through PHREEQC modelling, meaning they will be in the precipitated form. The Fe bearing minerals Fe (OH)3(a) and Gibbsite are found in near-neutral states whereas the rest of the Fe, Mn and carbonate minerals are all found in the unsaturated form.

The above results may be attributed to the mixing of oxic and anoxic groundwater, which leads to the precipitation of Fe, Mn and carbonate minerals and with time leads to Fe encrustation and clogging issues in boreholes (Smith and Roychoudhury, 2013). As Fe and Mn behave geochemically similarly and are widely found in aquifers and soils, their concentrations seen in Table 7 may be as a result of reducing conditions, residence time, well-depth, and salinity which are the key factors leading to the dissolution and migration of Fe and Mn in groundwater (Zhang *et al.*, 2020). The aquifers and soils of the site may release organic matter into the groundwater which deplete DO resulting in a more reductive hydrochemistry (Zhang *et al.*, 2020).

5.3.2 *Modelling*

PHREEQC was used to model the saturation indices of Fe and Mn minerals with the change in certain conditions such as Fe and Mn concentrations, pH, temperature and redox potential. The sample selected for modelling was the DP Marais Hospital BH2 and chosen as it had both Fe and Mn present in its samples. The natural presence of Fe and Mn in the groundwater made the site suitable for modelling as the change in the pH, temperature and redox potential parameters with the presence of Fe and Mn would mirror the natural settings found in the WCP as observed in Figure 9 and 11 earlier. Therefore, making the predictions of chemical changes in the groundwater during pumping from the modelling more reliable.

a.

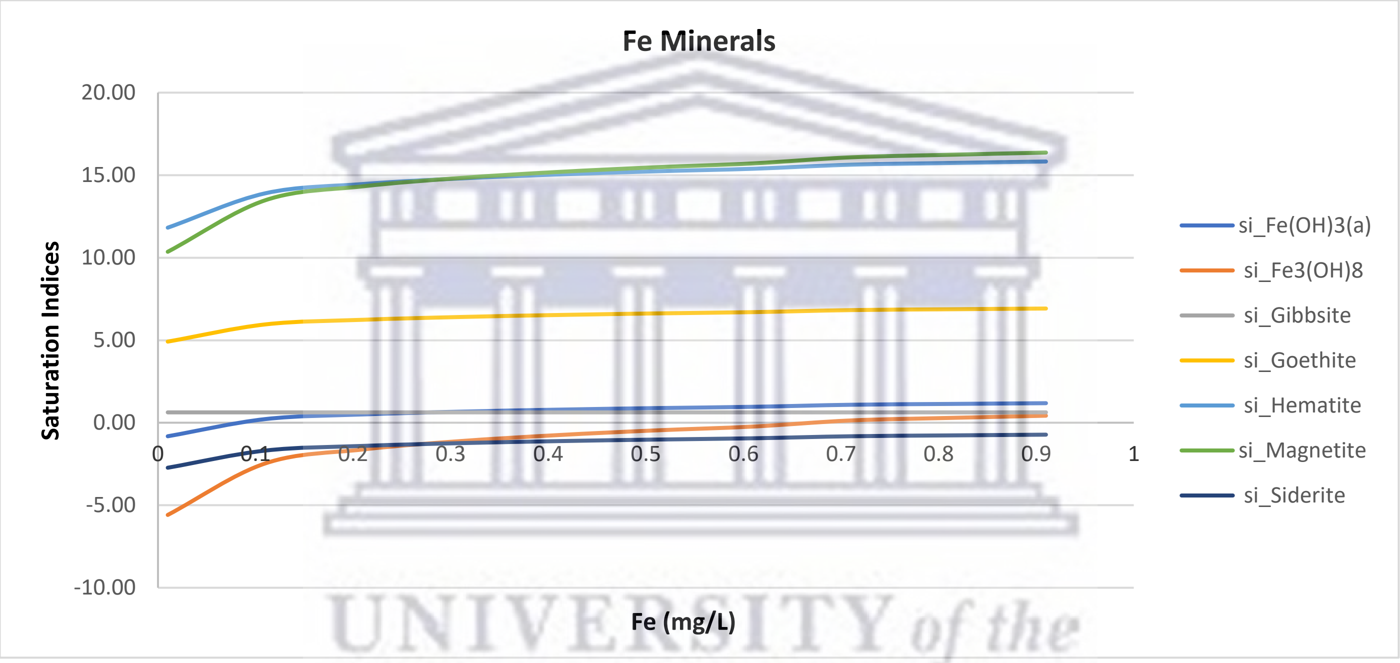

Figure 18a: Incremental modelling of Fe concentration against Fe (a.) and Mn (b.) minerals.

b.

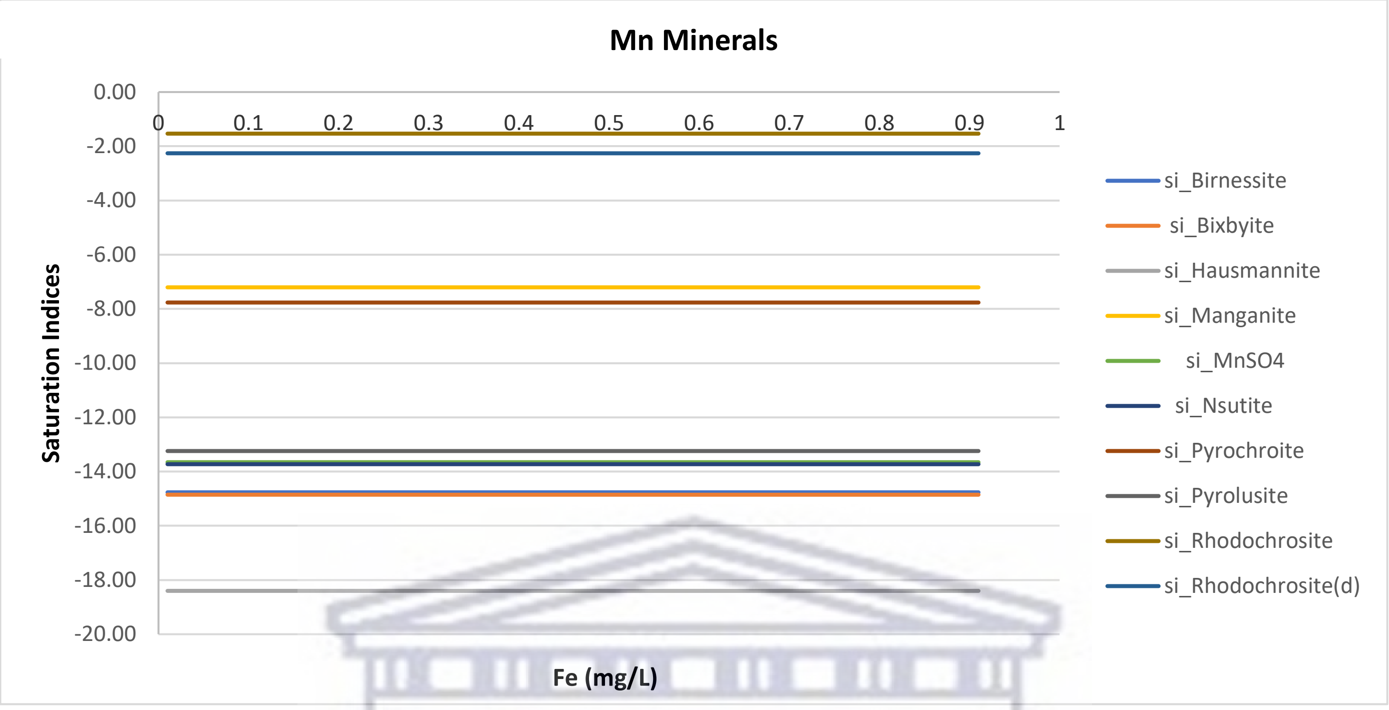

Figure 198b: Incremental modelling of Fe concentration against Fe (a.) and Mn (b.) minerals.

Figure 18 displays the incremental reaction modelling done for the sample from DP Marais Hospital BH2. The model included 10 steps from 0.01mg/L to 0.91 mg/L with the output minerals being either Fe (Figure 18a), Mn (Figure 18b) as well as carbonate minerals. The carbonate minerals of calcite and dolomite showed no change. The saturation indices of the Fe bearing minerals, except for Gibbsite indicate an increase in saturation indices, Figure 18 represents this precipitation trend. Therefore, with an increase in Fe concentration Fe bearing minerals (Figure 18a) will be in a precipitated state which may result in borehole clogging. Mn bearing minerals (Figure 18b) and reflected no change in saturation indices with the increase in Fe concentration. This indicted that there is a direct relationship between the increase in Fe concentration and the precipitation of Fe-bearing minerals.

a.

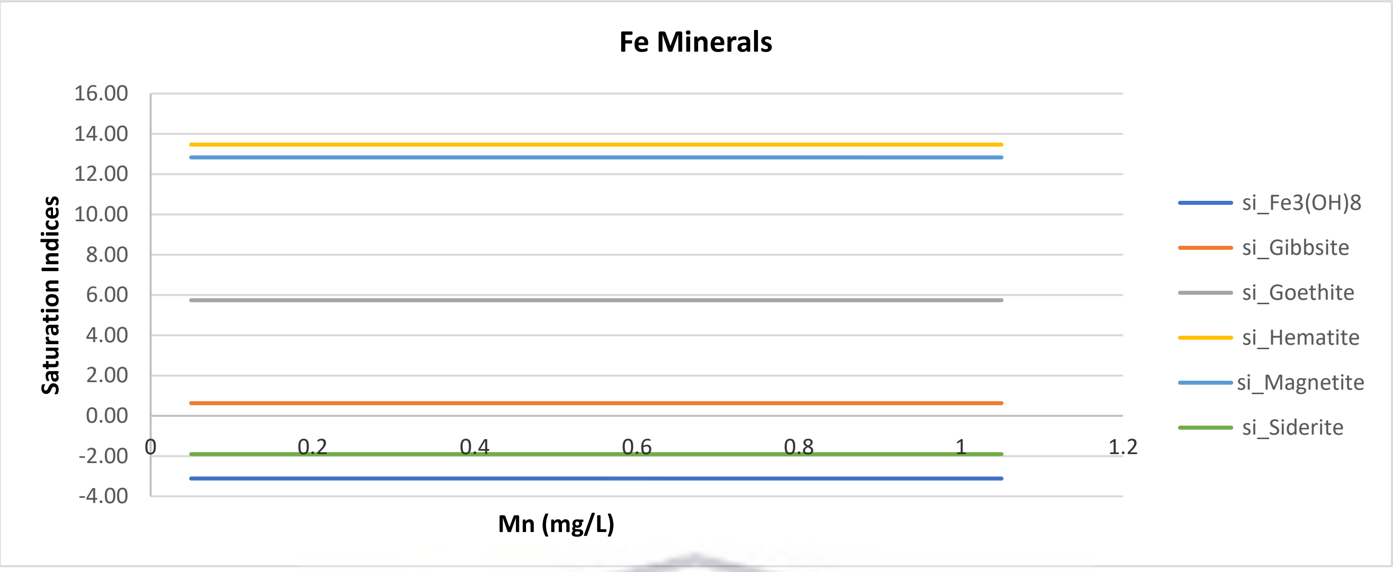

Figure 19a: Incremental modelling of Mn concentration against Fe (a.) and Mn (b.) minerals.

b.

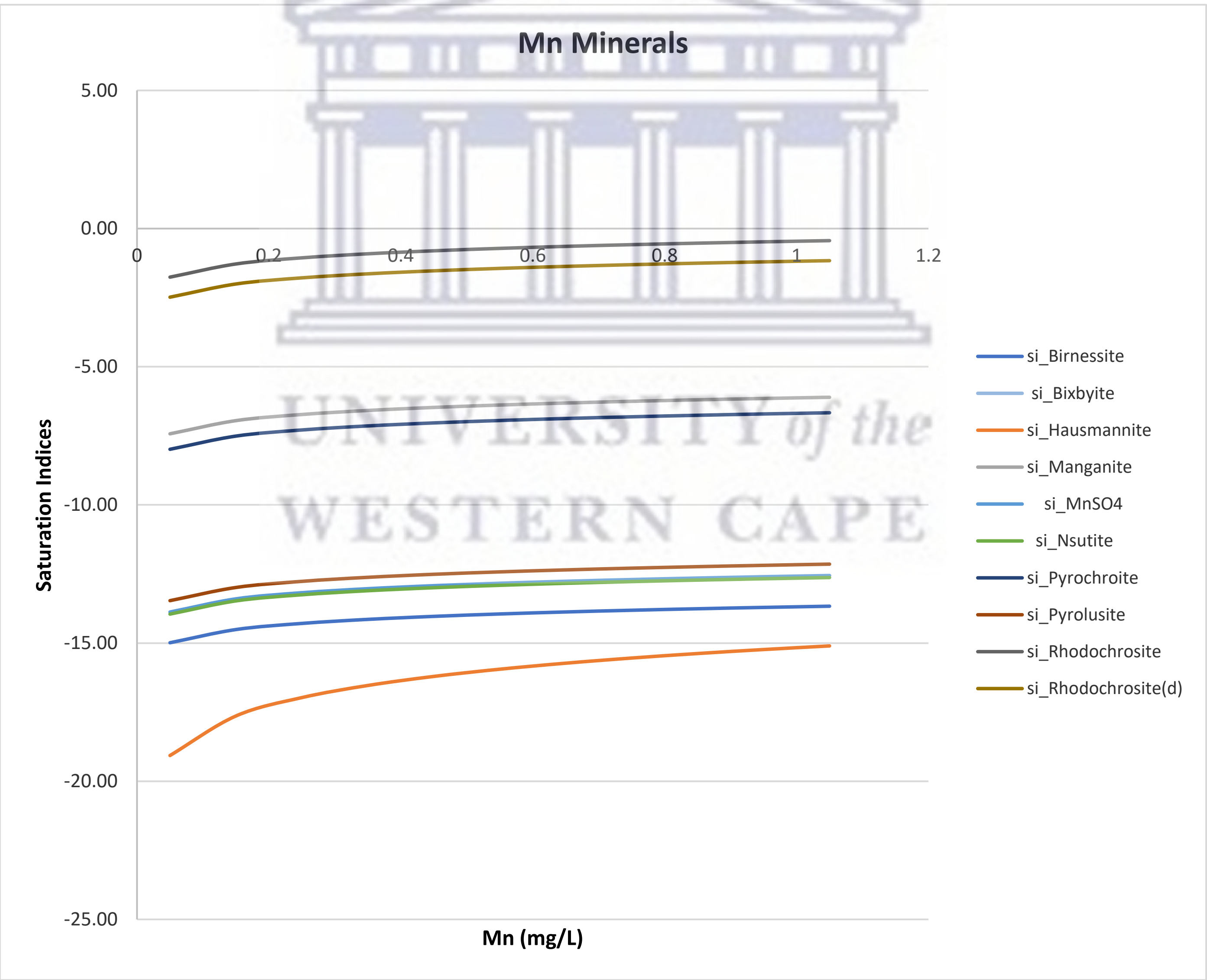

Figure 19b: Incremental modelling of Mn concentration against Fe (a.) and Mn (b.) minerals.

Figure 19 displays the increase of Mn concentration against Fe (Figure 19a.) and Mn (Figure

19b.) minerals which was modelled in 11 steps from 0.05 mg/L to 1.05 mg/L. It was observed that with an increase in Mn concentrations there is no change in the saturation indices for Fe bearing minerals, Mn bearing minerals and carbonate minerals (dolomite and calcite). The Fe bearing minerals Goethite, Hematite and Magnetite are all found in saturated states from the sample chemistry and remain so despite the increase in Mn concentration. All Mn bearing minerals are in an unsaturated state at concentrations of 1.05mg/L and below and may not be the cause of precipitation in boreholes, therefore these minerals found in boreholes may be as a result of weathering from the surrounding geology.

Figure 20 shows the effect of incrementally increasing the pH from 3 to 9, in 13 steps in 0.5 increments on Fe, Mn and carbonate minerals. The saturation indices for Fe bearing minerals increase as the pH value increases until a certain point at which the saturation indices begin to decrease, showing a trend of precipitation and dissolution.

a.

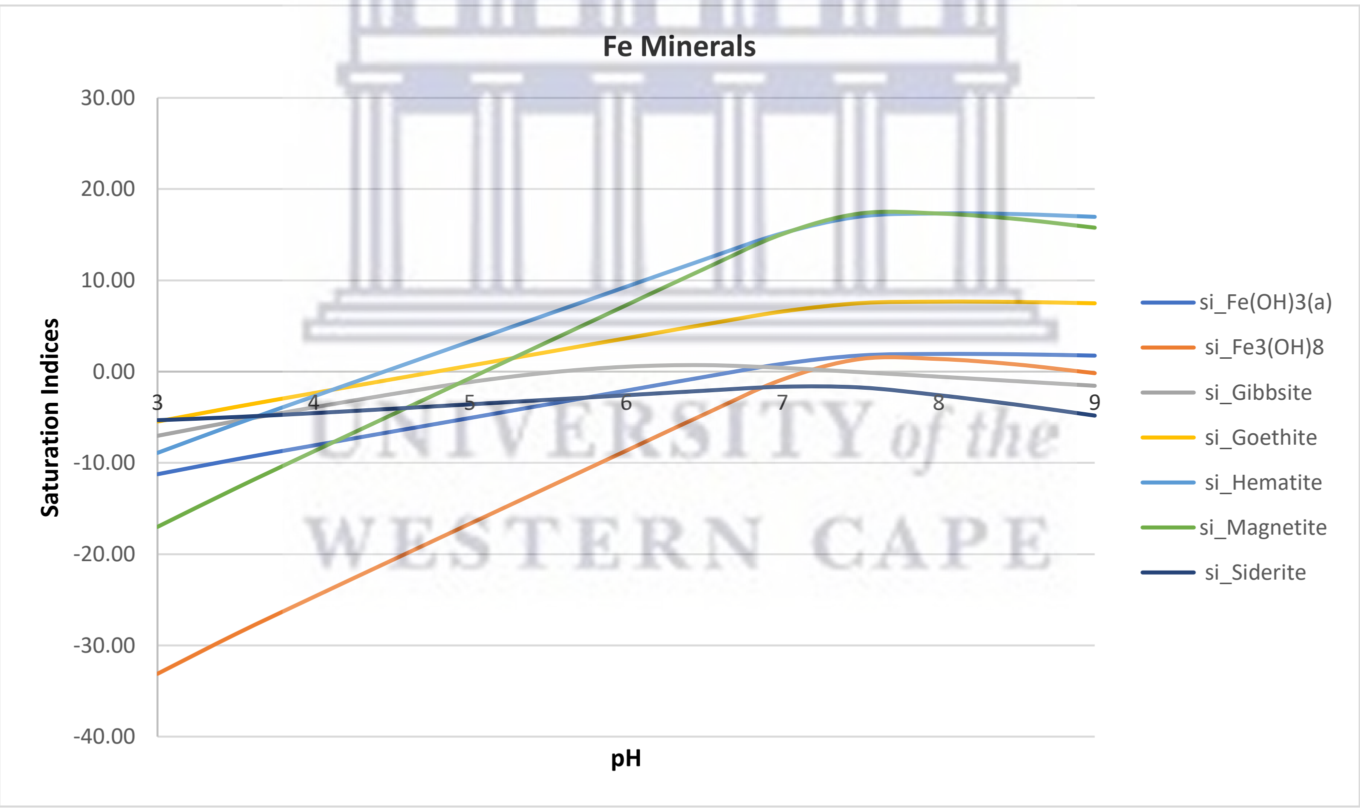

Figure 20a: Incremental modelling of pH levels against Fe (a.), Carbonate (b.) and Mn (c.) minerals.

b.

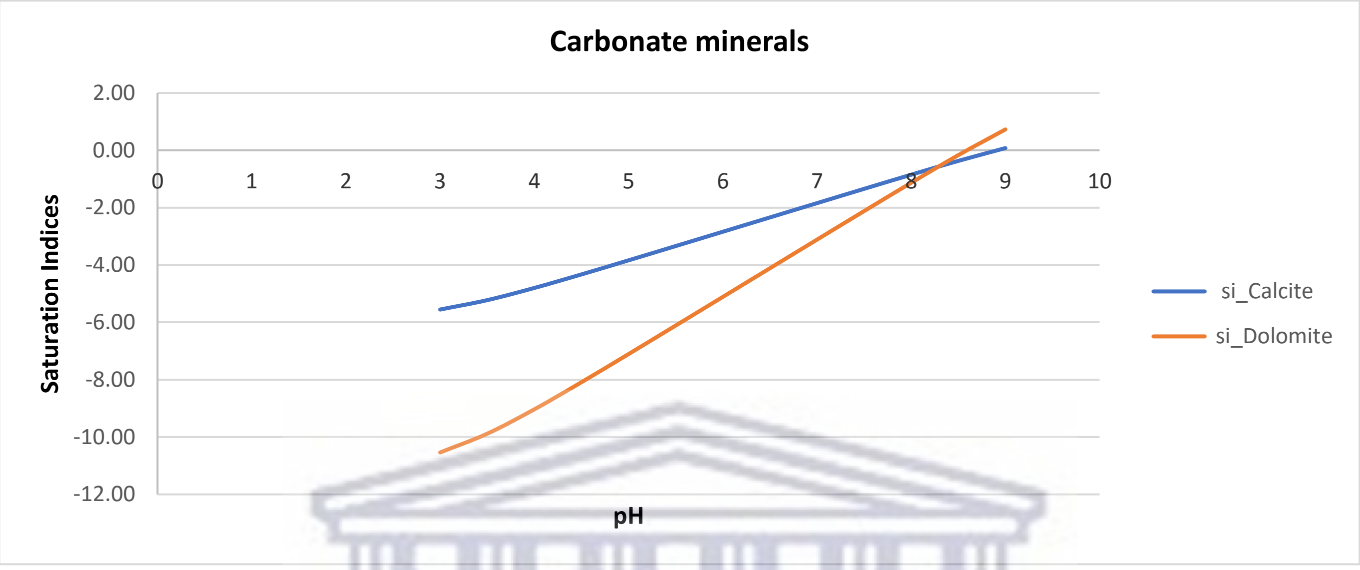

Figure 20b: Incremental modelling of pH levels against Fe (a.), Carbonate (b.) and Mn (c.) minerals.

c.

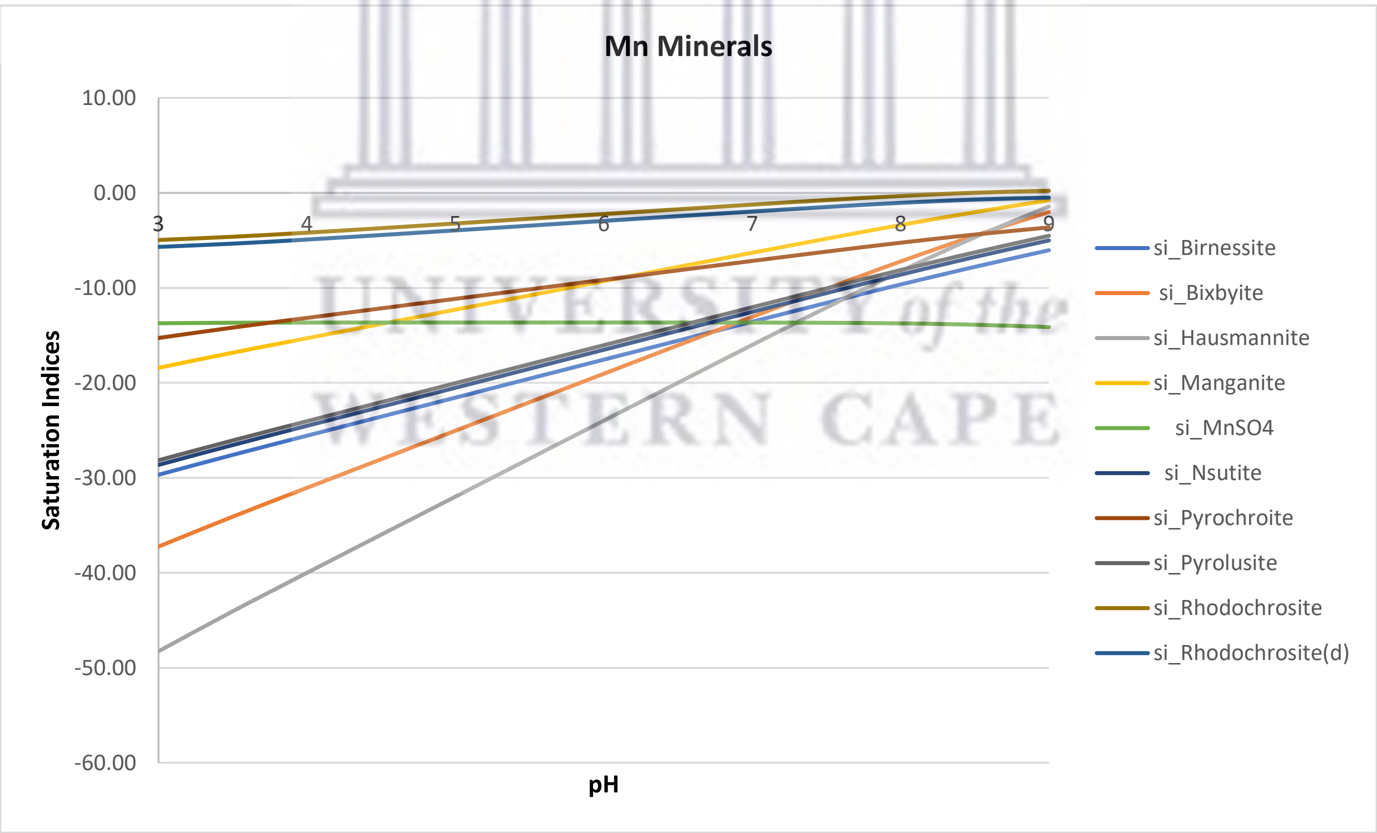

Figure 20c: Incremental modelling of pH levels against Fe (a.), Carbonate (b.) and Mn (c.) minerals.

All Mn bearing (Figure 20c.) minerals remain in an unsaturated state except for the mineral Rhodochrosite which reached a near-neutral stage. Mn2(SO_4)3 and $MnSO_4$ saturation indices increased but at a very minimal rate compared to the other minerals. Carbonate minerals both increased from an unsaturated to saturated states showing a strong precipitation trend however they increased from an unsaturated state to a state of equilibrium.

Fe is found in solution in water with a pH greater than 3, Fe^{3+} specifically is at near neutral pH (6.3 – 6.8) and is insoluble that precipitates as Fe oxy-hydroxide minerals according to (Smith and Roychoudhury, 2013). As seen from Figure 20a, between the pH 3 and pH 7 the major Fe minerals Goethite, Hematite and Magnetite are in the saturated form. Borehole pH may increase to near-neutral levels if the borehole is exposed to air which is likely to happen during pumping, the dissolved oxygen diffuses into the groundwater resulting in the degassing of CO_2 leading to the increase in pH and precipitation of Fe minerals. For future studies it is worth investigating the microbiological effects on pH levels against the precipitation of Fe, Mn and carbonate minerals.

a.

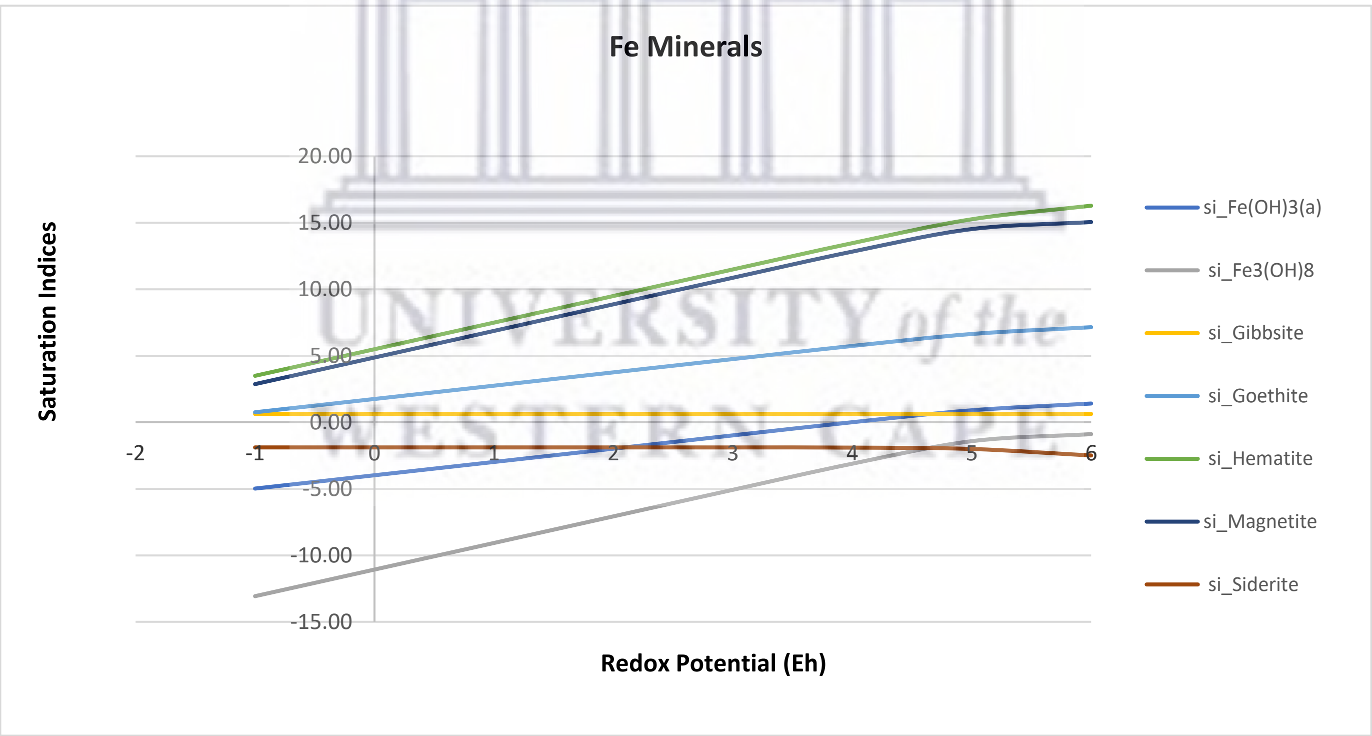

Figure 21a: Incremental modelling of Redox Potential (Eh) levels against Fe (a.) and Mn (b.) minerals

b.

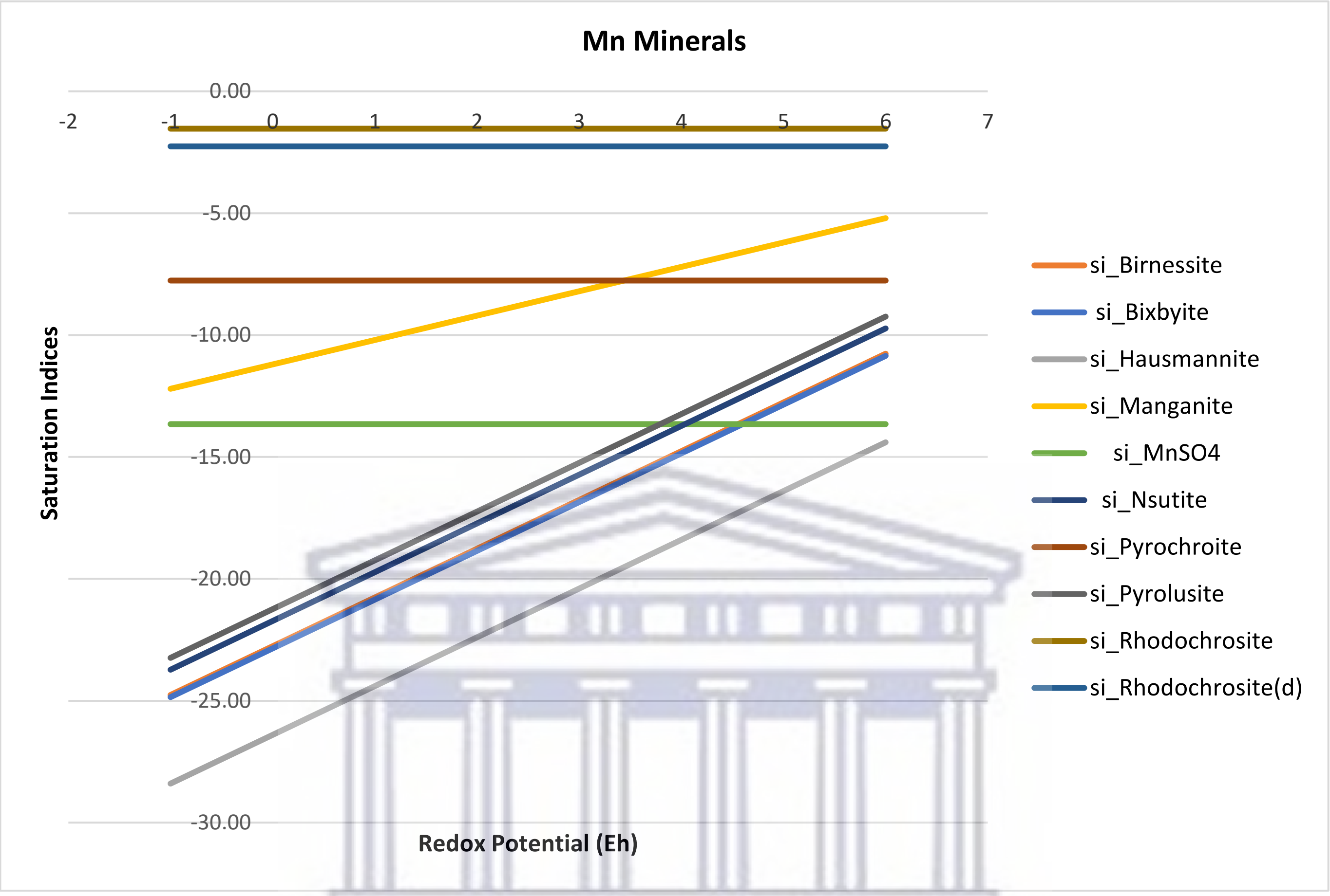

Figure 21b: Incremental modelling of Redox Potential (Eh) levels against Fe (a.) and Mn (b.) minerals

Figure 21 shows incremental modelling of the redox potential between -1 and 6 on Fe (a.) and Mn (b.) minerals, this modelling was conducted on carbonate minerals (dolomite and calcite) however no reaction took place. In the Fe bearing mineral model (Figure 21a), Gibbsite saturation indices increased with the increase in redox potential. Fe3(OH)8 and Siderite resulted in unsaturated saturation indices indicating a dissolution trend. The remaining Fe minerals indicated a precipitation trend indicating that with an increase in redox potential there will be an increase in the precipitation of Fe bearing minerals. Mn bearing minerals show an increase in saturation indices yet remained in the unsaturated state at a redox potential of 6. The precipitation of Fe may precipitate before Mn or increase in saturation indices due to the "level" of redox potential according to (Braester and Martinell, 1988). There are minerals that did not change in state with an increase in redox potential. Fe and Mn minerals did not change their saturation indices with an increase in redox potential.

Negative Eh values symbolize in-situ polluted groundwater therefore to account for this the model began at -1 (Weaver *et al.*, 2004). At low Eh value Fe^{2+} concentration is high in soil solutions but as Eh rises the formation of Fe oxy-hydroxides take place (Husson, 2013). As seen from Figure 31 the positive Eh values result in the saturation of major Fe minerals Goethite, Hematite and Magnetite. As stated by (Houben, 2003), Fe and Mn oxides rarely occur together in the same borehole due to different potentials required for formation which is seen in Figure 20 for the Mn mineral saturation indices. The effect of the redox reactions on the influence of Fe and Mn concentrations have been documented in many studies such as (Braester and Martinell, 1988; Houben, 2003; Morris *et al.*, 2003; Pullin and Cabaniss, 2003; Diliūnas and Jurevičius, 2006; Pinti, 2015).

a.

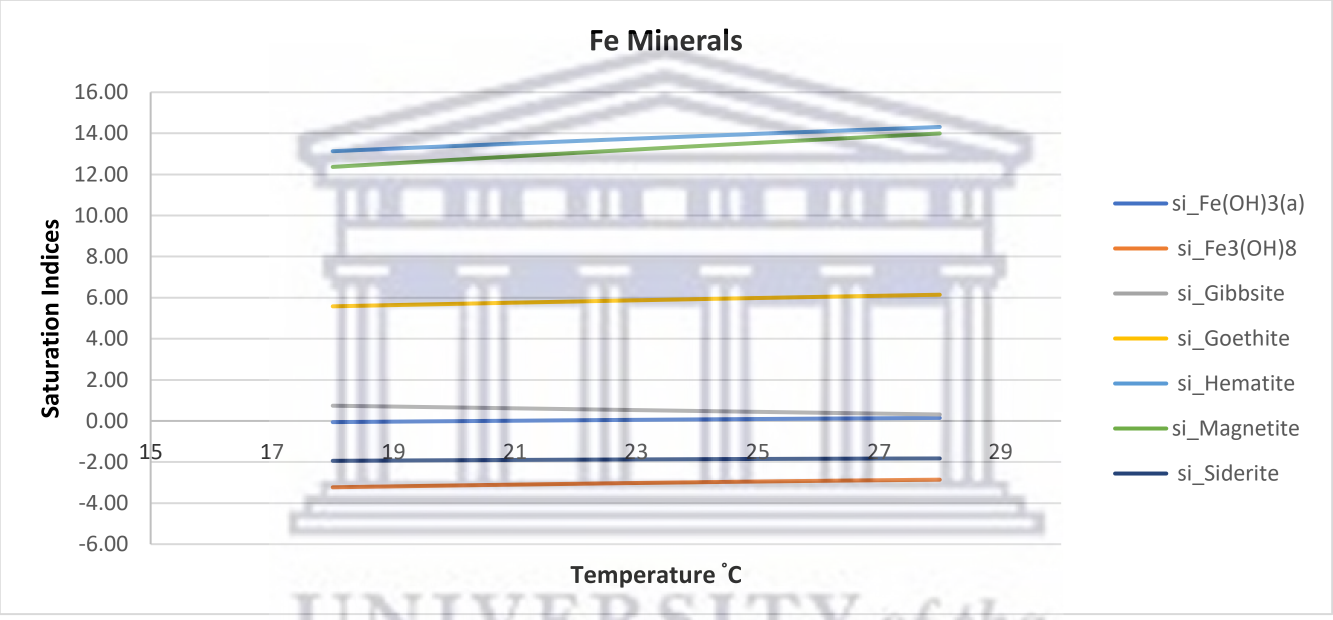

Figure 22a: Incremental modelling of Temperature against Fe (a.), carbonate (b.) and Mn (c.) minerals.

b.

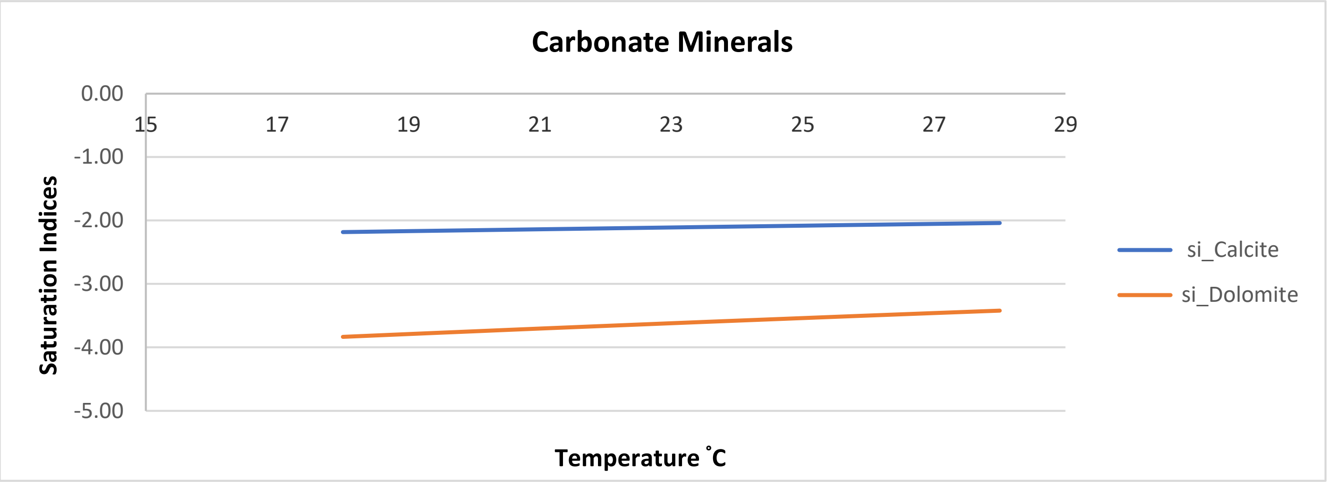

Figure 22b: Incremental modelling of Temperature against Fe (a.), carbonate (b.) and Mn (c.) minerals.

c.

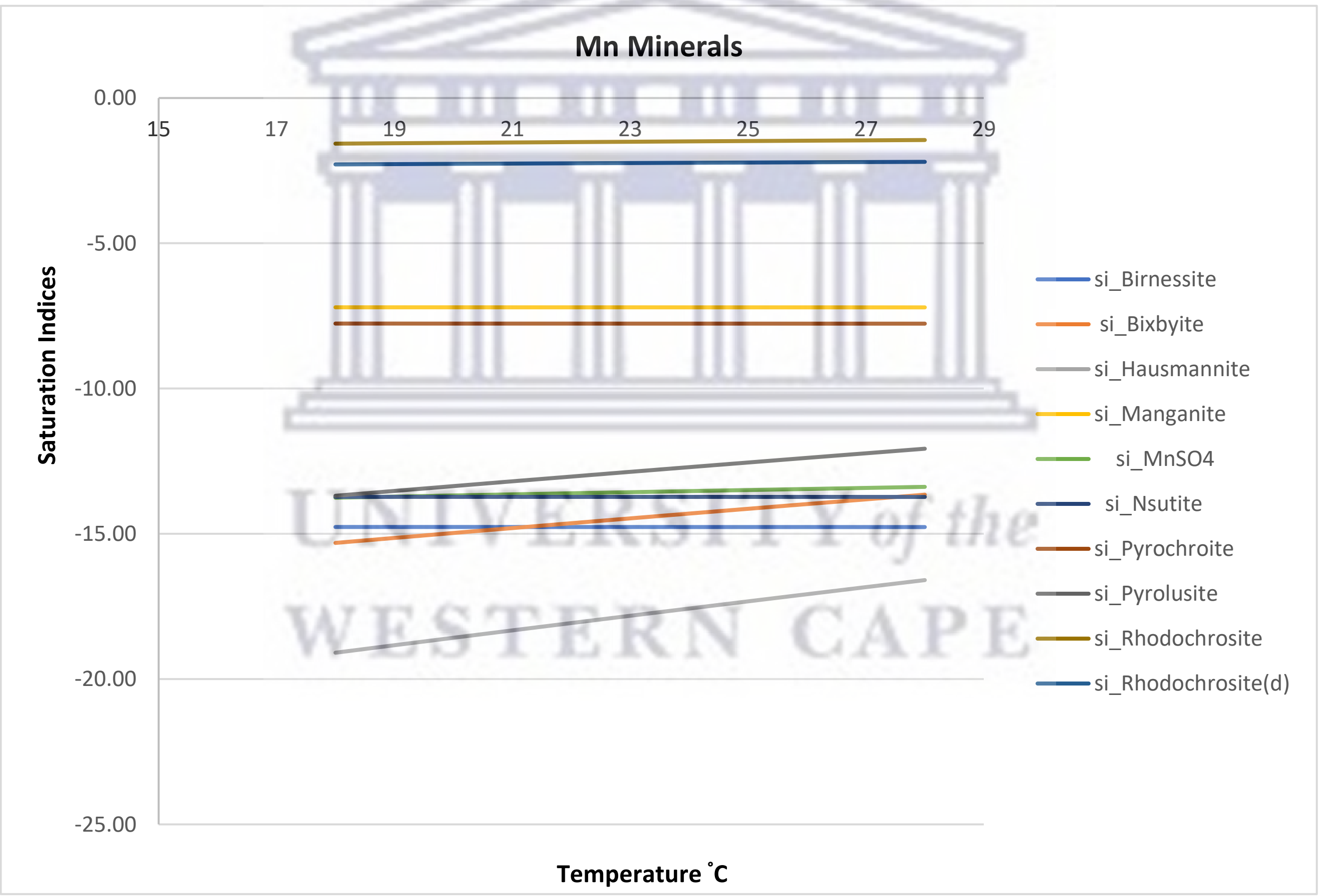

Figure 22c: Incremental modelling of Temperature against Fe (a.), carbonate (b.) and Mn (c.) minerals.

Figure 22 shows the incremental modelling of temperature between 18°C and 28°C on Fe (Figure 22a), Mn (Figure 22b) and carbonate minerals (Figure 22c). It was stated earlier that groundwater is generally characterised by low temperatures (7 – 10°C) stated by (El Araby, Hawash and El Diwani, 2009). However, the temperature taken at the sites were in the range of 20 – 23°C (Appendix A) so an increased range was selected for this model. Temperature is an important parameter to model Fe stability and its speciation forms are affected by temperature (Diliūnas and Jurevičius, 2006; Rossel *et al.*, 2010). Fe bearing minerals (Figure 22a.) increased in their saturation indices with the increase in temperature. Goethite, Hematite and Magnetite precipitate in the temperature range of 18°C to 28°C. The remaining Fe minerals remain in an unsaturated and equilibrium state. Mn bearing minerals (Figure 22c.) are all found to increase in their saturation indices yet, remain in the unsaturated state indicating a dissolution trend with the increase of temperature from 18°C to 28°C. Mn bearing minerals Bixbyite, Hausmannite, Mn2(SO4)3) and Pyrolusite show a larger change than the remaining Mn bearing minerals indicating that the change in temperature from 18°C and 28°C has a small effect on the precipitation of Mn bearing minerals. Carbonate minerals (Figure 22b.) show a very small increase in their saturation indices yet remain in the unsaturated state at 28°C and 18°C. This indicates that an increase in temperature has a very small impact on carbonate mineral precipitation as was confirmed by (Smith and Roychoudhury, 2013).

5.3.3 Correlation Analysis for Fe and Mn

In order to understand the relationship between the Fe and Mn minerals and parameters modelled a correlation analysis was conducted from 1 water sample that was collected where the use of PHREEQC in the previous section was used to model 10 different concentrations of Fe, pH, redox, temperature and Mn, this is seen in Table 6 and 7 respectively.

Table 6: Correlation coefficients between the modelled parameters and Fe minerals.

Correlation	**Iron Minerals**						
Parameter	Iron Hydroxide	Iron Oxide Hydroxide	Gibbsite	Geothite	Hematite	Magnetite	Siderite
Fe	0.8653	0.8647	#N/A	0.8643	0.866	0.8655	0.8668
pH	0.9719	0.9625	0.7015	0.972	0.972	0.9627	0.5024
Redox	**0.9977**	**0.9945**	#N/A	**0.9977**	**0.9977**	**0.9945**	-0.6639
Temperature	**0.9993**	**0.9967**	-0.9998	**0.9996**	**0.9997**	**0.9998**	**0.9906**
Mn	#N/A	#N/A	#N/A	#N/A	#N/A	#N/A	#N/A

It is evident that there are strong correlations (the correlation between two variables is generally considered strong when their correlation value is larger than 0.7) between the parameters and resulting Fe minerals as displayed in Table 5. The strongest relationships are between pH, redox potential, temperature and Fe minerals. Therefore, as the parameters increase, we can expect a linear directional change in the Fe minerals. This, however, does not necessarily mean that the changes experienced are significant. In order to show the significance of these changes, summary statistics for each mineral is shown in the table in the Appendix C.

The statistics shown in Appendix C indicate that even though the parameters may be highly correlated to the Fe minerals, the extent of change in the minerals is minimum. This is seen, for example, in temperature that shows near perfect correlation to Fe hydroxide but as temperature increases from 18 degrees to 28 degrees, Fe hydroxide changes minimally by 0.20 in its saturation indices. This is also seen through a low standard deviation. The pH and redox potential parameters are therefore both correlated with the resultant changes seen as material and therefore a significant predictor of the precipitation of Fe minerals.

Table 7: Correlation coefficients between the parameters modelled and Mn minerals.

Correlations	**Manganese Minerals**										
Parameter	Birnessite	Bixbyite	Hausmannite	Manganite	Manganese Sulphate	Manganese Sulphate Two	Nsutite	Pyrochroite	Pyrolusite	Rhodochrosite	RhodochrositeD
Fe	#N/A	#N/A	#N/A	#N/A	-0.6963	#N/A	#N/A	#N/A	#N/A	#N/A	#N/A
pH	**0.9999**	**0.9998**	**0.9998**	**0.9998**	-0.5725	-0.5999	**0.9999**	**0.9995**	**0.9999**	**0.9982**	**0.9982**
Redox Potential	**1**	**1**	**1**	**1**	**1**	#N/A	**1**	#N/A	**1**	#N/A	#N/A
Temperature	-0.866	**1**	**1**	-0.7746	**0.9999**	**0.9997**	#N/A	-0.7746	**0.9999**	**0.996**	**0.9933**
Mn	0.9197	0.9208	0.9215	0.9211	0.9208	0.9197	0.922	0.9211	0.9224	0.9197	0.922

As the Fe minerals, it is evident that there are strong correlations between the parameters and resulting Mn minerals. Therefore, as the parameters increase, we can expect a linear directional change in the Mn minerals. This, however, does not necessarily mean that the changes experienced are significant. To show the significance of the changes, summary statistics for each mineral is shown in Appendix C.

While temperature shows a strong correlation, the extent of the change in variables is minimal. An increase in the temperature does cause a decrease in Birnessite, however, over the full temperature range (18-28) the Birnessite mineral minimally changed by 0.003 in the saturation indices. This trend is seen across the Mn minerals. Redox potential and pH show a strong correlation with the Mn minerals, and this is equally seen in the extent of the change as seen in Appendix C.

5.4 Comparing various sampling techniques of iron and manganese

The comparison of sampling techniques was done to understand and demonstrate the sensitivity of Fe and Mn minerals (dissolved and total) to different environments (Table 8). The following sampling techniques were used, pipe outlet, filtered, preserved, flow through cell and immediate analysis. All sampled were analysed at the lab except for the immediate analysis which was done using the DR900. The DR900 is a multi parameter handheld portable colorimeter for water testing of over 90 colorimetric parameters. All analyses results are compared to the South African water quality guidelines for domestic use.

Table 8: Comparison of sampling techniques to measure Fe and Mn concentrations.

Sampling Techniques		Fe II (LAB)	Total Fe (LAB)	Fe III	Dissolved Mn (LAB)	Total Mn (LAB)	Precipitated Mn
		mg/l	mg/l	mg/l	mg/l	mg/l	mg/l
Paarl Pipe Outlet	Lab Analysis	**0.01**	**0.29**	**0.28**	**BDL**	**BDL**	
Paarl Filtered	Lab Analysis	**BDL**	**0.23**		**BDL**	**BDL**	
Paarl Preserved	Lab Analysis	**0.01**	**0.43**	**0.42**	**BDL**	**BDL**	
Paarl Flow Through Cell	Lab Analysis	**0.01**	**0.33**	**0.33**	**BDL**	**BDL**	
Paarl Immediate Analysis	DR 900	**0.00**	**0.03**	**0.03**		**0.50**	
Sonstraal Pipe Outlet	Lab Analysis	**0.01**	**2.14**	**2.13**	**BDL**	**0.15**	
Sonstraal Filtered	Lab Analysis	**0.01**	**4.10**	**4.10**	**BDL**	**0.25**	
Sonstraal Preserved	Lab Analysis	**0.33**	**4.01**	**3.68**	**0.08**	**0.43**	
Sonstraal Flow Through Cell	Lab Analysis	**0.01**	**2.90**	**2.89**	**0.02**	**0.25**	
Sonstraal Immediate Analysis	DR 900	**0.14**	**0.16**	**0.02**		**0.70**	
DPMH BH1 Pipe Outlet	Lab Analysis	**0.95**	**544.03**	**543.08**	**BDL**	**0.08**	
DPMH BH1 Filtered	Lab Analysis	**1.07**	**200.49**	**199.42**	**BDL**	**BDL**	
DPMH BH1 Preserved	Lab Analysis	**12.75**	**73.46**	**60.71**	**BDL**	**BDL**	
DPMH BH1 Flow Through Cell	Lab Analysis	**1.72**	**36.31**	**34.59**	**BDL**	**BDL**	
DPMH BH1 Immediate Analysis	DR 900	**0.97**	**0.99**	**0.02**		**0.29**	
DPMH BH2 Pipe Outlet	Lab Analysis	**0.09**	**120.16**	**120.07**	**0.08**	**0.56**	**0.48**
DPMH BH2 Filtered	Lab Analysis	**0.11**	**178.55**	**178.44**	**0.10**	**0.57**	**0.48**
DPMH BH2 Preserved	Lab Analysis	**36.75**	**198.94**	**162.19**	**0.11**	**0.58**	**0.47**
DPMH BH2 Flow Through Cell	Lab Analysis	**0.40**	**71.19**	**70.79**	**0.09**	**0.51**	**0.42**
DPMH BH2 Immediate Anlysis	DR 900	**2.18**	**2.80**	**0.62**		**0.00**	
UWC BH4 Pipe Outlet	Lab Analysis	**0.01**	**1.89**	**1.87**	**BDL**	**BDL**	
UWC BH4 Filtered	Lab Analysis	**0.04**	**11.36**	**11.33**	**BDL**	**BDL**	
UWC BH4 Preserved	Lab Analysis	**1.21**	**6.55**	**5.34**	**BDL**	**BDL**	
UWC BH4 Flow Through Cell	Lab Analysis	**0.06**	**1.89**	**1.83**	**BDL**	**BDL**	
UWC BH4 Immediate Analysis	DR 900	**0.24**	**0.35**	**0.11**		**2.50**	
UWC BH5 Pipe Outlet	Lab Analysis	**0.02**	**3.12**	**3.11**	**0.07**	**0.42**	**0.35**
UWC BH5 Filtered	Lab Analysis	**0.11**	**41.27**	**41.16**	**0.05**	**0.33**	**0.28**
UWC BH5 Preserved	Lab Analysis	**10.68**	**53.42**	**42.74**	**0.10**	**0.52**	**0.41**
UWC BH5 Flow Through Cell	Lab Analysis	**0.16**	**29.10**	**28.94**	**0.09**	**0.48**	**0.39**
UWC BH5 Immediate Analysis	DR 900	**1.07**	**Too High for DR900**			**20.80**	

Paarl Hospital (Table 8) – All samples analysed at the lab reflected that the water has Fe concentrations that are around the minimum limit of 0.3 mg/L, in the precipitated form of Fe^{3+}. This was calculated for all samples by subtracting the Total Fe/Mn from dissolved Fe/ Mn. The South African water quality guideline tolerable maximum concentration of Fe is 0.3 mg/L however the immediate measurements show significantly lower level of Fe with no Fe^{2+} and only the precipitated form of Fe^{3+} present. All analysed Mn concentrations from the lab analysis are below detection limit although the Total Mn concentrations analysed by the DR900 are higher than the South African water quality guidelines tolerable maximum concentration of 0.1 mg/L.

Sonstraal Hospital (Table 8) – According to the samples analysed by the lab, the concentrations of Total Fe and Mn is significantly higher than the immediate measurements and the maximum tolerable concentrations of Fe (0.3 mg/L) and Mn (0.1 mg/L) according to the South African water quality guidelines. However, the immediate measurements for Total Fe, Fe^{2+} and Fe^{3+} is below the minimum concentration but the Total Mn measured immediately was higher than the lab analysis. Through the lab analysis, the concentrations of Total and Fe^{3+} will result in the clogging of the boreholes at the Sonstraal Hospital as well as due to the Total Mn concentrations.

DP Marais Hospital BH1 (Table 8) - From the results of the lab analysed samples and the immediate measurements the BH01 of DP Marais Hospital will result in the clogging of borehole and equipment because of the large volume of Total Fe present. The immediate measurements showed higher concentrations of Fe^{2+} than the Fe^{3+} unlike the lab analysed sample where Fe^{3+} is always higher than the Fe^{2+}. All concentrations of Fe and Mn analysed indicated that Fe clogging is likely to occur.

DPMH BH2 (Table 8) - The results for BH2 from DP Marais Hospital mirrored that of BH1 in terms of trends of this site. However, the immediate measurements of Mn indicated 0 concentrations of Mn unlike the lab analysed samples that confirmed high concentrations of Mn in the various types of samples collected. This borehole also likely to be clogged due to the high concentrations of Fe and Mn found as Fe^{2+} and Fe^{3+}.

UWC BH4 (Table 8) – The labs analysis of the samples for Fe concentrations are higher than the field measurements except for Fe^{2+} concentrations. Mn concentrations are below detection limit for all samples taken for lab unlike immediately analysis that show high concentrations of Total Mn. From these concentrations of Fe and Mn, there is potential for Fe clogging to take place.

UWC BH5 (Table 8) – All immediate measurements taken are higher than the South African water quality guidelines maximum tolerable concentrations of Fe (0.3 mg/L) and Mn. (0.1 mg/L). All lab Fe^{2+} concentrations at this borehole, the pipe outlet sample, filtered sample and the flow through sample were beneath the South African water quality guideline tolerable limits. From these results borehole clogging is likely to occur.

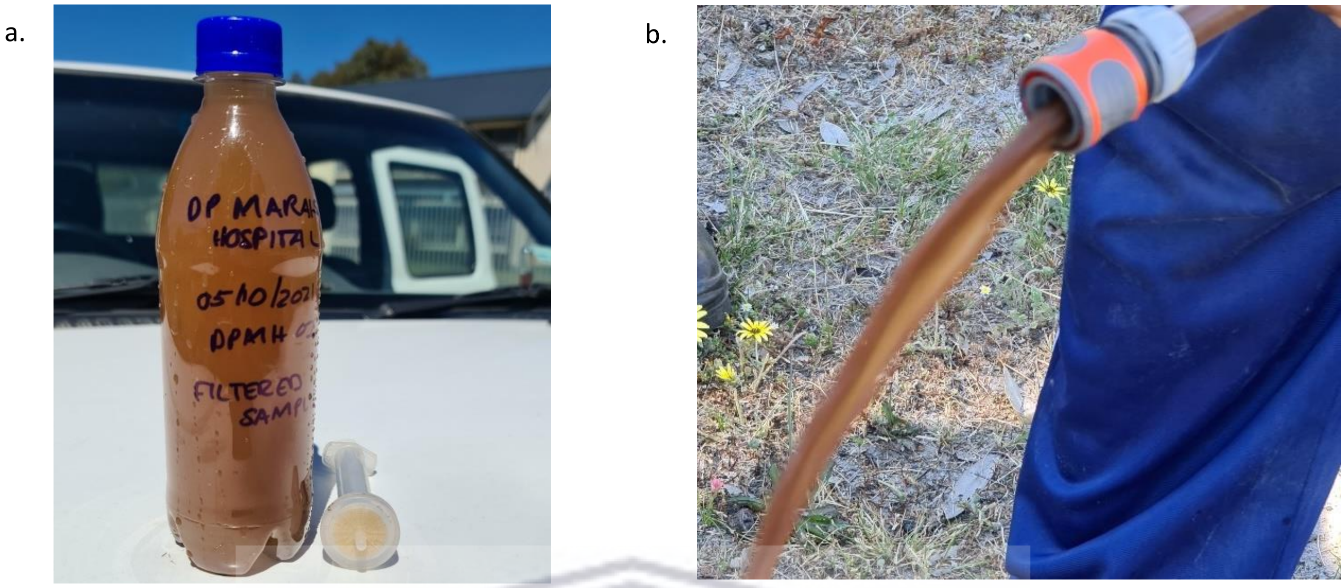

Figure 202: (a.) Image of filtered sampled collected at DP Marais Hospital and filter used to collect the sample. (b.) Image of the water being purged from DP Marais Hospital.

Apart from the correct sampling procedure being followed an important consideration for the ensuring the integrity of the samples collected is to minimize sample handling and storage which may cause alterations in chemical constituents as stated by (Barcelona *et al.*, 1985). Due to the miscommunication with the lab, there was increased storage and transport which resulted in the loss of the sample integrity. Finalising what was to be measured was done a month and a half after samples were collected, despite the samples being kept in refrigeration storage it still allowed for chemical changes to take place resulting in inaccurate data. The increased time due to the storage and transportation will result in "false positives" or "false negatives" as suggested by (Friends of Groundwater in the World Water Quality Alliance, 2021). Mn in groundwater behaves similarly to Fe thus the sampling procedure was the same as suggest by Weaver *et al.*, 2004.

In this research project it was observed that analysis done immediately was lower than the samples done at the lab which can be attributed to the change in chemistry that takes place when the samples during storage and transportation. When collecting the samples for Fe and Mn a key factor is to avoid contact with the atmosphere which is recommended by Weaver *et al.*, 2004. This was attempted through the flow through cell sampling which proved to work in the case of DP Marais Hospital site that had the most about of Fe and Mn in its groundwater. In the case of Lithuanian hydrogeochemical conditions, a significant factor determining the formation and stability of Fe compounds in groundwater is aquifer-atmosphere interaction (Diliūnas and Jurevičius, 2006).

As seen from Figure 22b, the purging was conducted by a pump and not a bailer. The method of using a bailer is only recommended if the use of Light Non-Aqueous Phase Liquids and Dense Non-Aqueous Phase Liquids by Weaver *et al.*, 2004 and suggests that when sampling for Fe the use of a bailer to purge is not recommend. This recommendation is made as the bailer is likely to physically dislodge the built-up Fe oxides on the borehole casing walls which may influence the results measured (Weaver, Cave and Talma, 2004). This advised the decision to make use of a low flow pump to purge each borehole sampled at.

To try and gain insight into the Fe^{2+} concentration of the groundwater at each site that was sampled the filtration technique was used as well as the immediate analysis using the DR900. From the results of this sampling technique in Table 8 it was noticed that the concentration of Total Fe for the filtered samples was one of the highest for this sampling technique than the others, this is evident in the DP Marais Hospital and UWC boreholes. Weaver *et al.*, 2004 stated that if Fe^{3+} is present in groundwater it is important to filter the sample as quickly and as soon as possible to prevent contact with air. (Weaver, Cave and Talma, 2004) also mentioned that by using the pressure filtering technique there should be no cause for concern with the sample being exposed to air as the sample chemistry change should be insignificant with this type of exposure. However, (Kerr Environmental *et al.*, 1989) provided a different view and stated that in previous research, errors of various kinds were found when determining dissolved concentrations of certain metals with Fe and Mn being among them, using a 0.45 micron filter. These errors can be attributed to the filter passage of fine-grained clay particles, the process of Fe oxidation and colloidal formation through the process of filtering anoxic groundwater which results in the removal of previously dissolved Fe and clogging of filter pores with fine particles (Kerr Environmental *et al.*, 1989). Comparing the results in Table 7 of the DR900 Fe^{2+} to the Filtered sample of Fe^{2+} the DR900 measurements appear increased except for the DP Marais Hospital BH1 site, this trend could be attributed to the potential sources of error. The elevated Fe^{2+} concentration may also be explained by (Hem and Cropper, 1962) that observed that Fe^{2+} is stable at high concentrations within the aquifer and loses its stability once the water is pumped and brought to the surface and the oxidation reaction takes place. (Barcelona *et al.*, 1985). It is also suggested by (Barcelona *et al.*, 1985) and (Weaver *et al.*, 2004) that it is more effective to conduct a field analysis for certain specific inorganic constituents such as Fe^{2+} rather than preserving the sample to be analysed by a lab. By looking at Figure 22(a.) that the filter used is stained through the build-up of colloids. Figure 22(b.) it can be seen when compared to the sample taken in Figure 22(a.) that despite purging there was no change in the colour of the water being pumped. It can be concluded that when trying to understand the Fe^{2+} content of an aquifer there should be an immediate analysis done and the use of a filter should require careful consideration and used depending on what the data generated will be used for.

From Table 7 it can be seen that the preserved samples would have the highest amount of Total Fe as seen at Paarl Hospital, Sonstraal Hospital, DP Marais Hospital BH2 and UWC BH5 compared to samples taken at the pipe outlet. The use of a strong acid for preservation of the samples is meant to slow down the oxidation of Fe however it may be rapid when pH is at a normal range for natural waters. The pH of the samples taken (Appendix A) range between 5 and 7.5 which is in the range of near-neutral which may be responsible to enhance the precipitation of Fe oxides.

The flow through cell technique was used to as it is used to replicate conditions found within the aquifer. Weaver *et al*., 2004 states that the following changes occur once groundwater is brought to the surface, the hydrostatic pressure changes, temperature change and the sample encounters the atmosphere, these changes will cause the chemical condition to change in the water. Mahed, 2015 also advised that once purging is complete that the use of a flow through cell should be used to take field measurements and to avoid sample contamination. According to Table 8 the flow through cell method produced one of the lowest concentrations of Fe when compared to the other sampling techniques. This can be seen in DP Marais Hospital BH1 and DP Marais Hospital BH2. As mentioned earlier the DR900 is used to measure the in-situ Fe and Mn concentrations of the aquifer and the flow through cell is used to replicate the conditions of the aquifer, it would be expected to that these two methods would produce similar results however this trend was not observed. The errors that occurred with the lab shows that the results are inconclusive as the results do not show any trend.

In this study a comparison was done to compare the infield site analysis to the lab analysis however this resulted in an unclear conclusion due to the loss in sample integrity. In Table 8 the Mn results from all sites were mainly below detection limit which provide no insight on the effect of the various sampling techniques on the concentration of Mn. In summary, (Petersen, Minkkinen and Esbensen, 2005) has said that any sampling that occurs will generate sampling errors and the way in which these errors may be addressed is by understanding how the sampling errors originate and occur.

CHAPTER 6: CONCLUSION

This study was set with 4 objectives that are as follows:

1. To assess the spatial variations in Fe and Mn concentrations.
2. To establish site-specific processes controlling the concentration of Fe and Mn in groundwater.
3. To model the likelihood of precipitation of Fe and Mn based on detected solution composition.
4. To assess the best practice method/techniques for sampling Fe and Mn.

According to the spatial variation maps made to address the first objective, Fe and Mn are widely found within the WCP in low concentrations. The low concentrations are still a concern as the South African water quality guidelines maximum tolerable concentrations for Fe and Mn are 0.3 mg/L and 0.1 mg/L respectively. Therefore, caution should always be taken when drilling boreholes due to the potential precipitation and clogging that can take place increasing the maintenance of the boreholes and supply equipment.

For the second objective, all sites geological logs and maps show that these boreholes were drilled into different geological formations. However, Fe and Mn was found to be present. The boreholes are also drilled to various depths which can cause a change in chemistry if Fe^{2+} and Mn^{2+} is present and brought to the surface. Land use of all sites in this research project were based in built up areas, with some areas having open fields/spaces. It is concluded that the Fe and Mn concentrations are not as a result of the built-up areas as there is no heavy metal industries which studies suggest influence Fe and Mn concentrations in groundwater. The interviews conducted at each site proved to be a useful exercise as it revealed information that cannot be analysed through samples collected as well as confirming the data that was analysed. The interviews highlighted the importance of site maintenance personnel being able to understand Fe clogging and why users are complaining about the taste. All conditions mentioned in this section are necessary to understand as it creates a wholistic understanding of all factors contributing to the concentrations of Fe and Mn in groundwater. Understanding the site geology, lithological logs and land use, it can be concluded water rock interaction (geogenic contamination) of groundwater is taking place, which is defined as groundwater being rich or deficient in certain components due to geological processes taking place in the aquifer rather than human induce activities.

To model as part of the third objective, all sites sampled at require the determination of these samples saturation indices to be understood and analysed. This was done according to the standard chemistry analysed at the lab. From here the sample DPMH01 was selected to model the likelihood of precipitation of Fe and Mn minerals. The parameters modelled were Fe, Mn, pH, redox potential and temperature which have a high influence on the concentration of Mn and Fe. From the modelled scenarios it was concluded that pH, temperature and redox potential had the most influence on the precipitation of Fe and Mn in boreholes. This is also reflected in the statistics and correlation analysis ran on the saturation indices.

As seen from the modelling, the precipitation of Fe and Mn may be considered sensitive, therefore the sampling for these minerals is very important. The main objective for different sampling methods was to reduce the samples exposure to oxygen and the change of water chemistry. Another important reason to conduct different sampling techniques was to compare the infield analysis to the analysis done by the lab. To understand which method/technique provides the most accurate/representative concentration of Fe and Mn. This is due to the chemical changes that occur during the transportation of the samples and storage. This research project set out to compare these methods to establish the best practice methods to sample Fe and Mn, however the sampling errors that occurred resulted in the data being inconclusive to make any recommendations.

From this research project the aim was to investigate and understand the spatial distribution of Fe and Mn in groundwater within the WCP and to delineate the site-specific processes that influence the concentrations of Fe and Mn was achieved through modelling, interviews, spatial distribution maps and sampling techniques.

Recommendations

It is suggested that future research should take into consideration the following recommendations. The recommendations for the first objective would be to geographically map out the precipitate concentrations of Fe and Mn in order to understand its spatial variation. The recommendations for the second objective would be to look at the land-use activities surrounding the study area as this falls part of the site-specific processes controlling the concentration of groundwater. The recommendations for the third objective would be to use more samples to do extensive modelling. The recommendations for the fourth objective would be that the sampling technique should be repeated with decreased time between sample collection and lab analysis in order to achieve the most representative results. The sampling technique used should also be mentioned when reporting on Fe and Mn as this provides insight to the quality of the data and results which will be useful when it comes to decision making.

Not only site-specific processes that take place influence the Fe and Mn concentrations in groundwater but there is also a strong microbial influence that needs to be considered in the future. This study does provide errors that highly influence and alter the results therefore thee sampling techniques practiced should be repeated in future studies for further understanding and recommendations.

APPENDICES

Appendix A: Field Measurements

Site Name	Borehole Name	No. Samples	Total Fe (mg/L)	Fe2+ (mg/L)	Fe3+ (mg/L)	Total Mn (mg/L)	pH	Temp (C)	EC (uS/cm)
Kraaifontein Hospital	Couldn't sample due to pump being removed								
Paarl Hospital	Tap Sample	5	0.03	0.00	0.03	0.5	7.39	21	445
Sonstraal Hospital	BH1	5	0.16	0.14	0.02	0.7	6.96	23	755
DP Marais Hospital	DPMH01	5	0.99	0.97	0.02	0.29	5.28	20.8	500
	DPMH02	5	2.8	2.18	0.62	0.00	6.7	20.7	520
Brooklyn Chest Hospital	Couldn't sample due to pump being removed								
UWC	BH4	5	0.35	0.24	0.11	2.5	7.42	20.7	575
	BH5	5	Too high	1.07	N/A	20.8	7.01	20.6	1155

Appendix B: Incremental Modelling Saturation Indices Data

Fe Minerals Saturation Indices With Increase in Fe Concentration

soln	pH	pe	Fe (mg/L)	si_Fe(OH)3(a)	si_Fe3(OH)8	si_Gibbsite	si_Goethite	si_Hematite	si_Magnetite	si_Siderite
1	6.7	4	0.01	-0.82	-5.59	0.63	4.92	11.82	10.36	-2.73
2	6.7	4	0.11	0.22	-2.46	0.63	5.96	13.90	13.48	-1.69
3	6.7	4	0.21	0.50	-1.62	0.63	6.24	14.46	14.32	-1.41
4	6.7	4	0.31	0.67	-1.11	0.63	6.41	14.80	14.83	-1.24
5	6.7	4	0.41	0.79	-0.75	0.63	6.53	15.04	15.19	-1.12
6	6.7	4	0.51	0.89	-0.47	0.63	6.62	15.23	15.48	-1.02
7	6.7	4	0.61	0.96	-0.23	0.63	6.70	15.39	15.71	-0.94
8	6.7	4	0.71	1.09	0.14	0.63	6.82	15.63	16.08	-0.82
9	6.7	4	0.81	1.14	0.29	0.63	6.87	15.74	16.23	-0.77
10	6.7	4	0.91	1.18	0.42	0.63	6.92	15.83	16.37	-0.72

Mn Minerals Saturation Indices With Increase in Fe Concentration

soln	pH	pe	Fe (mg/L)	si_Birnessite	si_Bixbyite	si_Hausmannite	si_Manganite	si_Mn2(SO4)3	si_MnSO4	si_Nsutite	si_Pyrochroite	si_Pyrolusite	si_Rhodochrosite	si_Rhodochrosite(d)
1	6.7	4	0.01	-14.76	-14.85	-18.40	-7.20	-64.77	-13.65	-13.73	-7.76	-13.24	-1.53	-2.26
2	6.7	4	0.11	-14.76	-14.85	-18.40	-7.20	-64.77	-13.65	-13.73	-7.76	-13.24	-1.53	-2.26
3	6.7	4	0.21	-14.76	-14.85	-18.40	-7.20	-64.77	-13.65	-13.73	-7.76	-13.24	-1.53	-2.26
4	6.7	4	0.31	-14.76	-14.85	-18.40	-7.20	-64.77	-13.65	-13.73	-7.76	-13.24	-1.53	-2.26
5	6.7	4	0.41	-14.76	-14.85	-18.40	-7.20	-64.77	-13.65	-13.73	-7.76	-13.24	-1.53	-2.26
6	6.7	4	0.51	-14.76	-14.85	-18.40	-7.20	-64.77	-13.65	-13.73	-7.76	-13.24	-1.53	-2.26
7	6.7	4	0.61	-14.76	-14.85	-18.40	-7.20	-64.77	-13.65	-13.73	-7.76	-13.24	-1.53	-2.26
8	6.7	4	0.71	-14.76	-14.85	-18.40	-7.20	-64.77	-13.65	-13.73	-7.76	-13.24	-1.53	-2.26
9	6.7	4	0.81	-14.76	-14.85	-18.40	-7.20	-64.78	-13.65	-13.73	-7.76	-13.24	-1.53	-2.26
10	6.7	4	0.91	-14.76	-14.85	-18.40	-7.20	-64.78	-13.65	-13.73	-7.76	-13.24	-1.53	-2.26

Carbonate Minerals Saturation Indices With The Increase In Fe Concentration

soln	pH	pe	Fe (mg/L)	si_Calcite	si_Dolomite
1	6.7	4	0.01	-2.14	-3.72
2	6.7	4	0.11	-2.14	-3.72
3	6.7	4	0.21	-2.14	-3.72
4	6.7	4	0.31	-2.14	-3.72
5	6.7	4	0.41	-2.14	-3.72
6	6.7	4	0.51	-2.14	-3.72
7	6.7	4	0.61	-2.14	-3.72
8	6.7	4	0.71	-2.14	-3.72
9	6.7	4	0.81	-2.14	-3.72
10	6.7	4	0.91	-2.14	-3.72

Fe Minerals Saturation Indice With Increase in Mn Concentration

soln	pH	pe	Mn (mg/L)	si_Fe3(OH)8	si_Gibbsite	si_Goethite	si_Hematite	si_Magnetite	si_Siderite
1	6.7	4	**0.05**	-3.11	0.63	5.74	13.47	12.83	-1.90
2	6.7	4	**0.15**	-3.11	0.63	5.74	13.47	12.83	-1.90
3	6.7	4	**0.25**	-3.11	0.63	5.74	13.47	12.83	-1.90
4	6.7	4	**0.35**	-3.11	0.63	5.74	13.47	12.83	-1.90
5	6.7	4	**0.45**	-3.11	0.63	5.74	13.47	12.83	-1.90
6	6.7	4	**0.55**	-3.11	0.63	5.74	13.47	12.83	-1.90
7	6.7	4	**0.65**	-3.11	0.63	5.74	13.47	12.83	-1.90
8	6.7	4	**0.75**	-3.11	0.63	5.74	13.47	12.83	-1.90
9	6.7	4	**0.85**	-3.11	0.63	5.74	13.47	12.83	-1.90
10	6.7	4	**0.95**	-3.11	0.63	5.74	13.47	12.83	-1.90
11	6.7	4	**1.05**	-3.11	0.63	5.74	13.47	12.83	-1.90

Mn Minerals Saturation Indice With Increase in Mn Concentration

soln	pH	pe	Mn (mg/L)	si_Bixbyite	si_Birnessite	si_Hausmannite	si_Manganite	si_Mn2(SO4)3	si_MnSO4	si_Nsutite	si_Pyrochroite	si_Pyrolusite	si_Rhodochrosite	si_Rhodochrosite(d)
1	6.7	4	**0.05**	-15.30	-14.99	-19.07	-7.43	-65.22	-13.88	-13.95	-7.99	-13.46	-1.76	-2.48
2	6.7	4	**0.15**	-14.34	-14.51	-17.64	-6.95	-64.26	-13.40	-13.47	-7.51	-12.99	-1.28	-2.00
3	6.7	4	**0.25**	-13.90	-14.29	-16.97	-6.73	-63.82	-13.18	-13.25	-7.29	-12.77	-1.06	-1.78
4	6.7	4	**0.35**	-13.61	-14.14	-16.53	-6.58	-63.53	-13.03	-13.11	-7.14	-12.62	-0.91	-1.64
5	6.7	4	**0.45**	-13.39	-14.03	-16.21	-6.47	-63.31	-12.92	-13.00	-7.03	-12.51	-0.80	-1.53
6	6.7	4	**0.55**	-13.22	-13.95	-15.95	-6.39	-63.14	-12.84	-12.91	-6.95	-12.42	-0.72	-1.44
7	6.7	4	**0.65**	-13.07	-13.87	-15.73	-6.31	-62.99	-12.76	-12.84	-6.87	-12.35	-0.64	-1.37
8	6.7	4	**0.75**	-12.95	-13.81	-15.54	-6.25	-62.87	-12.70	-12.77	-6.81	-12.29	-0.58	-1.31
9	6.7	4	**0.85**	-12.84	-13.76	-15.38	-6.20	-62.76	-12.65	-12.72	-6.76	-12.23	-0.53	-1.25
10	6.7	4	**0.95**	-12.74	-13.71	-15.23	-6.15	-62.66	-12.60	-12.67	-6.71	-12.19	-0.48	-1.20
11	6.7	4	**1.05**	-12.66	-13.67	-15.10	-6.10	-62.58	-12.56	-12.63	-6.66	-12.14	-0.44	-1.16

Carbonate Minerals Saturation Indice With Increase in Mn Concentration

soln	pH	pe	Mn (mg/L)	si_Calcite	si_Dolomite
1	6.7	4	**0.05**	-2.14	-3.72
2	6.7	4	**0.15**	-2.14	-3.72
3	6.7	4	**0.25**	-2.14	-3.72
4	6.7	4	**0.35**	-2.14	-3.72
5	6.7	4	**0.45**	-2.14	-3.72
6	6.7	4	**0.55**	-2.14	-3.72
7	6.7	4	**0.65**	-2.14	-3.72
8	6.7	4	**0.75**	-2.14	-3.72
9	6.7	4	**0.85**	-2.14	-3.72
10	6.7	4	**0.95**	-2.14	-3.72
11	6.7	4	**1.05**	-2.14	-3.72

Fe Minerals Saturation Indice With Increase in pH Concentration

soln	pe	pH	si_Fe(OH)3(a)	si_Fe3(OH)8	si_Gibbsite	si_Goethite	si_Hematite	si_Magnetite	si_Siderite
1	4	**3**	-11.24	-33.11	-7.03	-5.47	-8.91	-17.01	-5.33
2	4	**3.5**	-9.62	-28.77	-5.43	-3.87	-5.75	-12.80	-4.98
3	4	**4**	-8.09	-24.70	-3.92	-2.35	-2.72	-8.75	-4.55
4	4	**4.5**	-6.58	-20.68	-2.47	-0.85	0.29	-4.73	-4.08
5	4	**5**	-5.08	-16.67	-1.14	0.65	3.30	-0.73	-3.58
6	4	**5.5**	-3.58	-12.67	-0.11	2.15	6.30	3.27	-3.09
7	4	**6**	-2.08	-8.67	0.54	3.65	9.30	7.27	-2.59
8	4	**6.5**	-0.59	-4.69	0.71	5.15	12.29	11.26	-2.09
9	4	**7**	0.85	-0.87	0.41	6.59	15.16	15.07	-1.66
10	4	**7.5**	1.77	1.39	-0.06	7.51	17.00	17.33	-1.74
11	4	**8**	1.94	1.38	-0.55	7.67	17.33	17.33	-2.58
12	4	**8.5**	1.90	0.78	-1.05	7.64	17.26	16.73	-3.63
13	4	**9**	1.75	-0.17	-1.55	7.49	16.96	15.77	-4.82

Mn Minerals Saturation Indice With Increase in pH Concentration

soln	pe	pH	si_Birnessite	si_Bixbyite	si_Hausmannite	si_Manganite	si_Mn2(SO4)3	si_MnSO4	si_Nsutite	si_Pyrochroite	si_Pyrolusite	si_Rhodochrosite	si_Rhodochrosite(d)
1	4	**3**	-29.68	-37.24	-48.26	-18.42	-64.96	-13.73	-28.64	-15.28	-28.16	-4.96	-5.69
2	4	**3.5**	-27.59	-34.09	-44.05	-16.83	-64.83	-13.67	-26.55	-14.19	-26.06	-4.62	-5.34
3	4	**4**	-25.57	-31.06	-40.00	-15.31	-64.78	-13.66	-24.53	-13.17	-24.04	-4.19	-4.92
4	4	**4.5**	-23.56	-28.05	-35.99	-13.80	-64.77	-13.65	-22.52	-12.16	-22.04	-3.72	-4.44
5	4	**5**	-21.56	-25.04	-31.99	-12.30	-64.76	-13.65	-20.52	-11.16	-20.04	-3.22	-3.95
6	4	**5.5**	-19.56	-22.04	-27.99	-10.80	-64.76	-13.65	-18.52	-10.16	-18.04	-2.73	-3.45
7	4	**6**	-17.56	-19.04	-23.99	-9.30	-64.76	-13.65	-16.52	-9.16	-16.04	-2.23	-2.95
8	4	**6.5**	-15.56	-16.05	-19.99	-7.80	-64.77	-13.65	-14.53	-8.16	-14.04	-1.73	-2.46
9	4	**7**	-13.57	-13.06	-16.01	-6.31	-64.78	-13.66	-12.53	-7.17	-12.05	-1.24	-1.96
10	4	**7.5**	-11.59	-10.10	-12.08	-4.83	-64.82	-13.68	-10.55	-6.19	-10.07	-0.76	-1.49
11	4	**8**	-9.65	-7.22	-8.26	-3.39	-64.94	-13.74	-8.61	-5.25	-8.13	-0.33	-1.05
12	4	**8.5**	-7.79	-4.51	-4.69	-2.03	-65.23	-13.88	-6.76	-4.39	-6.27	0.02	-0.71
13	4	**9**	-6.04	-2.01	-1.43	-0.78	-65.73	-14.13	-5.01	-3.64	-4.52	0.22	-0.50

Carbonate Minerals Saturation Indice With Increase in pH Concentration

state	soln	pe	pH	si_Calcite	si_Dolomite
i_soln	1	4	**3**	-5.55	-10.54
i_soln	2	4	**3.5**	-5.23	-9.88
i_soln	3	4	**4**	-4.80	-9.03
i_soln	4	4	**4.5**	-4.33	-8.09
i_soln	5	4	**5**	-3.84	-7.11
i_soln	6	4	**5.5**	-3.34	-6.11
i_soln	7	4	**6**	-2.84	-5.11
i_soln	8	4	**6.5**	-2.34	-4.12
i_soln	9	4	**7**	-1.84	-3.12
i_soln	10	4	**7.5**	-1.34	-2.12
i_soln	11	4	**8**	-0.85	-1.13
i_soln	12	4	**8.5**	-0.37	-0.17
i_soln	13	4	**9**	0.08	0.73

Mn Minerals Saturation Indice With Increase in Redox Potential

soln	pH	Eh	si_Birnessite	si_Bixbyite	si_Hausmannite	si_Manganite	si_Mn2(SO4)3	si_MnSO4	si_Nsutite	si_Pyrochroite	si_Pyrolusite	si_Rhodochrosite	si_Rhodochrosite(d)
1	6.7	**-1**	-24.76	-24.85	-28.40	-12.20	-74.77	-13.65	-23.73	-7.76	-23.24	-1.53	-2.26
2	6.7	**0**	-22.76	-22.85	-26.40	-11.20	-72.77	-13.65	-21.73	-7.76	-21.24	-1.53	-2.26
3	6.7	**1**	-20.76	-20.85	-24.40	-10.20	-70.77	-13.65	-19.73	-7.76	-19.24	-1.53	-2.26
4	6.7	**2**	-18.76	-18.85	-22.40	-9.20	-68.77	-13.65	-17.73	-7.76	-17.24	-1.53	-2.26
5	6.7	**3**	-16.76	-16.85	-20.40	-8.20	-66.77	-13.65	-15.73	-7.76	-15.24	-1.53	-2.26
6	6.7	**4**	-14.76	-14.85	-18.40	-7.20	-64.77	-13.65	-13.73	-7.76	-13.24	-1.53	-2.26
7	6.7	**5**	-12.76	-12.85	-16.40	-6.20	-62.77	-13.65	-11.73	-7.76	-11.24	-1.53	-2.26
8	6.7	**6**	-10.76	-10.85	-14.40	-5.20	-60.77	-13.65	-9.73	-7.76	-9.24	-1.53	-2.26

Fe Minerals Saturation Indice With Increase in Redox Potential

soln	pH	Eh	si_Fe(OH)3(a)	si_Fe3(OH)8	si_Gibbsite	si_Goethite	si_Hematite	si_Magnetite	si_Siderite
1	6.7	**-1**	-4.98	-13.07	0.63	0.75	3.49	2.87	-1.89
2	6.7	**0**	-3.98	-11.07	0.63	1.75	5.49	4.87	-1.89
3	6.7	**1**	-2.98	-9.07	0.63	2.75	7.49	6.87	-1.89
4	6.7	**2**	-1.98	-7.07	0.63	3.75	9.49	8.87	-1.89
5	6.7	**3**	-0.98	-5.08	0.63	4.75	11.49	10.87	-1.89
6	6.7	**4**	0.00	-3.11	0.63	5.74	13.47	12.83	-1.90
7	6.7	**5**	0.90	-1.42	0.63	6.64	15.26	14.53	-2.00
8	6.7	**6**	1.41	-0.89	0.63	7.15	16.28	15.05	-2.50

Carbonate Minerals Saturation Indice With Increase in Redox Potential

soln	pH	Eh	si_Calcite	si_Dolomite
1	6.7	**-1**	-2.14	-3.72
2	6.7	**0**	-2.14	-3.72
3	6.7	**1**	-2.14	-3.72
4	6.7	**2**	-2.14	-3.72
5	6.7	**3**	-2.14	-3.72
6	6.7	**4**	-2.14	-3.72
7	6.7	**5**	-2.14	-3.72
8	6.7	**6**	-2.14	-3.72

Mn Minerals Saturation Indice With Increase in Temperature

soln	pH	pe	Temperature	si_Birnessite	si_Bixbyite	si_Hausmannite	si_Manganite	si_Mn2(SO4)3	si_MnSO4	si_Nsutite	si_Pyrochroite	si_Pyrolusite	si_Rhodochrosite	si_Rhodochrosite(d)
1	6.7	4	**18**	-14.76	-15.31	-19.09	-7.20	-65.39	-13.76	-13.73	-7.76	-13.69	-1.57	-2.28
2	6.7	4	**19**	-14.76	-15.14	-18.83	-7.20	-65.16	-13.72	-13.73	-7.76	-13.52	-1.56	-2.27
3	6.7	4	**20**	-14.76	-14.97	-18.58	-7.20	-64.93	-13.68	-13.73	-7.76	-13.36	-1.54	-2.27
4	6.7	4	**21**	-14.76	-14.80	-18.32	-7.20	-64.70	-13.64	-13.73	-7.76	-13.19	-1.53	-2.26
5	6.7	4	**22**	-14.76	-14.63	-18.07	-7.20	-64.48	-13.60	-13.73	-7.76	-13.03	-1.52	-2.25
6	6.7	4	**23**	-14.77	-14.47	-17.82	-7.20	-64.26	-13.57	-13.73	-7.76	-12.87	-1.50	-2.24
7	6.7	4	**24**	-14.77	-14.30	-17.57	-7.20	-64.03	-13.53	-13.73	-7.76	-12.71	-1.49	-2.23
8	6.7	4	**25**	-14.77	-14.14	-17.32	-7.20	-63.81	-13.49	-13.73	-7.76	-12.54	-1.48	-2.22
9	6.7	4	**26**	-14.77	-13.98	-17.08	-7.21	-63.60	-13.46	-13.73	-7.77	-12.39	-1.47	-2.21
10	6.7	4	**27**	-14.77	-13.81	-16.83	-7.21	-63.38	-13.42	-13.73	-7.77	-12.23	-1.46	-2.20
11	6.7	4	**28**	-14.77	-13.65	-16.59	-7.21	-63.16	-13.38	-13.73	-7.77	-12.07	-1.45	-2.20

Fe Minerals Saturation Indice With Increase in Temperature

soln	pH	pe	Temperature	si_Fe(OH)3(a)	si_Fe3(OH)8	si_Gibbsite	si_Goethite	si_Hematite	si_Magnetite	si_Siderite
1	6.7	4	**18**	-0.06	-3.23	0.74	5.58	13.13	12.37	-1.94
2	6.7	4	**19**	-0.03	-3.19	0.70	5.64	13.26	12.54	-1.93
3	6.7	4	**20**	-0.01	-3.14	0.66	5.70	13.38	12.71	-1.91
4	6.7	4	**21**	0.01	-3.10	0.61	5.76	13.50	12.88	-1.90
5	6.7	4	**22**	0.03	-3.06	0.57	5.82	13.63	13.05	-1.89
6	6.7	4	**23**	0.05	-3.02	0.53	5.87	13.74	13.21	-1.87
7	6.7	4	**24**	0.07	-2.98	0.49	5.93	13.86	13.38	-1.86
8	6.7	4	**25**	0.09	-2.95	0.44	5.98	13.98	13.54	-1.85
9	6.7	4	**26**	0.11	-2.92	0.40	6.04	14.09	13.69	-1.84
10	6.7	4	**27**	0.13	-2.89	0.36	6.09	14.20	13.85	-1.83
11	6.7	4	**28**	0.15	-2.86	0.31	6.14	14.31	14.00	-1.83

Carbonate Minerals Saturation Indice With Increase in Temperature

soln	pH	pe	Temperature	si_Calcite	si_Dolomite
1	6.7	4	**18**	-2.18	-3.83
2	6.7	4	**19**	-2.17	-3.79
3	6.7	4	**20**	-2.15	-3.75
4	6.7	4	**21**	-2.14	-3.70
5	6.7	4	**22**	-2.12	-3.66
6	6.7	4	**23**	-2.11	-3.62
7	6.7	4	**24**	-2.09	-3.58
8	6.7	4	**25**	-2.08	-3.54
9	6.7	4	**26**	-2.07	-3.50
10	6.7	4	**27**	-2.05	-3.46
11	6.7	4	**28**	-2.04	-3.42

Appendix C: Statistics of Incremental Modelling

Statistics	Iron Hydroxide	Iron Oxide Hydroxide	Gibbsite	Geothite	Hematite	Magnetite	Siderite
Fe							
Range	2	6.01	0	2	4.01	6.01	2
Mean	0.66	-1.14	0.63	6.4	14.78	14.81	-1.24
Standard Deviation	0.6	1.8	0	0.6	1.2	1.8	0.6
pH							
Range	13.18	34.5	7.74	13.14	26.24	34.34	3.67
Mean	-2.97	-11.34	-1.67	2.77	7.52	4.62	-3.44
Standard Deviation	4.75	12.35	2.42	4.74	9.47	12.32	1.26
Redox Potential							
Range	6.39	12.18	0	6.39	12.79	12.18	0.61
Mean	-1.57	-6.35	0.63	4.16	10.31	9.59	-1.98
Standard Deviation	2.31	4.5	0	2.31	4.63	4.5	0.21
Mn							
Range		0	0	0	0	0	0
Mean		-3.11	0.63	5.74	13.47	12.83	-1.9
Standard Deviation		0	0	0	0	0	0
Temperature							
Range	0.2	0.37	0.43	0.57	1.18	1.63	0.12
Mean	0.05	-3.03	0.53	5.87	13.73	13.2	-1.88
Standard Deviation	0.07	0.12	0.14	0.19	0.39	0.54	0.04

Regression of modelled parameters on Fe minerals

Fe	Coef.Estimate	Coef.Std..Error	Coef.t.value	Coef.Pr...t..
(Intercept)	-284.64	175.9	-1.62	0.18
Data$IronHydroxide	-19.01	25.02	-0.76	0.49
Data$IronOxideHydroxide	-10.24	10.63	-0.96	0.39
Data$Geothite	-42.02	25.89	-1.62	0.18
Data$Hematite	20.48	14.49	1.41	0.23
Data$Magnetite	17.03	17.72	0.96	0.39

$$\begin{aligned} Fe = {} & -284.64 - 19.01(Iron\ Hydroxide) - 10.24(Iron\ Oxide\ Hydroxide) \\ & - 42.02(Geothite) + 20.48(Hematite) + 17.03(Magnetite) \end{aligned}$$

- Residual standard error: 0.1125 on 4 degrees of freedom
- Multiple R-squared: 0.9387, Adjusted R-squared: 0.862
- F-statistic: 12.24 on 5 and 4 DF, p-value: 0.01546

pH	Coef.Estimate	Coef.Std..Error	Coef.t.value	Coef.Pr...t..
(Intercept)	-6.26	1.56	-4.03	0.01
Data$IronHydroxide	0.21	0.51	0.42	0.69
Data$IronOxideHydroxide	-0.52	0.13	-4.16	0.01
Data$Gibbsite	0	0	-1.18	0.29
Data$Geothite	0.2	0.5	0.4	0.7
Data$Hematite	0.85	0.23	3.73	0.01
Data$Magnetite	-0.13	0.15	-0.87	0.42
Data$Siderite	-0.17	0.11	-1.56	0.18

$$\begin{aligned} ph = {} & -6.626 - 0.21(Iron\ Hydroxide) - 0.52(Iron\ Oxide\ Hydroxide) \\ & + 0.2(Geothite) + 0.85(Hematite) - 0.13(Magnetite) - 0.17(Siderite) \end{aligned}$$

- Residual standard error: 0.001833 on 5 degrees of freedom
- Multiple R-squared: 1, Adjusted R-squared: 1
- F-statistic: 1.935e+06 on 7 and 5 DF, p-value: 8.99e-16

Mn	Coef.Estimate	Coef.Std..Error	Coef.t.value	Coef.Pr...t..
(Intercept)	0.55	0.1	5.5	0

$$Mn = 0.55$$

Residual standard error: 0.3317 on 10 degrees of freedom

Temperature	Coef.Estimate	Coef.Std..Error	Coef.t.value	Coef.Pr...t..
(Intercept)	-62.19	41.98	-1.48	0.24
Data$IronHydroxide	4.2	5.78	0.73	0.52
Data$IronOxideHydroxide	-7.74	2.79	-2.78	0.07
Data$Gibbsite	-3.77	4.49	-0.84	0.46
Data$Geothite	2.5	4.78	0.52	0.64
Data$Hematite	-4.2	4.57	-0.92	0.43
Data$Magnetite	8.38	3.49	2.4	0.1
Data$Siderite	2.21	4.93	0.45	0.68

$$ph = -62.19 + 4.2(Iron\ Hydroxide) - 7.74(Iron\ Oxide\ Hydroxide) - 3.77(Gibbsite) + 2.5(Geothite) - 4.2(Hematite) + 8.38(Magnetite) + 2.21(Siderite)$$

- Residual standard error: 0.0343 on 3 degrees of freedom
- Multiple R-squared: 1, Adjusted R-squared: 0.9999
- F-statistic: 1.335e+04 on 7 and 3 DF, p-value: 9.877e-07

Redox Potential	Coef.Estimate	Coef.Std..Error	Coef.t.value	Coef.Pr...t..
(Intercept)	5.49	0	7.39E+12	0
Redox Potential	0.96	0	2.52E+13	0
Data$Geothite	2.4	0	3.23E+13	0
Data$Hematite	-0.2	0	-4.30E+12	0
Data$Magnetite	-0.98	0	-3.10E+13	0

$$Redox = 5.49 + 0.96(Iron\ Hydroxide) + 2.4(Geothite) - 0.2(Hematite) - 0.98(Magnetite)$$

- Residual standard error: 2.033e-16 on 2 degrees of freedom
- Multiple R-squared: 1, Adjusted R-squared: 1
- F-statistic: 2.032e+32 on 5 and 2 DF, p-value: < 2.2e-16

Parameter	Birnessite	Bixbyite	Hausmannite	Manganite	Manganese Sulfate	Manganese Sulfate 2	Nsutite	Pyrochroite	Pyrolusite	Rhodochrosite	RhodochrositeD
Fe											
Range	0	0.001	0.001	0	0.004	0.001	0	0	0	0.001	0.001
Mean	-14.765	-14.853	-18.4	-7.204	-64.774	-13.654	-13.728	-7.764	-13.242	-1.534	-2.259
Standard Deviation	0	0	0	0	0.001	0	0	0	0	0	0
Regression coefficient											
pH											
Range	23.635	35.231	46.827	17.635	0.962	0.481	23.635	11.635	23.635	5.187	5.187
Mean	-17.637	-19.194	-24.21	-9.376	-64.915	-13.723	-16.6	-9.236	-16.114	-2.269	-2.993
Standard Deviation	7.711	11.523	15.335	5.765	0.277	0.139	7.711	3.818	7.712	1.792	1.792
Regression coefficient											
Redox Potential											
Range	14	14	14	7	14	0	14	0	14		0
Mean	-17.764	-17.853	-21.4	-8.703	-67.772	-13.653	-16.727	-7.763	-16.242	-1.534	-2.259
Standard Deviation	4.899	4.899	4.899	2.45	4.899	0	4.899	0	4.899		0
Regression coefficient											
Mn											
Range	1.32	2.64	3.97	1.33	2.64	1.32	1.32	1.33	1.32	1.32	1.32
Mean	-14.066	-13.456	-16.305	-6.505	-63.376	-12.956	-13.029	-7.065	-12.543	-0.836	-1.56
Standard Deviation	0.4	0.8	1.201	0.401	0.8	0.4	0.4	0.401	0.4	0.4	0.399
Regression coefficient											
Temperature											
Range	0.003	1.66	2.5	0.003	2.226	0.374	0.003	0.003	1.62	0.124	0.089
Mean	-14.765	-14.474	-17.829	-7.204	-64.264	-13.568	-13.728	-7.764	-12.872	-1.506	-2.239
Standard Deviation	0.001	0.551	0.829	0.001	0.738	0.124	0.001	0.001	0.537	0.041	0.029
Regression coefficient											

Regression of modelled parameters on Mn minerals

Fe	Coef.Estimate	Coef.Std..Error	Coef.t.value	Coef.Pr...t..
(Intercept)	-3238.14	1180.26	-2.74	0.03
Data$ManganeseSulfate	-50	18.22	-2.74	0.03

$$Fe = -3238.14 - 50(Manganese\ Sulfate)$$

- Residual standard error: 0.2305 on 8 degrees of freedom
- Multiple R-squared: 0.4848, Adjusted R-squared: 0.4205
- F-statistic: 7.529 on 1 and 8 DF, p-value: 0.02529

pH	Coef.Estimate	Coef.Std..Error	Coef.t.value	Coef.Pr...t..
(Intercept)	14.3	0	7.95E+11	0
Data$Birnessite	1	0	7.20E+11	0
Data$Manganite	-1	0	-4.80E+11	0

$$ph = 14.3 + 1(Birnessite) - 1(Manganite)$$

- Residual standard error: 3.942e-16 on 2 degrees of freedom
- Multiple R-squared: 1, Adjusted R-squared: 1
- F-statistic: 2.928e+31 on 10 and 2 DF, p-value: < 2.2e-16

Mn	Coef.Estimate	Coef.Std..Error	Coef.t.value	Coef.Pr...t..
(Intercept)	-82.54	270.08	-0.31	0.78
Data$Birnessite	-26.88	23.82	-1.13	0.32
Data$Bixbyite	-4.28	19.5	-0.22	0.84
Data$Hausmannite	0.83	12.6	0.07	0.95
Data$Manganite	14.74	21.37	0.69	0.53
Data$Nsutite	11.28	18.57	0.61	0.58
Data$Pyrolusite	7.68	12.52	0.61	0.57

$$Mn = -82.54 - 26.88(Birnessite) - 4.28(Bixybite) + 0.83(Hausmannite) \\ + 14.74(Magnatite) + 11.28(Nsutite) + 7.68(Pyrolusite)$$

- Residual standard error: 0.1435 on 4 degrees of freedom
- Multiple R-squared: 0.9251, Adjusted R-squared: 0.8127
- F-statistic: 8.231 on 6 and 4 DF, p-value: 0.03041

Temperature	Coef.Estimate	Coef.Std..Error	Coef.t.value	Coef.Pr...t..
(Intercept)	-187	0	-1.50E+11	0
Data$Birnessite	-25	0	-3.90E+11	0
Data$Manganite	-25	0	-3.70E+11	0
Data$ManganeseSulfateTwo	25	0	2.52E+11	0

$$temperature = -187 - 25(Birnessite) - 25(Manganite) \\ + 25(ManganeseSulfateTwo)$$

- Residual standard error: 1.297e-13 on 2 degrees of freedom
- Multiple R-squared: 1, Adjusted R-squared: 1
- F-statistic: 8.178e+26 on 8 and 2 DF, p-value: < 2.2e-16

Redox Potential	Coef.Estimate	Coef.Std..Error	Coef.t.value	Coef.Pr...t..
(Intercept)	11.38	0	9.33E+15	0
Data$Birnessite	0.5	0	7.52E+15	0

$$Redox\ Potential = 11.38 - 0.5(Birnessite)$$

- Residual standard error: 8.624e-16 on 6 degrees of freedom
- Multiple R-squared: 1, Adjusted R-squared: 1
- F-statistic: 5.648e+31 on 1 and 6 DF, p-value: < 2.2e-16

Correlation matrixes for Fe minerals

	Fe	Iron Hydroxide	Iron OxideHydroxide	Gibbsite	Geothite	Hematite	Magnetite	Siderite	Iron Hydroxide Norm	Iron OxideHydroxide Norm	Gibbsite Norm	Geothite Norm	Hematite Norm	Magnetite Norm	Siderite Norm
Fe	1	0.865292793	0.864709895	#N/A	0.864314658	0.865982025	0.865465723	0.866762793	0.865292793	0.864709895	#N/A	0.86431466	0.865982	0.8654657	-0.866762793
Iron Hydroxide	0.865292793	1	0.999989178	#N/A	0.999973629	0.999984678	0.999991685	0.999978673	1	0.999989178	#N/A	0.99997363	0.9999847	0.9999917	-0.999978673
Iron OxideHydroxide	0.864709895	0.999989178	1	#N/A	0.999993063	0.999994217	0.999996702	0.99998516	0.999989178	1	#N/A	0.99999306	0.9999942	0.9999967	-0.99998516
Gibbsite	#N/A	#N/A	#N/A	1	#N/A	#N/A	#N/A	#N/A	#N/A	#N/A	#N/A	#N/A	#N/A	#N/A	#N/A
Geothite	0.864314658	0.999973629	0.999993063	#N/A	1	0.999989985	0.999991929	0.999979494	0.999973629	0.999993063	#N/A	1	0.99999	0.9999919	-0.999979494
Hematite	0.865982025	0.999984678	0.999994217	#N/A	0.999989985	1	0.999996924	0.999993372	0.999984678	0.999994217	#N/A	0.99998999	1	0.9999969	-0.999993372
Magnetite	0.865465723	0.999991685	0.999996702	#N/A	0.999991929	0.999996924	1	0.999993652	0.999991685	0.999996702	#N/A	0.99999193	0.9999969	1	-0.999993652
Siderite	0.866762793	0.999978673	0.99998516	#N/A	0.999979494	0.999993372	0.999993652	1	0.999978673	0.99998516	#N/A	0.99997949	0.9999934	0.9999937	-1
Iron Hydroxide Norm	0.865292793	1	0.999989178	#N/A	0.999973629	0.999984678	0.999991685	0.999978673	1	0.999989178	#N/A	0.99997363	0.9999847	0.9999917	-0.999978673
Iron OxideHydroxide Norm	0.864709895	0.999989178	1	#N/A	0.999993063	0.999994217	0.999996702	0.99998516	0.999989178	1	#N/A	0.99999306	0.9999942	0.9999967	-0.99998516
Gibbsite Norm	#N/A	#N/A	#N/A	#N/A	#N/A	#N/A	#N/A	#N/A	#N/A	#N/A	1	#N/A	#N/A	#N/A	#N/A
Geothite Norm	0.864314658	0.999973629	0.999993063	#N/A	1	0.999989985	0.999991929	0.999979494	0.999973629	0.999993063	#N/A	1	0.99999	0.9999919	-0.999979494
Hematite Norm	0.865982025	0.999984678	0.999994217	#N/A	0.999989985	1	0.999996924	0.999993372	0.999984678	0.999994217	#N/A	0.99998999	1	0.9999969	-0.999993372
Magnetite Norm	0.865465723	0.999991685	0.999996702	#N/A	0.999991929	0.999996924	1	0.999993652	0.999991685	0.999996702	#N/A	0.99999193	0.9999969	1	-0.999993652
Siderite Norm	-0.866762793	-0.999978673	-0.99998516	#N/A	-0.999979494	-0.999993372	-0.999993652	-1	-0.999978673	-0.99998516	#N/A	-0.9999795	-0.9999934	-0.999994	1

	pH	Iron Hydroxide	Iron Oxide Hydroxide	Gibbsite	Geothite	Hematite	Magnetite	Siderite	Iron Hydroxide Norm	Iron Oxide Hydroxide Norm	Gibbsite Norm	Geothite Norm	Hematite Norm	Magnetite Norm	Siderite Norm
pH	1	0.971862303	0.962515386	0.701520643	0.972025819	0.972007124	0.962701128	0.502364926	0.97188528	0.962523968	0.701449348	0.971997678	0.972053301	0.962699353	-0.502436527
Iron Hydroxide	0.971862303	1	0.999319483	0.826106923	0.99999789	0.999996499	0.999339706	0.691321464	0.999999865	0.999320699	0.826039216	0.999998208	0.999996171	0.999339745	-0.691368449
Iron Oxide Hydroxide	0.962515386	0.999319483	1	0.84121527	0.999293202	0.999294962	0.999996109	0.717436879	0.999316041	0.999999983	0.841148345	0.999297801	0.999287385	0.999996412	-0.717479911
Gibbsite	0.701520643	0.826106923	0.84121527	1	0.825276857	0.825306934	0.840334179	0.864094888	0.826029353	0.841214115	0.999999572	0.825449635	0.825155678	0.84037101	-0.863853311
Geothite	0.972025819	0.99999789	0.999293202	0.825276857	1	0.999999294	0.999318198	0.690926342	0.999998333	0.999294335	0.825208787	0.999999774	0.999999299	0.999318112	-0.690974099
Hematite	0.972007124	0.999996499	0.999294962	0.825306934	0.999999294	1	0.999322249	0.691029039	0.999996761	0.999296032	0.825238278	0.999999669	0.999999938	0.999322087	-0.691077301
Magnetite	0.962701128	0.999339706	0.999996109	0.840334179	0.999318198	0.999322249	1	0.717114763	0.999336357	0.999995992	0.840266003	0.999323038	0.999315106	0.999999974	-0.717160023
Siderite	0.502364926	0.691321464	0.717436879	0.864094888	0.690926342	0.691029039	0.717114763	1	0.691255797	0.717411317	0.864038807	0.691015326	0.690892982	0.717113778	-0.999997558
Iron Hydroxide Norm	0.97188528	0.999999865	0.999316041	0.826029353	0.999998333	0.999996761	0.999336357	0.691255797	1	0.999317261	0.825961883	0.99999842	0.999996421	0.999336418	-0.691302405
Iron OxideHydroxide Norm	0.962523968	0.999320699	0.999999983	0.841214115	0.999294335	0.999296032	0.999995992	0.717411317	0.999317261	1	0.841147273	0.999298925	0.999288461	0.999996278	-0.717454273
Gibbsite Norm	0.701449348	0.826039216	0.841148345	0.999999572	0.825208787	0.825238278	0.840266003	0.864038807	0.825961883	0.841147273	1	0.825381325	0.825086943	0.840302867	-0.863796566
Geothite Norm	0.971997678	0.999998208	0.999297801	0.825449635	0.999999774	0.999999669	0.999323038	0.691015326	0.99999842	0.999298925	0.825381325	1	0.999999597	0.99932293	-0.691063326
Hematite Norm	0.972053301	0.999996171	0.999287385	0.825155678	0.999999299	0.999999938	0.999315106	0.690892982	0.999996421	0.999288461	0.825086943	0.999999597	1	0.999314914	-0.690941688
Magnetite Norm	0.962699353	0.999339745	0.999996412	0.84037101	0.999318112	0.999322087	0.999999974	0.717113778	0.999336418	0.999996278	0.840302867	0.99932293	0.999314914	1	-0.717158885
Siderite Norm	-0.502436527	-0.691368449	-0.717479911	-0.863853311	-0.690974099	-0.691077301	-0.717160023	-0.999997558	-0.691302405	-0.717454273	-0.863796566	-0.691063326	-0.690941688	-0.717158885	1

	Redox	Iron Hydroxide	Iron Oxide Hydroxide	Gibbsite	Geothite	Hematite	Magnetite	Siderite	Iron Hydroxide Norm	Iron Oxide Hydroxide Norm	Gibbsite Norm	Geothite Norm	Hematite Norm	Magnetite Norm	Siderite Norm
Redox	1	0.997698191	0.994517192	#N/A	0.997713754	0.997684981	0.99447066	-0.6638761	0.997698678	-0.994515185	#N/A	0.997698699	0.997698784	0.994515614	0.669812045
Iron Hydroxide	0.997698191	1	0.999318256	#N/A	0.999999264	0.999999326	0.999302191	-0.611645456	0.999999554	-0.999317815	#N/A	0.999999561	0.999999557	0.999317972	0.617923451
Iron Oxide Hydroxide	0.994517192	0.999318256	1	#N/A	0.999310521	0.999326235	0.999999566	-0.58203559	0.999318888	-0.999999914	#N/A	0.999318872	0.999318829	0.999999912	0.588491365
Gibbsite	#N/A	#N/A	#N/A	1	#N/A	#N/A	#N/A	#N/A	#N/A	#N/A	#N/A	#N/A	#N/A	#N/A	#N/A
Geothite	0.997713754	0.999999264	0.999310521	#N/A	1	0.999999766	0.999294011	-0.611818234	0.999999915	-0.999309895	#N/A	0.999999915	0.999999915	0.999310045	0.618100003
Hematite	0.997684981	0.999999326	0.999326235	#N/A	0.999999766	1	0.999309682	-0.611485393	0.99999991	-0.999325554	#N/A	0.99999991	0.999999909	0.999325704	0.617766347
Magnetite	0.99447066	0.999302191	0.999999566	#N/A	0.999294011	0.999309682	1	-0.581672718	0.999302395	-0.999999812	#N/A	0.999302386	0.999302338	0.999999811	0.588132464
Siderite	-0.6638761	-0.611645456	-0.58203559	#N/A	-0.611818234	-0.611485393	-0.581672718	1	-0.611643401	0.582018795	#N/A	-0.611643653	-0.611644641	-0.582022161	-0.999949899
IronHydroxide Norm	0.997698678	0.999999554	0.999318888	#N/A	0.999999915	0.99999991	0.999302395	-0.611643401	1	-0.999318234	#N/A	1	1	0.999318386	0.617924231
Iron Oxide Hydroxide Norm	-0.994515185	-0.999317815	-0.999999914	#N/A	-0.999309895	-0.999325554	-0.999999812	0.582018795	-0.999318234	1	#N/A	-0.999318223	-0.999318177	-1	-0.58847527
Gibbsite Norm	#N/A	#N/A	#N/A	#N/A	#N/A	#N/A	#N/A	#N/A	#N/A	#N/A	1	#N/A	#N/A	#N/A	#N/A
Geothite Norm	0.997698699	0.999999561	0.999318872	#N/A	0.999999915	0.99999991	0.999302386	-0.611643653	1	-0.999318223	#N/A	1	1	0.999318374	0.617924474
Hematite Norm	0.997698784	0.999999557	0.999318829	#N/A	0.999999915	0.999999909	0.999302338	-0.611644641	1	-0.999318177	#N/A	1	1	0.999318328	0.617925461
Magnetite Norm	0.994515614	0.999317972	0.999999912	#N/A	0.999310045	0.999325704	0.999999811	-0.582022161	0.999318386	-1	#N/A	0.999318374	0.999318328	1	0.588478584
Siderite Norm	0.669812045	0.617923451	0.588491365	#N/A	0.618100003	0.617766347	0.588132464	-0.999949899	0.617924231	-0.58847527	#N/A	0.617924474	0.617925461	0.588478584	1

	Temperature	Iron Hydroxide	Iron Oxide Hydroxide	Gibbsite	Geothite	Hematite	Magnetite	Siderite	Iron Hydroxide Norm	Iron Oxide Hydroxide Norm	Gibbsite Norm	Geothite Norm	Hematite Norm	Magnetite Norm	Siderite Norm
Temperature	1	0.999260081	0.996672016	-0.999776942	0.99959178	0.999728269	0.99978725	0.990550876	0.998909466	-0.997516135	-0.999997745	0.99973914	0.999749874	0.999725567	-0.99547986
Iron Hydroxide	0.999260081	1	0.997503812	-0.998801511	0.999463742	0.999535849	0.999442613	0.99135255	0.999189643	-0.998304255	-0.999189345	0.999511034	0.999512987	0.999511792	-0.996856882
Iron Oxide Hydroxide	0.996672016	0.997503812	1	-0.995834157	0.99830622	0.998105395	0.998083292	0.996778655	0.999295349	-0.999783859	-0.996531747	0.998226147	0.998199708	0.998259007	-0.999710957
Gibbsite	-0.999776942	-0.998801511	-0.995834157	1	-0.999172796	-0.99937775	-0.999424961	-0.988716294	-0.998349623	0.996784788	0.999782949	-0.999354699	-0.999367519	-0.999336756	0.994580631
Geothite	0.99959178	0.999463742	0.99830622	-0.999172796	1	0.999911617	0.999896208	0.99284602	0.999712256	-0.998934184	-0.999542009	0.999925677	0.999923772	0.999927009	-0.997541237
Hematite	0.999728269	0.999535849	0.998105395	-0.99937775	0.999911617	1	0.99997212	0.992517272	0.999668786	-0.998801445	-0.999687584	0.99997306	0.999973012	0.9999722	-0.997310753
Magnetite	0.99978725	0.999442613	0.998083292	-0.999424961	0.999896208	0.99997212	1	0.992637275	0.999634567	-0.998718787	-0.999752046	0.999984569	0.999985604	0.999982496	-0.99717463
Siderite	0.990550876	0.99135255	0.996778655	-0.988716294	0.99284602	0.992517272	0.992637275	1	0.994941868	-0.996363984	-0.990391368	0.992939075	0.992895377	0.992993039	-0.997123045
Iron Hydroxide Norm	0.998909466	0.999189643	0.999295349	-0.998349623	0.999712256	0.999668786	0.999634567	0.994941868	1	-0.999716789	-0.998827191	0.999714936	0.999703411	0.999728708	-0.998827869
Iron Oxide Hydroxide Norm	-0.997516135	-0.998304255	-0.999783859	0.996784788	-0.998934184	-0.998801445	-0.998718787	-0.996363984	-0.999716789	1	0.99739394	-0.998863823	-0.998840905	-0.998891466	0.999694866
Gibbsite Norm	-0.999997745	-0.999189345	-0.996531747	0.999782949	-0.999542009	-0.999687584	-0.999752046	-0.990391368	-0.998827191	0.99739394	1	-0.999697096	-0.999708556	-0.999682443	0.995313083
Geothite Norm	0.99973914	0.999511034	0.998226147	-0.999354699	0.999925677	0.99997306	0.999984569	0.992939075	0.999714936	-0.998863823	-0.999697096	1	0.999999877	0.999999822	-0.997389229
Hematite Norm	0.999749874	0.999512987	0.998199708	-0.999367519	0.999923772	0.999973012	0.999985604	0.992895377	0.999703411	-0.998840905	-0.999708556	0.999999877	1	0.999999432	-0.99735472
Magnetite Norm	0.999725567	0.999511792	0.998259007	-0.999336756	0.999927009	0.9999722	0.999982496	0.992993039	0.999728708	-0.998891466	-0.999682443	0.999999822	0.999999432	1	-0.997431353
Siderite Norm	-0.99547986	-0.996856882	-0.999710957	0.994580631	-0.997541237	-0.997310753	-0.99717463	-0.997123045	-0.998827869	0.999694866	0.995313083	-0.997389229	-0.99735472	-0.997431353	1

	Mn	Iron Oxide Hydroxide	Gibbsite	Geothite	Hematite	Magnetite	Siderite	Iron Oxide Hydroxide Norm	Gibbsite Norm	Geothite Norm	Hematite Norm	Magnetite Norm	Siderite Norm
Mn	1	#N/A	#N/A	#N/A	#N/A	#N/A	#N/A	1	-0.674199862	-0.969087827	-0.990768368	-0.997279717	0.996790617
IronOxideHydroxide	#N/A	1	#N/A	#N/A	#N/A	#N/A	#N/A	#N/A	#N/A	#N/A	#N/A	#N/A	#N/A
Gibbsite	#N/A	#N/A	1	#N/A	#N/A	#N/A	#N/A	#N/A	#N/A	#N/A	#N/A	#N/A	#N/A
Geothite	#N/A	#N/A	#N/A	1	#N/A	#N/A	#N/A	#N/A	#N/A	#N/A	#N/A	#N/A	#N/A
Hematite	#N/A	#N/A	#N/A	#N/A	1	#N/A	#N/A	#N/A	#N/A	#N/A	#N/A	#N/A	#N/A
Magnetite	#N/A	#N/A	#N/A	#N/A	#N/A	1	#N/A	#N/A	#N/A	#N/A	#N/A	#N/A	#N/A
Siderite	#N/A	#N/A	#N/A	#N/A	#N/A	#N/A	1	#N/A	#N/A	#N/A	#N/A	#N/A	#N/A
Iron Oxide Hydroxide Norm	1	#N/A	#N/A	#N/A	#N/A	#N/A	#N/A	1	-0.674200244	-0.969087735	-0.990768171	-0.99727979	0.996790654
Gibbsite Norm	-0.674199862	#N/A	#N/A	#N/A	#N/A	#N/A	#N/A	-0.674200244	1	0.598912306	0.667977066	0.656098007	-0.666527906
Geothite Norm	-0.969087827	#N/A	#N/A	#N/A	#N/A	#N/A	#N/A	-0.969087735	0.598912306	1	0.976768704	0.965583619	-0.965537114
Hematite Norm	-0.990768368	#N/A	#N/A	#N/A	#N/A	#N/A	#N/A	-0.990768171	0.667977066	0.976768704	1	0.986210158	-0.99137316
Magnetite Norm	-0.997279717	#N/A	#N/A	#N/A	#N/A	#N/A	#N/A	-0.99727979	0.656098007	0.965583619	0.986210158	1	-0.996838908
Siderite Norm	0.996790617	#N/A	#N/A	#N/A	#N/A	#N/A	#N/A	0.996790654	-0.666527906	-0.965537114	-0.99137316	-0.996838908	1

Correlation matrixes for Mn minerals

	Fe	Birnessite	Bixbyite	Hausmannite	Manganite	Manganese Sulfate	Manganese SulfateTwo	Nsutite	Pyrochroite	Pyrolusite	Rhodochrosite	RhodochrositeD	Birnessite Norm	Bixbyite Norm	Hausmannite Norm	Manganite Norm	Manganese Sulfate Norm	Manganese Sulfate Two Norm	Nsutite Norm	Pyrochroite Norm	Pyrolusite Norm	Rhodochrosite Norm	RhodochrositeD Norm
Fe	1	#N/A	#N/A	#N/A	#N/A	-0.696310624	#N/A	#N/A	#N/A	#N/A	#N/A	#N/A	0.965581029	0.989375688	0.996376998	0.965582723	0.996143896	0.994148637	0.965577799	0.965581029	0.969223369	0.997489021	0.988441298
Birnessite	#N/A	1	#N/A	#N/A	#N/A	#N/A	#N/A	#N/A	#N/A	#N/A	#N/A	#N/A	#N/A	#N/A	#N/A	#N/A	#N/A	#N/A	#N/A	#N/A	#N/A	#N/A	#N/A
Bixbyite	#N/A	#N/A	1	#N/A	#N/A	#N/A	#N/A	#N/A	#N/A	#N/A	#N/A	#N/A	#N/A	#N/A	#N/A	#N/A	#N/A	#N/A	#N/A	#N/A	#N/A	#N/A	#N/A
Hausmannite	#N/A	#N/A	#N/A	1	#N/A	#N/A	#N/A	#N/A	#N/A	#N/A	#N/A	#N/A	#N/A	#N/A	#N/A	#N/A	#N/A	#N/A	#N/A	#N/A	#N/A	#N/A	#N/A
Manganite	#N/A	#N/A	#N/A	#N/A	1	#N/A	#N/A	#N/A	#N/A	#N/A	#N/A	#N/A	#N/A	#N/A	#N/A	#N/A	#N/A	#N/A	#N/A	#N/A	#N/A	#N/A	#N/A
Manganese Sulfate	-0.696310624	#N/A	#N/A	#N/A	#N/A	1	#N/A	#N/A	#N/A	#N/A	#N/A	#N/A	-0.704360725	-0.756272327	-0.723167818	-0.704355317	-0.729987652	-0.722473297	-0.704371031	-0.704360725	-0.628618557	-0.692045442	-0.740629655
Manganese Sulfate Two	#N/A	#N/A	#N/A	#N/A	#N/A	#N/A	1	#N/A	#N/A	#N/A	#N/A	#N/A	#N/A	#N/A	#N/A	#N/A	#N/A	#N/A	#N/A	#N/A	#N/A	#N/A	#N/A
Nsutite	#N/A	#N/A	#N/A	#N/A	#N/A	#N/A	#N/A	1	#N/A	#N/A	#N/A	#N/A	#N/A	#N/A	#N/A	#N/A	#N/A	#N/A	#N/A	#N/A	#N/A	#N/A	#N/A
Pyrochroite	#N/A	#N/A	#N/A	#N/A	#N/A	#N/A	#N/A	#N/A	1	#N/A	#N/A	#N/A	#N/A	#N/A	#N/A	#N/A	#N/A	#N/A	#N/A	#N/A	#N/A	#N/A	#N/A
Pyrolusite	#N/A	#N/A	#N/A	#N/A	#N/A	#N/A	#N/A	#N/A	#N/A	1	#N/A	#N/A	#N/A	#N/A	#N/A	#N/A	#N/A	#N/A	#N/A	#N/A	#N/A	#N/A	#N/A
Rhodochrosite	#N/A	#N/A	#N/A	#N/A	#N/A	#N/A	#N/A	#N/A	#N/A	#N/A	1	#N/A	#N/A	#N/A	#N/A	#N/A	#N/A	#N/A	#N/A	#N/A	#N/A	#N/A	#N/A
RhodochrositeD	#N/A	#N/A	#N/A	#N/A	#N/A	#N/A	#N/A	#N/A	#N/A	#N/A	#N/A	1	#N/A	#N/A	#N/A	#N/A	#N/A	#N/A	#N/A	#N/A	#N/A	#N/A	#N/A
Birnessite Norm	0.965581029	#N/A	#N/A	#N/A	#N/A	-0.704360725	#N/A	#N/A	#N/A	#N/A	#N/A	#N/A	1	0.976602621	0.969964709	1	0.972199908	0.983428941	0.999999999	1	0.917175176	0.962713485	0.968471826
Bixbyite Norm	0.989375688	#N/A	#N/A	#N/A	#N/A	-0.756272327	#N/A	#N/A	#N/A	#N/A	#N/A	#N/A	0.976602621	1	0.992972928	0.976603117	0.995303878	0.994482402	0.976601676	0.976602621	0.938471522	0.989659299	0.99074202
Hausmannite Norm	0.996376998	#N/A	#N/A	#N/A	#N/A	-0.723167818	#N/A	#N/A	#N/A	#N/A	#N/A	#N/A	0.969964709	0.992972928	1	0.969965556	0.999765255	0.997990352	0.969963094	0.969964709	0.972746914	0.99666313	0.997753545
Manganite Norm	0.965582723	#N/A	#N/A	#N/A	#N/A	-0.704355317	#N/A	#N/A	#N/A	#N/A	#N/A	#N/A	1	0.976603117	0.969965556	1	0.972200692	0.983429572	0.999999999	1	0.917176677	0.962715091	0.968472001
ManganeseSulfate Norm	0.996143896	#N/A	#N/A	#N/A	#N/A	-0.729987652	#N/A	#N/A	#N/A	#N/A	#N/A	#N/A	0.972199908	0.995303878	0.999765255	0.972200692	1	0.998397709	0.972198414	0.972199908	0.967494778	0.996430016	0.997518702
Manganese Sulfate Two Norm	0.994148637	#N/A	#N/A	#N/A	#N/A	-0.722473297	#N/A	#N/A	#N/A	#N/A	#N/A	#N/A	0.983428941	0.994482402	0.997990352	0.983429572	0.998397709	1	0.983427737	0.983428941	0.963926062	0.993614812	0.995926739
Nsutite Norm	0.965577799	#N/A	#N/A	#N/A	#N/A	-0.704371031	#N/A	#N/A	#N/A	#N/A	#N/A	#N/A	0.999999999	0.976601676	0.969963094	0.999999999	0.972198414	0.983427737	1	0.999999999	0.917172314	0.962710424	0.968471491
Pyrochroite Norm	0.965581029	#N/A	#N/A	#N/A	#N/A	-0.704360725	#N/A	#N/A	#N/A	#N/A	#N/A	#N/A	1	0.976602621	0.969964709	1	0.972199908	0.983428941	0.999999999	1	0.917175176	0.962713485	0.968471826
Pyrolusite Norm	0.969223369	#N/A	#N/A	#N/A	#N/A	-0.628618557	#N/A	#N/A	#N/A	#N/A	#N/A	#N/A	0.917175176	0.938471522	0.972746914	0.917176677	0.967494778	0.963926062	0.917172314	0.917175176	1	0.969501429	0.970561115
Rhodochrosite Norm	0.997489021	#N/A	#N/A	#N/A	#N/A	-0.692045442	#N/A	#N/A	#N/A	#N/A	#N/A	#N/A	0.962713485	0.989659299	0.99666313	0.962715091	0.996430016	0.993614812	0.962710424	0.962713485	0.969501429	1	0.990929601
RhodochrositeD Norm	0.988441298	#N/A	#N/A	#N/A	#N/A	-0.740629655	#N/A	#N/A	#N/A	#N/A	#N/A	#N/A	0.968471826	0.99074202	0.997753545	0.968472001	0.997518702	0.995926739	0.968471491	0.968471826	0.970561115	0.990929601	1

	pH	Birnessite	Bixbyite	Hausmannite	Manganite	Manganese Sulfate	Manganese Sulfate Two	Nsutite	Pyrochroite	Pyrolusite	Rhodochrosite	RhodochrositeD	Birnessite Norm	Bixbyite Norm	Hausmannite Norm	Manganite Norm	Manganese Sulfate Norm	Manganese SulfateTwo Norm	Nsutite Norm	Pyrochroite Norm	Pyrolusite Norm	Rhodochrosite Norm	RhodochrositeD Norm
pH	1	0.999887884	0.99980462	0.99975952	0.99979938	-0.572506228	-0.599857846	0.999884	0.999542705	0.999888633	0.998187765	0.998223318	0.999887884	0.99980462	0.99975952	0.99979938	-0.572506228	-0.599857846	0.999884304	0.999542705	0.999888633	0.998187765	0.998223318
Birnessite	0.999888	1	0.999988236	0.999975412	0.999987214	-0.560180347	-0.587840081	1	0.999883433	0.999999913	0.99874044	0.998775029	1	0.999988236	0.999975412	0.999987214	-0.560180347	-0.587840081	0.999999893	0.999883433	0.999999913	0.99874044	0.998775029
Bixbyite	0.999805	0.999988236	1	0.999997585	0.999999597	-0.556191617	-0.583935364	0.999989	0.999944577	0.999987767	0.998901135	0.998935021	0.999988236	1	0.999997585	0.999999597	-0.556191617	-0.583935364	0.999989371	0.999944577	0.999987767	0.998901135	0.998935021
Hausmannite	0.99976	0.999975412	0.999997585	1	0.999997673	-0.554394769	-0.582175992	0.999977	0.999964666	0.999974818	0.998961144	0.998994563	0.999975412	0.999997585	1	0.999997673	-0.554394769	-0.582175992	0.999976995	0.999964666	0.999974818	0.998961144	0.998994563
Manganite	0.999799	0.999987214	0.999999597	0.999997673	1	-0.555989434	-0.58375182	0.999988	0.999947858	0.999986845	0.998876498	0.998910759	0.999987214	0.999999597	0.999997673	1	-0.555989434	-0.58375182	0.99998828	0.999947858	0.999986845	0.998876498	0.998910759
Manganese Sulfate	-0.57251	-0.560180347	-0.556191617	-0.554394769	-0.555989434	1	0.998963144	-0.55998	-0.547482854	-0.560235715	-0.533738211	-0.533845363	-0.560180347	-0.556191618	-0.554394769	-0.555989434	1	0.998963144	-0.55998266	-0.547482854	-0.560235715	-0.53373821	-0.533845363
Manganese Sulfate Two	-0.59986	-0.587840081	-0.583935364	-0.582175992	-0.58375182	0.998963144	1	-0.58765	-0.575450375	-0.587896656	-0.561074073	-0.561189929	-0.587840081	-0.583935364	-0.582175992	-0.58375182	0.998963144	1	-0.587650532	-0.575450375	-0.587896656	-0.561074072	-0.561189929
Nsutite	0.999884	0.999999893	0.999989371	0.999976995	0.99998828	-0.55998266	-0.587650532	1	0.999886867	0.999999787	0.998748794	0.99878387	0.999999893	0.999989371	0.999976995	0.99998828	-0.55998266	-0.587650532	1	0.999886867	0.999999787	0.998748794	0.99878387
Pyrochroite	0.999543	0.999883433	0.999944577	0.999964666	0.999947858	-0.547482854	-0.575450375	0.999887	1	0.999882494	0.999073383	0.99910698	0.999883433	0.999944577	0.999964666	0.999947858	-0.547482854	-0.575450374	0.999886867	1	0.999882494	0.999073383	0.99910698
Pyrolusite	0.999889	0.999999913	0.999987767	0.999974818	0.999986845	-0.560235715	-0.587896656	1	0.999882494	1	0.998732848	0.998767482	0.999999913	0.999987767	0.999974818	0.999986845	-0.560235715	-0.587896656	0.999999787	0.999882494	1	0.998732848	0.998767482
Rhodochrosite	0.998188	0.99874044	0.998901135	0.998961144	0.998876498	-0.533738211	-0.561074073	0.998749	0.999073383	0.998732848	1	0.999995858	0.99874044	0.998901135	0.998961144	0.998876498	-0.533738211	-0.561074072	0.998748794	0.999073383	0.998732848	1	0.999995858
RhodochrositeD	0.998223	0.998775029	0.998935021	0.998994563	0.998910759	-0.533845363	-0.561189929	0.998784	0.99910698	0.998767482	0.999995858	1	0.998775029	0.998935021	0.998994563	0.998910759	-0.533845363	-0.561189929	0.99878387	0.99910698	0.998767482	0.999995858	1
Birnessite Norm	0.999888	1	0.999988236	0.999975412	0.999987214	-0.560180347	-0.587840081	1	0.999883433	0.999999913	0.99874044	0.998775029	1	0.999988236	0.999975412	0.999987214	-0.560180347	-0.587840081	0.999999893	0.999883433	0.999999913	0.99874044	0.998775029
Bixbyite Norm	0.999805	0.999988236	1	0.999997585	0.999999597	-0.556191618	-0.583935364	0.999989	0.999944577	0.999987767	0.998901135	0.998935021	0.999988236	1	0.999997585	0.999999597	-0.556191617	-0.583935364	0.999989371	0.999944577	0.999987767	0.998901135	0.998935021
Hausmannite Norm	0.99976	0.999975412	0.999997585	1	0.999997673	-0.554394769	-0.582175992	0.999977	0.999964666	0.999974818	0.998961144	0.998994563	0.999975412	0.999997585	1	0.999997673	-0.554394769	-0.582175992	0.999976995	0.999964666	0.999974818	0.998961144	0.998994563
Manganite Norm	0.999799	0.999987214	0.999999597	0.999997673	1	-0.555989434	-0.58375182	0.999988	0.999947858	0.999986845	0.998876498	0.998910759	0.999987214	0.999999597	0.999997673	1	-0.555989434	-0.58375182	0.99998828	0.999947858	0.999986845	0.998876498	0.998910759
Manganese Sulfate Norm	-0.57251	-0.560180347	-0.556191617	-0.554394769	-0.555989434	1	0.998963144	-0.55998	-0.547482854	-0.560235715	-0.533738211	-0.533845363	-0.560180347	-0.556191617	-0.554394769	-0.555989434	1	0.998963145	-0.55998266	-0.547482854	-0.560235715	-0.53373821	-0.533845363
Manganese Sulfate Two Norm	-0.59986	-0.587840081	-0.583935364	-0.582175992	-0.58375182	0.998963144	1	-0.58765	-0.575450374	-0.587896656	-0.561074072	-0.561189929	-0.587840081	-0.583935364	-0.582175992	-0.58375182	0.998963145	1	-0.587650532	-0.575450374	-0.587896656	-0.561074072	-0.561189929
Nsutite Norm	0.999884	0.999999893	0.999989371	0.999976995	0.99998828	-0.55998266	-0.587650532	1	0.999886867	0.999999787	0.998748794	0.99878387	0.999999893	0.999989371	0.999976995	0.99998828	-0.55998266	-0.587650532	1	0.999886867	0.999999787	0.998748794	0.99878387
Pyrochroite Norm	0.999543	0.999883433	0.999944577	0.999964666	0.999947858	-0.547482854	-0.575450375	0.999887	1	0.999882494	0.999073383	0.99910698	0.999883433	0.999944577	0.999964666	0.999947858	-0.547482854	-0.575450374	0.999886867	1	0.999882494	0.999073383	0.99910698
Pyrolusite Norm	0.999889	0.999999913	0.999987767	0.999974818	0.999986845	-0.560235715	-0.587896656	1	0.999882494	1	0.998732848	0.998767482	0.999999913	0.999987767	0.999974818	0.999986845	-0.560235715	-0.587896656	0.999999787	0.999882494	1	0.998732848	0.998767482
Rhodochrosite Norm	0.998188	0.99874044	0.998901135	0.998961144	0.998876498	-0.53373821	-0.561074072	0.998749	0.999073383	0.998732848	1	0.999995858	0.99874044	0.998901135	0.998961144	0.998876498	-0.53373821	-0.561074072	0.998748794	0.999073383	0.998732848	1	0.999995858
RhodochrositeD Norm	0.998223	0.998775029	0.998935021	0.998994563	0.998910759	-0.533845363	-0.561189929	0.998784	0.99910698	0.998767482	0.999995858	1	0.998775029	0.998935021	0.998994563	0.998910759	-0.533845363	-0.561189929	0.99878387	0.99910698	0.998767482	0.999995858	1

	Temperature	Birnessite	Bixbyite	Hausmannite	Manganite	Manganese Sulfate	Manganese Sulfate Two	Nsutite	Pyrochroite	Pyrolusite	Rhodochrosite	Rhodochrosite D	Birnessite Norm	Bixbyite Norm	Hausmannite Norm	Manganite Norm	Manganese Sulfate Norm	Manganese Sulfate Two Norm	Nsutite Norm	Pyrochroite Norm	Pyrolusite Norm	Rhodochrosite Norm	RhodochrositeD Norm
Temperature	1	-0.866025404	0.999951311	0.999955044	-0.774596669	0.999936731	0.999674777	#N/A	-0.774596669	0.999949606	0.996014156	0.993339705	0.999525648	-0.999955354	-0.999955097	0.999525682	-0.999951664	-0.999948027	0.99952574	0.99952568	-0.999955031	-0.999566382	-0.999271492
Birnessite	-0.866025404	1	-0.865666723	-0.866826216	0.559016994	-0.866559947	-0.859455057	#N/A	0.559016994	-0.866144022	-0.888322026	-0.884153458	-0.865613799	0.866917791	0.866947154	-0.865615025	0.86696329	0.866949567	-0.865613935	-0.865615053	0.866937473	0.868709011	0.869180742
Bixbyite	0.999951311	-0.865666723	1	0.999990081	-0.77002937	0.999987429	0.999809226	#N/A	-0.77002937	0.999973026	0.996470946	0.992928294	0.999249507	-0.999988614	-0.999988403	0.999249567	-0.999988087	-0.999988194	0.999249622	0.99924956	-0.999988487	-0.999771812	-0.999552136
Hausmannite	0.999955044	-0.866826216	0.999990081	1	-0.769867533	0.999991251	0.99977066	#N/A	-0.769867533	0.999990495	0.99653696	0.993182174	0.999252109	-0.999996536	-0.999996525	0.999252169	-0.999996365	-0.999996049	0.999252224	0.999252165	-0.999996503	-0.99978985	-0.999574201
Manganite	-0.774596669	0.559016994	-0.77002937	-0.769867533	1	-0.768538512	-0.764032656	#N/A	1	-0.769550657	-0.734085292	-0.788139236	-0.785187567	0.770201773	0.77018175	-0.785184876	0.770015812	0.769838948	-0.78518644	-0.785185524	0.77017619	0.760655416	0.756544146
ManganeseSulfate	0.999936731	-0.866559947	0.999987429	0.999991251	-0.768538512	1	0.999812155	#N/A	-0.768538512	0.999984796	0.996661306	0.992837473	0.999215973	-0.999990268	-0.999990222	0.99921604	-0.999990566	-0.999991069	0.99921609	0.999216037	-0.999990353	-0.999808915	-0.999603724
ManganeseSulfateTwo	0.999674777	-0.859455057	0.999809226	0.99977066	-0.764032656	0.999812155	1	#N/A	-0.764032656	0.999805352	0.996014078	0.991313532	0.998789692	-0.999754617	-0.999753863	0.998789778	-0.999755753	-0.999759087	0.998789826	0.99878975	-0.999754408	-0.999623229	-0.999443552
Nsutite	#N/A	#N/A	#N/A	#N/A	#N/A	#N/A	#N/A	1	#N/A	#N/A	#N/A	#N/A	#N/A	#N/A	#N/A	#N/A	#N/A	#N/A	#N/A	#N/A	#N/A	#N/A	#N/A
Pyrochroite	-0.774596669	0.559016994	-0.77002937	-0.769867533	1	-0.768538512	-0.764032656	#N/A	1	-0.769550657	-0.734085292	-0.788139236	-0.785187567	0.770201773	0.77018175	-0.785184876	0.770015812	0.769838948	-0.78518644	-0.785185524	0.77017619	0.760655416	0.756544146
Pyrolusite	0.999949606	-0.866144022	0.999973026	0.999990495	-0.769550657	0.999984796	0.999805352	#N/A	-0.769550657	1	0.99639847	0.993091901	0.999259714	-0.999982996	-0.999982957	0.999259774	-0.999982624	-0.9999819	0.999259828	0.999259767	-0.999982946	-0.999759076	-0.9995363
Rhodochrosite	0.996014156	-0.888322026	0.996470946	0.99653696	-0.734085292	0.996661306	0.996014078	#N/A	-0.734085292	0.99639847	1	0.986765441	0.994326621	-0.996621237	-0.996624272	0.994326903	-0.996644255	-0.996658955	0.994326842	0.994326984	-0.996625054	-0.997615023	-0.997917737
RhodochrositeD	0.993339705	-0.884153458	0.992928294	0.993182174	-0.788139236	0.992837473	0.991313532	#N/A	-0.788139236	0.993091901	0.986765441	1	0.993584116	-0.993075629	-0.993078944	0.99358411	-0.993065517	-0.993048427	0.993584133	0.993584033	-0.99307506	-0.992241989	-0.991733904
Birnessite Norm	0.999525648	-0.865613799	0.999249507	0.999252109	-0.785187567	0.999215973	0.998789692	#N/A	-0.785187567	0.999259714	0.994326621	0.993584116	1	-0.999268375	-0.999267302	1	-0.999256054	-0.999241522	1	1	-0.99926734	-0.998431517	-0.997935536
Bixbyite Norm	-0.999955354	0.866917791	-0.999988614	-0.999996536	0.770201773	-0.999990268	-0.999754617	#N/A	0.770201773	-0.999982996	-0.996621237	-0.993075629	-0.999268375	1	0.999999997	-0.999268434	0.999999926	0.999999695	-0.999268488	-0.999268433	0.999999998	0.999799941	0.999587465
Hausmannite Norm	-0.999955097	0.866947154	-0.999988403	-0.999996525	0.77018175	-0.999990222	-0.999753863	#N/A	0.77018175	-0.999982957	-0.996624272	-0.993078944	-0.999267302	0.999999997	1	-0.999267362	0.999999936	0.999999713	-0.999267415	-0.99926736	0.999999999	0.999800494	0.999588245
Manganite Norm	0.999525682	-0.865615025	0.999249567	0.999252169	-0.785184876	0.99921604	0.998789778	#N/A	-0.785184876	0.999259774	0.994326903	0.99358411	1	-0.999268434	-0.999267362	1	-0.999256114	-0.999241583	1	1	-0.999267399	-0.998431631	-0.997935671
Manganese Sulfate Norm	-0.999951664	0.86696329	-0.999988087	-0.999996365	0.770015812	-0.999990566	-0.999755753	#N/A	0.770015812	-0.999982624	-0.996644255	-0.993065517	-0.999256054	0.999999926	0.999999936	-0.999256114	1	0.999999904	-0.999256168	-0.999256113	0.999999938	0.999807524	0.999598384
Manganese Sulfate Two Norm	-0.999948027	0.866949567	-0.999988194	-0.999996049	0.769838948	-0.999991069	-0.999759087	#N/A	0.769838948	-0.9999819	-0.996658955	-0.993048427	-0.999241522	0.999999695	0.999999713	-0.999241583	0.999999904	1	-0.999241637	-0.999241581	0.999999719	0.9998145	0.999608489
Nsutite Norm	0.99952574	-0.865613935	0.999249622	0.999252224	-0.78518644	0.99921609	0.998789826	#N/A	-0.78518644	0.999259828	0.994326842	0.993584133	1	-0.999268488	-0.999267415	1	-0.999256168	-0.999241637	1	1	-0.999267453	-0.998431676	-0.997935715
Pyrochroite Norm	0.99952568	-0.865615053	0.99924956	0.999252165	-0.785185524	0.999216037	0.99878975	#N/A	-0.785185524	0.999259767	0.994326984	0.993584033	1	-0.999268433	-0.99926736	1	-0.999256113	-0.999241581	1	1	-0.999267398	-0.998431631	-0.997935673
Pyrolusite Norm	-0.999955031	0.866937473	-0.999988487	-0.999996503	0.77017619	-0.999990353	-0.999754408	#N/A	0.77017619	-0.999982946	-0.996625054	-0.99307506	-0.99926734	0.999999998	0.999999999	-0.999267399	0.999999938	0.999999719	-0.999267453	-0.999267398	1	0.999800628	0.999588439
Rhodochrosite Norm	-0.999566382	0.868709011	-0.999771812	-0.99978985	0.760655416	-0.999808915	-0.999623229	#N/A	0.760655416	-0.999759076	-0.997615023	-0.992241989	-0.998431517	0.999799941	0.999800494	-0.998431631	0.999807524	0.9998145	-0.998431676	-0.998431631	0.999800628	1	0.999961775
RhodochrositeD Norm	-0.999271492	0.869180742	-0.999552136	-0.999574201	0.756544146	-0.999603724	-0.999443552	#N/A	0.756544146	-0.9995363	-0.997917737	-0.991733904	-0.997935536	0.999587465	0.999588245	-0.997935671	0.999598384	0.999608489	-0.997935715	-0.997935673	0.999588439	0.999961775	1

	Mn	Birnessite	Bixbyite	Hausmannite	Manganite	Manganese Sulfate	Manganese Sulfate Two	Nsutite	Pyrochroite	Pyrolusite	Rhodochrosite	RhodochrositeD	Birnessite Norm	Bixbyite Norm	Hausmannite Norm	Manganite Norm	Manganese Sulfate Norm	Manganese Sulfate Two Norm	Nsutite Norm	Pyrochroite Norm	Pyrolusite Norm	Rhodochrosite Norm	RhodochrositeD Norm
Mn	1	0.91965823	0.920834381	0.921522339	0.921122605	0.920834381	0.91965823	0.922018	0.921122605	0.922446532	0.91965823	0.921978256	-0.921246301	-0.92126561	-0.92126655	-0.921246301	-0.921067899	-0.921120777	-0.92125	-0.921246301	-0.921266229	-0.921174767	-0.921155605
Birnessite	0.919658	1	0.999980935	0.999969848	0.999974819	0.999980935	1	0.999932	0.999974819	0.999920695	1	0.99992355	-0.999974399	-0.999974065	-0.999974171	-0.999974399	-0.999976104	-0.999975644	-0.99997	-0.999974399	-0.999974122	-0.99997508	-0.999975291
Bixbyite	0.920834	0.999980935	1	0.999991048	0.99997029	1	0.999980935	0.999972	0.99997029	0.999946254	0.999980935	0.999980839	-0.999994793	-0.999994693	-0.999994722	-0.999994793	-0.999995109	-0.999995079	-0.99999	-0.999994793	-0.99999462	-0.999994893	-0.99999495
Hausmannite	0.921522	0.999969848	0.999991048	1	0.999975738	0.999991048	0.999969848	0.999973	0.999975738	0.999957002	0.999969848	0.999974027	-0.999996865	-0.999996848	-0.999996869	-0.999996865	-0.999996432	-0.999996581	-1	-0.999996865	-0.999996901	-0.99999666	-0.999996695
Manganite	0.921123	0.999974819	0.99997029	0.999975738	1	0.99997029	0.999974819	0.999927	1	0.999936762	0.999974819	0.999927477	-0.999974436	-0.999974318	-0.999974387	-0.999974436	-0.999974471	-0.999974467	-0.99997	-0.999974436	-0.999974463	-0.999974567	-0.999974519
Manganese Sulfate	0.920834	0.999980935	1	0.999991048	0.99997029	1	0.999980935	0.999972	0.99997029	0.999946254	0.999980935	0.999980839	-0.999994793	-0.999994693	-0.999994722	-0.999994793	-0.999995109	-0.999995079	-0.99999	-0.999994793	-0.99999462	-0.999994893	-0.99999495
Manganese Sulfate Two	0.919658	1	0.999980935	0.999969848	0.999974819	0.999980935	1	0.999932	0.999974819	0.999920695	1	0.99992355	-0.999974399	-0.999974065	-0.999974171	-0.999974399	-0.999976104	-0.999975644	-0.99997	-0.999974399	-0.999974122	-0.99997508	-0.999975291
Nsutite	0.922018	0.999932288	0.999971634	0.999972538	0.999926553	0.999971634	0.999932288	1	0.999926553	0.999920519	0.999932288	0.999972807	-0.999973226	-0.999973329	-0.999973335	-0.999973226	-0.999972277	-0.999972514	-0.99997	-0.999973226	-0.999973516	-0.999972941	-0.999972595
Pyrochroite	0.921123	0.999974819	0.99997029	0.999975738	1	0.99997029	0.999974819	0.999927	1	0.999936762	0.999974819	0.999927477	-0.999974436	-0.999974318	-0.999974387	-0.999974436	-0.999974471	-0.999974467	-0.99997	-0.999974436	-0.999974463	-0.999974567	-0.999974519
Pyrolusite	0.922447	0.999920695	0.999946254	0.999957002	0.999936762	0.999946254	0.999920695	0.999921	0.999936762	1	0.999920695	0.999933606	-0.999968603	-0.999968965	-0.999968862	-0.999968603	-0.999967133	-0.999967532	-0.99997	-0.999968603	-0.999968929	-0.999968112	-0.999968047
Rhodochrosite	0.919658	1	0.999980935	0.999969848	0.999974819	0.999980935	1	0.999932	0.999974819	0.999920695	1	0.99992355	-0.999974399	-0.999974065	-0.999974171	-0.999974399	-0.999976104	-0.999975644	-0.99997	-0.999974399	-0.999974122	-0.99997508	-0.999975291
RhodochrositeD	0.921978	0.99992355	0.999980839	0.999974027	0.999927477	0.999980839	0.99992355	0.999973	0.999927477	0.999933606	0.99992355	1	-0.999976965	-0.999977099	-0.999977051	-0.999976965	-0.99997589	-0.999976288	-0.99998	-0.999976965	-0.999976896	-0.999976483	-0.999976385
Birnessite Norm	-0.92125	-0.999974399	-0.999994793	-0.999996865	-0.999974436	-0.999994793	-0.999974399	-0.99997	-0.999974436	-0.999968603	-0.999974399	-0.999976965	1	0.999999998	0.999999998	1	0.999999894	0.999999948	1	1	0.999999995	0.999999981	0.999999968
Bixbyite Norm	-0.92127	-0.999974065	-0.999994693	-0.999996848	-0.999974318	-0.999994693	-0.999974065	-0.99997	-0.999974318	-0.999968965	-0.999974065	-0.999977099	0.999999998	1	0.999999999	0.999999998	0.99999987	0.99999993	1	0.999999998	0.999999997	0.99999997	0.999999957
Hausmannite Norm	-0.92127	-0.999974171	-0.999994722	-0.999996869	-0.999974387	-0.999994722	-0.999974171	-0.99997	-0.999974387	-0.999968862	-0.999974171	-0.999977051	0.999999998	0.999999999	1	0.999999998	0.999999869	0.999999929	1	0.999999998	0.999999997	0.99999997	0.999999957
Manganite Norm	-0.92125	-0.999974399	-0.999994793	-0.999996865	-0.999974436	-0.999994793	-0.999974399	-0.99997	-0.999974436	-0.999968603	-0.999974399	-0.999976965	1	0.999999998	0.999999998	1	0.999999894	0.999999948	1	1	0.999999995	0.999999981	0.999999968
Manganese Sulfate Norm	-0.92107	-0.999976104	-0.999995109	-0.999996432	-0.999974471	-0.999995109	-0.999976104	-0.99997	-0.999974471	-0.999967133	-0.999976104	-0.99997589	0.999999894	0.99999987	0.999999869	0.999999894	1	0.99999999	1	0.999999894	0.999999869	0.999999961	0.999999972
Manganese Sulfate Two Norm	-0.92112	-0.999975644	-0.999995079	-0.999996581	-0.999974467	-0.999995079	-0.999975644	-0.99997	-0.999974467	-0.999967532	-0.999975644	-0.999976288	0.999999948	0.99999993	0.999999929	0.999999948	0.99999999	1	1	0.999999948	0.999999926	0.999999988	0.999999992
Nsutite Norm	-0.92125	-0.999974399	-0.999994793	-0.999996865	-0.999974436	-0.999994793	-0.999974399	-0.99997	-0.999974436	-0.999968603	-0.999974399	-0.999976965	1	0.999999998	0.999999998	1	0.999999894	0.999999948	1	1	0.999999995	0.999999981	0.999999968
Pyrochroite Norm	-0.92125	-0.999974399	-0.999994793	-0.999996865	-0.999974436	-0.999994793	-0.999974399	-0.99997	-0.999974436	-0.999968603	-0.999974399	-0.999976965	1	0.999999998	0.999999998	1	0.999999894	0.999999948	1	1	0.999999995	0.999999981	0.999999968
Pyrolusite Norm	-0.92127	-0.999974122	-0.99999462	-0.999996901	-0.999974463	-0.99999462	-0.999974122	-0.99997	-0.999974463	-0.999968929	-0.999974122	-0.999976896	0.999999995	0.999999997	0.999999997	0.999999995	0.999999869	0.999999926	1	0.999999995	1	0.99999997	0.999999956
Rhodochrosite Norm	-0.92117	-0.99997508	-0.999994893	-0.99999666	-0.999974567	-0.999994893	-0.99997508	-0.99997	-0.999974567	-0.999968112	-0.99997508	-0.999976483	0.999999981	0.99999997	0.99999997	0.999999981	0.999999961	0.999999988	1	0.999999981	0.99999997	1	0.999999992
RhodochrositeD Norm	-0.92116	-0.999975291	-0.99999495	-0.999996695	-0.999974519	-0.99999495	-0.999975291	-0.99997	-0.999974519	-0.999968047	-0.999975291	-0.999976385	0.999999968	0.999999957	0.999999957	0.999999968	0.999999972	0.999999992	1	0.999999968	0.999999956	0.999999992	1

	Redox	Birnessite	Bixbyite	Hausmannite	Manganite	Manganese Sulfate	Manganese Sulfate Two	Nsutite	Pyrochroite	Pyrolusite	Rhodochrosite	RhodochrositeD	Birnessite Norm	Bixbyite Norm	Hausmannite Norm	Manganite Norm	Manganese Sulfate Norm	Manganese Sulfate Two Norm	Nsutite Norm	Pyrochroite Norm	Pyrolusite Norm	Rhodochrosite Norm	RhodochrositeD Norm
Redox	1	1	1	1	1	1	#N/A	1	#N/A	1	#N/A	#N/A	-0.999983479	-0.999983394	-0.999966617	-0.999980138	-0.999370475	#N/A	-0.99999	#N/A	-0.9999842	#N/A	#N/A
Birnessite	1	1	1	1	1	1	#N/A	1	#N/A	1	#N/A	#N/A	-0.999983479	-0.999983394	-0.999966617	-0.999980138	-0.999370475	#N/A	-0.99999	#N/A	-0.9999842	#N/A	#N/A
Bixbyite	1	1	1	1	1	1	#N/A	1	#N/A	1	#N/A	#N/A	-0.999983479	-0.999983394	-0.999966617	-0.999980138	-0.999370475	#N/A	-0.99999	#N/A	-0.9999842	#N/A	#N/A
Hausmannite	1	1	1	1	1	1	#N/A	1	#N/A	1	#N/A	#N/A	-0.999983479	-0.999983394	-0.999966617	-0.999980138	-0.999370475	#N/A	-0.99999	#N/A	-0.9999842	#N/A	#N/A
Manganite	1	1	1	1	1	1	#N/A	1	#N/A	1	#N/A	#N/A	-0.999983479	-0.999983394	-0.999966617	-0.999980138	-0.999370475	#N/A	-0.99999	#N/A	-0.9999842	#N/A	#N/A
Manganese Sulfate	1	1	1	1	1	1	#N/A	1	#N/A	1	#N/A	#N/A	-0.999983479	-0.999983394	-0.999966617	-0.999980138	-0.999370475	#N/A	-0.99999	#N/A	-0.9999842	#N/A	#N/A
Manganese Sulfate Two	#N/A	#N/A	#N/A	#N/A	#N/A	#N/A	1	#N/A	#N/A	#N/A	#N/A	#N/A	#N/A	#N/A	#N/A	#N/A	#N/A	#N/A	#N/A	#N/A	#N/A	#N/A	#N/A
Nsutite	1	1	1	1	1	1	#N/A	1	#N/A	1	#N/A	#N/A	-0.999983479	-0.999983394	-0.999966617	-0.999980138	-0.999370475	#N/A	-0.99999	#N/A	-0.9999842	#N/A	#N/A
Pyrochroite	#N/A	#N/A	#N/A	#N/A	#N/A	#N/A	#N/A	#N/A	1	#N/A	#N/A	#N/A	#N/A	#N/A	#N/A	#N/A	#N/A	#N/A	#N/A	#N/A	#N/A	#N/A	#N/A
Pyrolusite	1	1	1	1	1	1	#N/A	1	#N/A	1	#N/A	#N/A	-0.999983479	-0.999983394	-0.999966617	-0.999980138	-0.999370475	#N/A	-0.99999	#N/A	-0.9999842	#N/A	#N/A
Rhodochrosite	#N/A	#N/A	#N/A	#N/A	#N/A	#N/A	#N/A	#N/A	#N/A	#N/A	1	#N/A	#N/A	#N/A	#N/A	#N/A	#N/A	#N/A	#N/A	#N/A	#N/A	#N/A	#N/A
RhodochrositeD	#N/A	#N/A	#N/A	#N/A	#N/A	#N/A	#N/A	#N/A	#N/A	#N/A	#N/A	1	#N/A	#N/A	#N/A	#N/A	#N/A	#N/A	#N/A	#N/A	#N/A	#N/A	#N/A
Birnessite Norm	-0.99998	-0.999983479	-0.99998	-0.999983479	-0.999983479	-0.999983479	#N/A	-0.999983479	#N/A	-0.9999835	#N/A	#N/A	1	0.999933747	0.999943454	0.999979505	0.999242268	#N/A	1	#N/A	0.99996201	#N/A	#N/A
Bixbyite Norm	-0.99998	-0.999983394	-0.99998	-0.999983394	-0.999983394	-0.999983394	#N/A	-0.999983394	#N/A	-0.9999834	#N/A	#N/A	0.999933747	1	0.999956671	0.999947603	0.999465865	#N/A	0.99994	#N/A	0.99997327	#N/A	#N/A
Hausmannite Norm	-0.99997	-0.999966617	-0.99997	-0.999966617	-0.999966617	-0.999966617	#N/A	-0.999966617	#N/A	-0.9999666	#N/A	#N/A	0.999943454	0.999956671	1	0.999965918	0.999411961	#N/A	0.999947	#N/A	0.99996791	#N/A	#N/A
Manganite Norm	-0.99998	-0.999980138	-0.99998	-0.999980138	-0.999980138	-0.999980138	#N/A	-0.999980138	#N/A	-0.9999801	#N/A	#N/A	0.999979505	0.999947603	0.999965918	1	0.999296917	#N/A	0.999981	#N/A	0.99996161	#N/A	#N/A
ManganeseSulfate Norm	-0.99937	-0.999370475	-0.99937	-0.999370475	-0.999370475	-0.999370475	#N/A	-0.999370475	#N/A	-0.9993705	#N/A	#N/A	0.999242268	0.999465865	0.999411961	0.999296917	1	#N/A	0.999256	#N/A	0.99930678	#N/A	#N/A
Manganese Sulfate Two Norm	#N/A	#N/A	#N/A	#N/A	#N/A	#N/A	#N/A	#N/A	#N/A	#N/A	#N/A	#N/A	#N/A	#N/A	#N/A	#N/A	#N/A	1	#N/A	#N/A	#N/A	#N/A	#N/A
Nsutite Norm	-0.99999	-0.999986542	-0.99999	-0.999986542	-0.999986542	-0.999986542	#N/A	-0.999986542	#N/A	-0.9999865	#N/A	#N/A	0.999999843	0.999940038	0.999947164	0.999981019	0.999256213	#N/A	1	#N/A	0.99996562	#N/A	#N/A
Pyrochroite Norm	#N/A	#N/A	#N/A	#N/A	#N/A	#N/A	#N/A	#N/A	#N/A	#N/A	#N/A	#N/A	#N/A	#N/A	#N/A	#N/A	#N/A	#N/A	#N/A	1	#N/A	#N/A	#N/A
Pyrolusite Norm	-0.99998	-0.999984198	-0.99998	-0.999984198	-0.999984198	-0.999984198	#N/A	-0.999984198	#N/A	-0.9999842	#N/A	#N/A	0.999962009	0.999973275	0.999967908	0.99996161	0.999306778	#N/A	0.999966	#N/A	1	#N/A	#N/A
Rhodochrosite Norm	#N/A	#N/A	#N/A	#N/A	#N/A	#N/A	#N/A	#N/A	#N/A	#N/A	#N/A	#N/A	#N/A	#N/A	#N/A	#N/A	#N/A	#N/A	#N/A	#N/A	#N/A	1	#N/A
RhodochrositeD Norm	#N/A	#N/A	#N/A	#N/A	#N/A	#N/A	#N/A	#N/A	#N/A	#N/A	#N/A	#N/A	#N/A	#N/A	#N/A	#N/A	#N/A	#N/A	#N/A	#N/A	#N/A	#N/A	1

Appendix D: Sampling Techniques

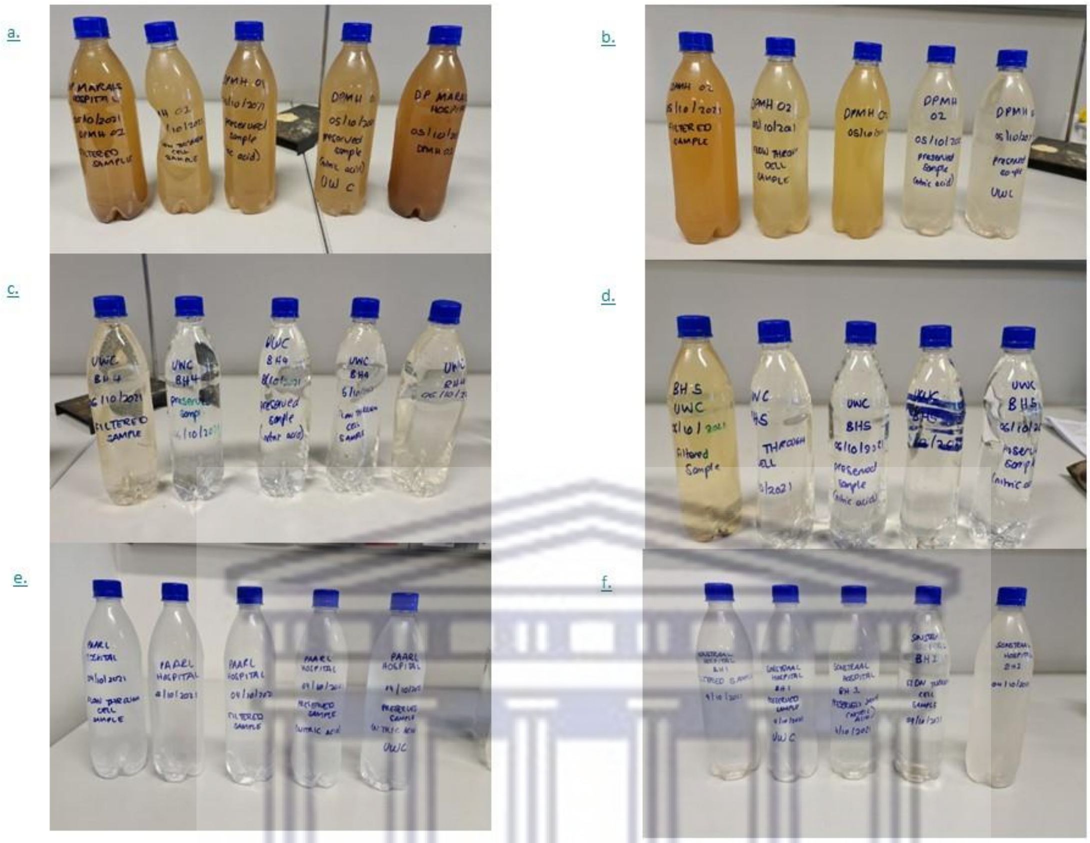

(a.) Image of samples collected from DP Marais Hospital BH1. (b.) Image of samples collected from DP Marais Hospital BH2. (c.) Image of samples collected from UWC BH4. (d.) Image of samples collected from UWC BH5. (e.) Image of samples collected from Paarl Hospital (Tap Sample). (f.) Image of samples collected from Sonstraal Hospital BH1

References

Abdullah, N., Alias, Y., Hodgkinson, J., Hussin, N., Raoov, M., Usman, A., & Yusoff, I. (2021). Natural sources of iron and manganese in groundwater of the lower Kelantan River Basin, North-eastern coast of Peninsula Malaysia: water quality assessment and an adsorption-based method for remediation. Environmental Earth Sciences, 1 - 17.

Adams, B., Calow, R., Chilton, P., Klinck, N., Lawrence, A. R., & Morris, B. L. (2003). *Groundwater and its susceptibility to degradation: A global assessment of the problem and options for management.* UNEP.

Adelana, S., Yongxin, X., & Vrbka, P. (2010). A conceptual model for the development and management of the cape flats aquifer, South Africa. *Water SA, 36*(4), 461 - 474.

Adeyeye, O., Liang, X., Xiao, C., Yang, W., & Zhang, Z. (2020). Source and mobilization mechanism of iron, manganese and arsenic in groundwater of Shuangliao City, Northeast China. *Water (Switzerland)*.

Ahmad, M. (2012). Iron and manganese removal from groundwater - geochemical modeling of the Vyredox method. Digitale Utgivelser ved UiO.

Ahn, Y., & Van Khanh, N. (2018). Electrochemical removal and recovery of iron from groundwater using non-corrosive electrodes. *Journal of Environmental Management*.

Alliance, F. o. (2021). *Assessing Groundwater Quality : A Global Perspective: Importance, Methods and Potential Data Sources.*

Amy, G., de Vet, W., Olivero, S., Verberk, J., van Dijk, J., & van Halem, D. (2010). Subsurface iron and arsenic removal for shallow tube well drinking water supply in rural Bangladesh. *Water Research, 44*(19), 5761 - 5769.

Apello, C., & Postma, D. (2009). *Geochemistry, groundwater and pollution* (2nd ed.). Amsterdam: CRC Press.

Barcelona, M. J., & Robert, P. W. (1989). Ground Water Sampling for Metals Analyses. *Superfund Ground Water Issue EPA.*

Barcelona, M. J., Gibb, J. P., Helfrich, J. A., & Garske, E. E. (1985). *Practical Guide for Ground-Water Sampling.* Champaign, Illinois: Illinois State Water Survey.

Bargmann, C. J. (2003). Geology and Wine 7 . Geology and Wine Production in the Coastal Region , Western Cape Province , South Africa. *Geoscience Canada, 30*(4), 162 - 182.

Behrens, S., Kappler, A., Lösekann-Behrens, T., Nitzsche, K., & Weigold, P. (2015). Microbial community composition of a household sand filter used for arsenic, iron, and manganese removal from groundwater in Vietnam. *Chemosphere,* 47 - 59.

Beknazarova, M., DeGaris, K., Harrington, N., Keerthirathne, T., Moser, B., Wallis, I., & Whiley, H. (2021). iron-related clogging of groundwater bores used for viticulture in the limestone coast, south Australia. *Water (Switzerland).*

Boghici, R. (2003). A field manual for groundwater sampling. *Texas Water Development Board, 51*(March), 1 - 47.

Bonzongo, J. J., Deliz Quiñones, K. Y., Harris, W., Oppong-Anane, A. B., & Townsend, T. (2018). Iron reductive dissolution in vadose zone soils: Implication for groundwater pollution in landfill impacted sites. *Applied Geochemistry*, 21 - 27.

Bourg, A. C., & Bertin, C. (1994). Seasonal and Spatial Trends in Manganese Solubility in an Alluvial Aquifer. *Environmental Science and Technology, 28*(5), 868 - 876.

Braester, C., & Martinell, R. (1988). The vyredox and nitredox methods of in situ treatment of groundwater. *Water Science and Technology, 20*(3), 149 - 163.

Bui, E., Caritat, P., Mckenzie, N., & Rossel, R. (2010). Mapping iron oxides and the color of Australian soil using visible – near - infrared reflectance spectra. *Journal of Geophysical Research*.

Cabaniss, S. E., & Pullin, M. J. (2003). The effects of pH, ionic strength, and iron-fulvic acid interactions on the kinetics of non-photochemical iron transformations. I. Iron(II) oxidation and iron(III) colloid formation. *Geochimica et Cosmochimica Acta*.

Cave, L., Talma, A. S., & Weaver, J. M. (2004). *Groundwater Sampling.*

Chevallier, L., Robey, K., & Tredoux, G. (2014). *Preventing Production Borehole Clogging by In-situ Iron Removal in South African Aquifer Systems.* Water Research Commission.

Colvin, C., Riemann, K., Brown, C., Le Maitre, D., Mlisa, A., Blake, D., . . . Prinsloo, E. (2009). *Ecological and Environmental Impacts of Large-scale Groundwater Development in the Table Mountain Group (TMG) Aquifer System.* WRC.

Conrad, J., Smit, L., Murray, K., & van Gend-Muller, J. (2019). The Malmesbury Group - An aquifer of surprising significance. *South African Journal of Geology, 122*.

Cornell, R., & Schwertmann, U. (2007). The Iron Oxides. *Iron Oxides in the Laboratary*, 5 - 18.

Cropper, W., & Hem, J. D. (1962). Survey of Ferrous-Ferric Chemical Equilibria and Redox Potentials. *Chemistry of Iron in Natural Water*.

Cullimore, R. (1999). *Microbiology of Well Biofouling.* Florida: CRC Press Lewis.

Danso-Amoako, E., & Prasad, T. (2014). Influence of chemical and biological parameters on iron and manganese accumulation in water distribution networks. *Procedia Engineering*, 1353 - 1361.

Diliūnas, J., & Jurevičius, A. (2006). Formation of iron compounds in the Quaternary groundwater of Lithuania. *Geologija Vilnius, 55*, 66 - 73.

Dippenaar, M. A. (2016). Hydrological Heritage Overview: Cape Town Where Sweet Waters Meet the Sea.

Du, X., Zhang, H., Ye, X., & Lu, Y. (2018). Flow velocity effects on Fe(III) clogging during managed aquifer recharge using Urban storm water. *Water (Switzerland), 10*(4), 1 - 11.

El Araby, R., Hawash, S., & El Diwani, G. (2009). Treatment of iron and manganese in simulated groundwater via ozone technology. *Desalination, 249*(3), 1345 - 1349.

Ellis, D., Bouchard, C., & Lantagne, G. (2000). Removal of iron and manganese from groundwater by oxidation and microfiltration. *Desalination, 130*(3), 255 - 264.

Emerson, D., Fleming, E. J., & McBeth, J. M. (2010). Iron-Oxidizing Bacteria: An Environmental and Genomic Perspective. *Annual Review of Microbiology, 64*(1), 561 - 583.

Esbensen, K. H., Minkkinen, P., & Petersen, L. (2005). Representative sampling for reliable data analysis: Theory of Sampling. *Chemometrics and Intelligent Laboratory Systems*, 261 - 277.

Forestry, D. o. (1996). *South African Water Quality Guidelines (second edition). Volume 1: Domestic Use.* Pretoria.

Gaffoor, Z., & Pietersen, K. (2018). *Sonstraal Hospital Facility Report.*

Hatva, T. (1989). Iron and manganese in groundwater in Finland: Occurrence in glacifluvial aquifers and removal by biofiltration. *Publications of the Water and Environment Research Institute*(4), 5 - 99.

Homoncik, S. C., Macdonald, A. M., Heal, K. V., Dochartaigh, B., & Ngwenya, B. T. (2010). Manganese concentrations in Scottish groundwater. *Science of the Total Environment*, 2467 - 2473.

Houben, G. J. (2003). Iron oxide incrustations in wells. Part 1: Genesis, mineralogy and geochemistry. *Applied Geochemistry*, 927 - 939.

Houben, G. J., & Weihe, U. (2010). Spatial distribution of incrustations around a water well after 38 years of use. *Ground Water*, 53 - 58.

Hughes, J., Titshall, L., & Trollip, D. (2013). Sources of manganese in the residue from a water treatment plant. *Water SA*, 265 - 270.

Husson, O. (2013). Redox potential (Eh) and pH as drivers of soil/plant/microorganism systems: A transdisciplinary overview pointing to integrative opportunities for agronomy. *Plant and Soil*, 389 - 417.

Jia, H. (2007). *Groundwater Resource Evaluation in Table Mountain Group Aquifer Systems.*

Joubert, S. J., & van Niekerk, A. (20``). Input variable selection for interpolating high-resolution climate surfaces for the western cape. *Water SA*, 271 - 280.

Kaliammal, M., & Udayanapilai, A. (2018). Speciation , Saturation Indices and Inverse Modelling Studies in the Metasedimentary Crystalline Limestone Terrain Pandalgudi, Aquifer Region, Viruthunagar District, Tamilnadu, India. *International Interdisciplinary Research Journal*.

Kang, H., Liu, Y., Li, D., & Xu, L. (2022). Study on the Removal of Iron and Manganese from Groundwater Using Modified Manganese Sand Based on Response Surface Methodology. *Applied Sciences*.

Karakish, A. A. (2005). Subsurface removal of iron and manganese from groundwater-case study. *Ninth International Water Technology Conference, IWTC9*, 415 - 429.

Khadse, G., Patni, P., & Labhasetwar, P. (2015). Removal of iron and manganese from drinking water supply. *Sustainable Water Resources Management*, 157 - 165.

Khozyem, H., Hamdan, A., Tantawy, A., Emam, A., & Elbadry, E. (2019). Distribution and origin of iron and manganese in groundwater: case study, Balat-Teneida area, El-Dakhla Basin, Egypt. *Arabian Journal of Geosciences*.

Lerner, D. N., & Harris, B. (2009). The relationship between land use and groundwater resources and quality. *Land Use Policy*, 265 - 273.

Lin, L., Jia, H., & Xu, Y. (2007). Fracture network characteristics of a deep borehole in the Table Mountain Group (TMG), South Africa. *Hydrogeology Journal*, 1419 - 1432.

Liu, B., Wang, X., Xie, G., Xing, D., & Zhao, X. (2018). Characterization of manganese oxidation by Brevibacillus at different ecological conditions. *Chemosphere*, 553-558.

Liu, X., Song, W., Yang, J., & Zheng, T. (2020). A review of recharge and clogging in sandstone aquifer. *Geothermics*.

Lock, B. E. (1980). Flat-plate subduction and the Cape Fold Belt of South Africa. *Geology*, 35 - 39.

Mahed, G. (2015). Development of a sampling protocol for radioactive elements in fractured rock aquifers using a case study from South Africa. *TOS Forum*, 19.

Majkić-Dursun, B., Petković, A., & Dimkić, M. (2015). The effect of iron oxidation in the groundwater of the alluvial aquifer of the Velika Morava River, Serbia, on the clogging of water supply wells. *Journal of the Serbian Chemical Society*, 947 - 957.

Mettler, S., Weidler, P., Abdelmoula, M., von Gunten, U., Schoenenberger, R., & Hoehn, E. (2001). Characterization of Iron and Manganese Precipitates from an In Situ Ground Water Treatment Plant. *Groundwater*, 921 - 930.

Olsthoorn, T. (2000). Background of subsurface iron and manganese removal.

Pegram, G., & Baleta, H. (2014). *Water in the Western Cape Economy.*

Pietersen, K., & Parsons, R. (2002). A Synthesis of the Hydrogeology of the Table Mountain Group - Formation of a Research Strategy. *Water Research Commission*.

Pinti, D. (2015). Redox Zonation. *Encyclopedia of Astrobiology*.

Post, J. E. (1999). Manganese oxide minerals: Crystal structures and economic and environmental significance. *Proceedings of the National Academy of Sciences of the United States of America*, 3447 - 3454.

Robey, K. (2014). A feasibility study of in-situ iron removal in the Atlantis Primary Aquifer, Western Cape Province, South Africa.

Sarkar, A., & Shekhar, S. (2018). Iron contamination in the waters of Upper Yamuna basin. *Groundwater for Sustainable Development*, 421 - 429.

Smith, M. (2006). Prediction, control and rehabilitation of iron encrustation in water supply boreholes, Western Cape, South Africa: A geochemical approach.

Smith, M., & Roychoudhury, A. N. (2013). Mobilisation of Iron from rocks in a fractured aquifer: Lithological and geochemical controls. *Applied Geochemistry*, 171 - 186.

Theis, T. L., & Singer, P. C. (1974). Complexation of Iron(II) by Organic Matter and Its Effect on Iron(II) Oxygenation. *Environmental Science and Technology*.

van Beek, C., Hofman-Caris, C., & Zweere, G. (2020). Drinking water treatment and chemical well clogging by iron(II) oxidation and hydrous ferric oxide (HFO) precipitation. *Journal of Water Supply: Research and Technology - AQUA*, *69*(5), 427 - 437.